Quantification of Nonclassical Correlations in a Doubly-resonant Optomechanical Cavity Coupled to a Nondegenerate Correlated Emission Laser

Mekonnen Bekele Tadesse

A Dissertation Submitted to the Department of Applied Physics
School of Applied Natural Science

Presented in the Partial Fulfilment of the Requirements for the Degree of Doctor of Philosophy in Physics
(Quantum Optics and Information)

Office of Graduate Studies
Adama Science and Technology University

June 2023
Adama, Ethiopia

Quantification of Nonclassical Correlations in a Doubly-resonant Optomechanical Cavity Coupled to a Nondegenerate Correlated Emission Laser

Mekonnen Bekele Tadesse

Major Supervisor: Sintayehu Tesfa Woldemariam (Ph. D.)

Co-Supervisor: Tewodros Yirgashewa Darge (Ph. D.)

A Dissertation Submitted to the Department of Applied Physics

School of Applied Natural Science

Presented in the Partial Fulfilment of the Requirements for the Degree of Doctor of Philosophy in Physics

(Quantum Optics and Information)

Office of Graduate Studies

Adama Science and Technology University

June 2023

Adama, Ethiopia

DECLARATION

I have a signed declaration and recommendation page.

Approval of Board of Reviewers

I have a partially signed Approval of Board of Reviewers page.

ACKNOWLEDGMENT

First and foremost, I give all the praise to the almighty God for giving me effort and time to complete this work. Next, I would like to express my deepest and heart felt thanks to Dr. Sintayehu Tesfa, the major dissertation supervisor, for drawing my attention towards cavity optomechanics, a particular study area in quantum optics and information. His excellent guidance, motivation, invaluable assistance, relentless attention during our encounters, timely feedback and meticulous evaluation of the entire work were indispensable for the success of my PhD research, and the publication of articles out of the work. It is also my pleasure to thank my co-advisor Dr. Tewodros Yirgashewa for his kind, considerable and constructive comments, opinion and suggestions during the proposal, the dissertation work and the final report. I am also grateful to all Physics staffs of Adama Science and Technology University for encouragement and support during up and down moments to be sane and complete the task. Particularly, the brotherly advice and console of Mr. Shunke Kebede, Dr. Mesfin Asfaw would not be forgotten. I owe my deepest thanks to all my family and friends, even if it is too long to include in the list. Especially, my heart felt thanks also goes to my brothers Demelash and Alemshet for financial and moral support they provided me during the difficulty time. It would be unfair if I failed to express my appreciation and respect to the Ethiopian Ministry of Education, Adama Science and Technology University and Bule Hora University for granting me the study leave, and financial support. Moreover, my heartfelt thanks go to my beloved family for understanding, care, and support from my wife Roza Dejene, sons Basliel and Natnael.

ABBREVIATIONS

BS	Beam Splitter
CEL	Correlated Emission Laser
CM	Covariance Matrix
COMS	Cavity Optomechanical System
CV	Continuous Variable
DCC	Doubly Coupled Cavity
EPR	Einstein-Podolski-Rosen
GQD	Gaussian Quantum Discord
HZ	Hillary-Zubairy
POVM	Positive Operator-Valued Measure
PPT	Positive Partial Transpose
QKD	Quantum Key Distribution
SQL	Standard Quantum Limit
SVR	Squeezed Vacuum Reservoir

List of Figures

List of Tables

Contents

Abstract

The detailed analysis of results of nonclassical correlations such as squeezing, entanglement, Gaussian quantum discord, Gaussian steering, correlations of number modes and statistical properties of quantum states of harmonically oscillating mirrors (mechanical modes) are presented. Particularly, traits of mechanical modes that can be attributed to the transfer of coherence to two separate mechanical modes via optical radiation pressure is explored in a doubly resonant optomechanical cavity, comprising pumped three-level atoms injected into cavity, a bichromatic drive laser, a beam splitter, and two separate harmonically oscillating mirrors using quantum Langevin approach. The results indicated that the degree of squeezing, entanglement, quantum discord, steering are sensitive to the specific choices of the frequencies of a bichromatic driving laser. It also turns out that the degree of these quantum features and the mean number of mechanical modes are enhanced with increasing rates of injection of the atoms, for stronger atom-field coupling but with decreasing initial lengths of a doubly resonant cavity and for smaller atomic decay rates. Besides, the degree of nonclassical correlations increase irrespective of the atomic decay rate up to the optimum value. There also appear significant degree of squeezing, entanglement using different measures, Gaussian quantum discord, Gaussian steering and mean number of mechanical modes for higher temperature of thermal baths coupled to mechanical modes. On the other hand, the degree of nonclassical correlations under consideration other than the squeezing show a decrease for an intense squeezed vacuum reservoir coupled to two-modes of a cavity. Interestingly, the degree of entanglement manifested in view of different criteria behave qualitatively in the same way, while the observed slight disparity between their magnitudes is attributed to the variations pertaining to the difference in the correlations leading to these phenomena. Robust degree of entanglement, quantum discord and steering using the quadrature and entropy measures is established in contrary to the correlations of number of mechanical modes when a vacuum reservoir is coupled to cavity radiations. These results entail that the various atomic, cavity and reservoir parameters can be deployed to control the squeezing, entanglement, discord, steering and the mean number of mechanical modes. In conclusion, one may argue that the possibility of generating mechanical modes, various realizable and robust degree of nonclassical features combined with significant controllability, the considered system to be applicable in the current quantum technology such as metrology and continuous variable information processing and allow the quantum features of cavity radiation to be accessible for application.

Keywords: *Nonclassical features, Squeezing, Entanglement, Quantum discord, Steering, Mechanical modes, Optomechanics, Radiation pressure, Bichromatic laser, Doubly resonant cavity, Quantum metrology, and Quantum Information processing.*

1

Introduction

1.1 Background

Our interpretation and understanding of the physical world may have been permeated as a result of correlations, classical or quantum, where the encoded information can be extracted from physical systems Henderson and Vedral [2001]; Luo [2008b]; Wheeler and Zurek [2014]. Particularly, the quantum correlations in composite systems are at the heart of the violation of Bell's inequalities that has been confirmed experimentally Poderini et al. [2022]. In this context, a state that can be verified using the Bell-type experiment and violates a Bell's inequality is known as Bell non-local Peres [1997]. A pure state is Bell non-local if and only if it is entangled. So far, the wide scope notion of quantum correlations in mixed states boast of novel features that have been playing a central role in quantum information processing and communication lying at the heart of quantum mechanics such as the entanglement (inseparable correlations of states) which is one of the non-local correlations Wheeler and Zurek [2014]; Nielsen [2000]. On the other hand, separable states might also possess non-zero quantum correlations (nonclassical correlations) even if their entanglement vanish Horodecki et al. [2009]; Modi et al. [2012]; Ollivier and Zurek [2001] whereby Oliver and Zurek introduced 'quantum discord' to exploit all non-classical correlations arising from the loss of information caused by quantum measurements Henderson and Vedral [2001]; Ollivier and Zurek [2001]. Separable states are generally considered as purely classical, since they do not violate Bell's inequalities.

Another recent inseparable form of quantum correlation, intermediating between entanglement (of mixed) Horodecki et al. [2009]; Einstein et al. [1935] and Bell nonlocality Horodecki et al. [2009]; Bell [1964b]; Brunner et al. [2014] was formulated by Wiseman and co-workers Wiseman et al. [2007]; Jones et al. [2007], exhibiting an intrinsic asymmetry between two entangled systems which allows one party to 'steer' the state of a distant party by exploiting their shared entanglement is known as Einstein-Podolski-Rosen (EPR) steering Kogias et al. [2015]. This phenomenon, which is at the heart of the EPR paradox Reid et al. [2009], was introduced by schrödinger Schrödinger [1935b]. Squeezing is also a different quantum feature at the expense of the transfer of the noise fluctuations in one quadrature operator to the conjugate quadrature with significance importance in ultra-high precision of measurements Tesfa [2021]; Walls and Milburn [2008]; Kassahun [2016].

Characterizing and quantifying various nonclassical features employing quantum correlations in continuous variable (CV) states play a crucial role in applications of quantum information processing and transmission Nielsen [2000]; Braunstein and Van Loock [2005]; Weedbrook et al. [2012]; Adesso et al. [2016]. In line with such proposal, many efforts have been carried out to quantify the quantum entanglement in bipartite Gaussian states owing to their theoretical as well as experimental interest and underpinning physical resource in quantum information tasks and protocols Nielsen [2000]; Horodecki et al. [2009]; Alber et al. [2003].

It is well-known that even some separable states contain nonclassical correlations Henderson and Vedral [2001]; Ollivier and Zurek [2001] where the "nonclassicality" of bipartite correlations can be measured via quantum discord which was first introduced in Henderson and Vedral [2001]; Ollivier and Zurek [2001]; Zurek [2000] as a measure of all quantum correlations in a bipartite state, including entanglement. For pure entangled states quantum discord coincides with the entropy of entanglement. Recently, it has been shown that almost all quantum states have nonvanishing discord Ferraro et al. [2010].

Gaussian quantum discord (GQD) that coincides with entanglement for pure states but differ for mixed ones can also be taken as weaker criteria for measure of quantumness and can go beyond the scope of entanglement Ollivier and Zurek [2001]; Zurek [2000]; Adesso and Datta [2010]; Giorda and Paris [2010]. Originally the notion of quantum discord was defined and evaluated for finite dimensional system but recently extended to the domain of continuous variable systems in analyzing the bipartite quantum correlations in states of Gaussian mode Adesso and Datta [2010]; Giorda and Paris [2010]; Olivares [2012]. In line with this, the concept of quantum discord has aroused great interest as a resource which is more robust than entanglement against the decoherence phenomenon offering exponential speed up of certain computational algorithms Henderson and Vedral [2001]; Ollivier and Zurek [2001].

On the other hand, the quantification and measure of Gaussian steering quantifier for CV systems has been proposed very recently by He et al. [2015]. It is noted that a measure of steering quantifies the amount of correlations in a given state as in Bennett et al. [2011], where a manifestation of these correlations can be observed by the violation of suitable EPR-steering criteria leading to a quantitative estimation of the degree of steerability by evaluating the maximum violation of a chosen steering criterion as revealed by optimal measurements. One expects that the higher the violation (i.e., the amount of correlations), the more useful the state will be in tasks and making it a subject of intense research that use quantum steering as a resource Reid et al. [2009].

Notably, the notion of steering has recently attracted significant theoretical Kogias et al. [2015]; Cavalcanti et al. [2011]; Olsen [2015]; Bowles et al. [2014]; Wang et al. [2016b] and experimental Wittmann et al. [2012]; Armstrong et al. [2015]; Kocsis et al. [2015] attention as a resource for a number of applications in nonclassical tasks that can be used in one-sided device-independent entanglement verification Wiseman et al. [2007] quantum key distribution Branciard et al. [2012]; Walk et al. [2016], signifying secure quantum teleportation Reid [2013a] and performing entanglement-assisted subchannel discrimination Piani and Watrous [2015].

Very recently, the interaction of cavity radiation with a movable mirror in a fabry-pérot cavity, cavity optomechanical system (COMS), has received a great deal of interest in quantum optics for generating, controlling, measuring and applying quantum states of bosonic systems such as photons and phonons (vibrational modes) by developing various schemes for their theoretical investigation and experimental verification with anticipated applications in sensing, quantum information processing, ultra-high precision measurements and tests of fundamental physics Kippenberg and Vahala [2007]; Aspelmeyer et al. [2014]; Agarwal [2012]. The quantum properties of these bosonic states, in particular the photons, can also be enhanced by the use of nonlinear elements such as atoms (two-, three-, four- level atoms), parametric amplifiers and other optical elements Tesfa [2021]; Walls and Milburn [2008]; Kassahun [2016].

Apart from encoding quantum information in quantum states of any realistic system encounters both the quantum decoherence and dissipation which leads to the loss of quantum correlation between the sub-systems induced by the unavoidable coupling with its environment such as the squeezed vacuum reservoir, thermal reservoir, biased noise fluctuation, vacuum reservoir and so on Tesfa [2021]; Walls and Milburn [2008]; Kassahun [2016] so that investigating the effect(s) of the coupling between the quantum systems and their own environment will make the exploitation of quantum properties for quantum information processing more relevant.

The extension to these undersigning could be achieved via investigating ways to generate coupling of COMS to various nonlinear elements, particularly with the atomic systems, and with their environment/s, where various quantum effects and their control is so well established as in the interaction of a cavity radiation in a two-level laser with one end of a cavity's quantum harmonically oscillating mirror with its anticipated potential as a source of squeezed and entangled mechanical and/or optical modes.

In this context, the various important features of cavity radiation originating from atomic coherence can be transferred to the modes of movable mirrors utilizing the non-conservative nature of radiation pressure that couples the mechanical-optical modes through different processes Aspelmeyer et al. [2014]; Agarwal [2012]; Marshall et al. [2003]; Zhang et al. [2003]; Braginsky and Khalili [1992]; Eisert et al. [2004]; Pinard et al. [2005]; Huang and Agarwal [2009]; Vitali et al. [2007]; Wang et al. [2014].

There is still a continuing effort to realize many more novel optomechanical systems which will have merits in achieving applications with better performance and ease of implementation which can provide a platform for classical and quantum information processing. Consequently, in this dissertation, we seek to study various quantum features that serves as indicators and quantifiers of nonclassicality in a doubly resonant optomechanical cavity coupled to a three level laser. Particularly, we intend to analyze the effects of different atomic, cavity and environmental parameters on the squeezing, entanglement, GQD, Gaussian steering, and the statistical properties of the two mechanical modes.

In this regard, the two mode cavity radiation generated by a nondegenerate three level cascade laser in which the top and bottom levels of the three level atoms are coupled by a strong coherent radiation. The two mode radiation is found to be separated by a beam splitter and coupled explicitly to two modes of the quantum harmonically oscillating mirrors (mechanical modes) via radiation pressure. The two mode cavity radiation is coupled to a two mode squeezed vacuum reservoir through a single stationary port mirror while the mechanical modes are coupled independently to the high-Q Markovian thermal environments.

The cavity is also driven by a bichromatic coherent laser. To this end, we first derive the master equation for the quantum optical system under consideration in the linear and adiabatic approximation schemes following the approach described in Ref. Tesfa [2021]; Kassahun [2016], and the master equation for the two quantum harmonically oscillating mirrors as in Ref. Aspelmeyer et al. [2014].

We then carry out our analysis by obtaining the quantum Langevin equations with the help of the master equation, for laser modes confining to adiabatic approximation, linear analysis and a good cavity limit following the procedure described in Refs. Kassahun [2016]; Scully; Fesseha [2001], and to those of the mechanical modes Aspelmeyer et al. [2014] employing the interaction Hamiltonian. Afterwards, correlation between the noise forces of the radiation and mechanical modes are manipulated analytically. With these aid, the steady state covariance matrix is obtained for a bipartite mechanical modes in a weak coupling of the optical and mechanical modes using the Lyapunov equation, and therefore calculate the correlation between these modes that can be used as a resource to carry out the accompanying analysis such as squeezing, entanglement, GQD, Gaussian steering, statistical properties and the induced correlation between the number of mechanical modes.

1.2 Statement of the Problem

The problems which have been encountering with information processing, storage, transferring, and computing are producing scalable and robust resources of information carrier in a condition that the information is encoded on a quantum resource than the classical bits.

Nowadays, investigating the mesoscopic quantum states and the various associated correlation properties is exciting research field as it gives

- a better compatibility to the current quantum technology (in storing, transferring, and computing information) to that of the microscopic quantum states such as photons and atoms in a cavity,
- a mechanism for evaluating different nonclassical behaviours at a scale between microscopic and macroscopic,

So far, the quantum behaviours of states of quantum harmonically oscillating mirrors such as optical bistability and entanglement using the logarithmic negativity criterion were studied. But the various nonclassical behaviors of the modes of quantum harmonically oscillating mirrors (mechanical modes) such as the squeezing, entanglement using different measures, quantum discord, steering, their interrelations, statistical properties, and the effects of atomic, cavity and reservoir parameters on these nonclassical properties were not yet studied. Therefore, in this research, “With the help of the correlation of the radiation emitted by CEL, can quantum correlation in the modes of the mechanical oscillators that has not physically coupled to each other in a doubly resonant optomechanical cavity be established? Also, in what ways do the atomic, cavity and reservoir parameters affect the squeezing, entanglement, quantum discord, Gaussian steering, and statistical properties of the mechanical modes?”

1.3 Objectives

1.3.1 General objective

The general objective of this research is to study nonclassical and statistical properties of mechanical modes of oscillating mirrors coupled to thermal baths induced by cavity modes generated by nondegenerate three-level atom pumped by coherent light and the cavity modes are driven by bichromatic light and coupled to squeezed vacuum reservoir.

1.3.2 Specific objectives

The specific objectives of the study in an optomechanical cavity coupled to a laser are to:

- derive the Hamiltonian equation, and the master equation for the mechanical modes,
- determine the evolution of expectation values of the cavity and mechanical modes, the corresponding noise correlations, the covariance matrix and correlations between cavity-cavity modes, mechanical-mechanical modes, and cavity-mechanical modes,
- evaluate the nonclassical features of mechanical modes using quadrature vari-

ances and entropic measures,

- assess the effects of various atomic parameters on the nonclassical behaviors of mechanical modes,
- investigate the effects of various cavity parameters on the nonclassical behaviors of mechanical modes,
- determine effects of temperatures of reservoirs coupled the mechanical modes and effects of squeezed vacuum reservoir coupled the cavity modes on squeezing, entanglement, GQD, and Gaussian Steering,
- demonstrate the interrelations between different entanglement measures and other nonclassical behaviors of of mechanical modes.

1.4 Significance of the Study

The overview presented in this research will move forward for unfamiliar encoding of information on quantum states of harmonically oscillating mirror (mechanical modes) which will be helpful to improve the storing, transferring and computing of quantum information. Nonclassical correlations of mechanical modes can also be affected when we consider different atomic, cavity and reservoir parameters. Therefore, there is great interest in understanding and quantifying the various quantum behaviours of mechanical modes and the effects of atomic injection rate, atomic decay rate, atom-field coupling strength, initial lengths of a doubly resonant cavity, frequencies of a bichromatic laser, a squeeze parameter of two-mode SVR, and temperature of thermal baths. Hence, this research is expected to

- put a platform for researchers and post graduate students to apply on other hybrid optomechanical systems.
- be helpful for recent applications in quantum technologies such as quantum metrology, quantum cryptography, quantum teleportation and others.

- identify the effects of various atomic, cavity and reservoir parameters have on different quantum properties.
- allow the quantum features of cavity radiation to be accessible for application.

1.5 Scope of the Study

Guided with the principles of quantum optics and their uses in a wide variety of areas including quantum information science and quantum mechanics, this study covers recent developments of micro-mechanical mirrors, their nonclassical correlations and control of decoherence using the quantum Langevin equations for different quantum states of the system in the rotating-wave and the adiabatic regime with the help of the master equation, confining to linear analysis and a good cavity limit, where the atom-field is considered as much stronger than the optomechanical coupling. On the other hand, the external environments coupled to cavity radiations and quantum harmonically oscillating mirrors are Markovian, and the parameters used in this study are limited to experimental values which has been employed in other optomechanical systems. The study also covered the interaction mechanism between optical and mechanical modes, the effects of different atomic parameters, cavity parameters, and parameters of reservoirs coupled to cavity modes and mechanical modes on various induced nonclassical features of mechanical modes in a cavity comprising a pumped three level atom injected into cavity, a strong bichromatic cavity drive laser, and two separate quantum harmonically oscillating mirrors.

Particularly, the main focus of these investigations were to see the effects of atomic injection rate, strength of atom-field coupling, atomic decay rate, frequencies of a bichromatic laser, initial lengths of a doubly resonant cavity, photon numbers of squeezed vacuum reservoirs, and temperature of the thermal reservoir coupled to mechanical modes on squeezing, entanglement, quantum discord, Gaussian steering and statistical properties of mechanical modes.

2

Literature Review

In quantized electromagnetic radiation, which can be considered as a system of Gaussian CVs, the role of the position and momentum observable is played by the electric field magnitudes measured at specific phases Kok and Lovett [2010]; Weedbrook et al. [2012]. For instance, the field at phase zero corresponds to the position observable, that at phase $\pi/2$ to the momentum observable, and so on. Accordingly, phase-sensitive measurements of the field in an electromagnetic wave are affected by quantum uncertainties.

For the coherent and vacuum states, this uncertainty is phase-independent and equals the standard quantum limit (SQL). In this limit the variances of the two conjugate quadrature operators takes a value of one Loudon and Knight [1987]. Note also that the position and momentum of a harmonic oscillator are both sinusoidal in time and exactly one quarter cycle out of phase.

In a squeezed state, the quantum noise in one quadrature is below the vacuum level or below SQL at the expense of enhanced fluctuations in the conjugate quadrature with the product of the uncertainties in the two quadrature satisfying the uncertainty relation Kassahun [2016]. The application of squeezing is tantamount to encoding quantum information onto the quadrature with minimum noise; and consequently, minimize the inherent loss of information in the process of encoding and decoding.

Quantum fluctuations using optomechanical methods have been employed in generating the squeezed states of the optical and mechanical modes Liao et al. [2011]; Purdy et al. [2013]; Kronwald et al. [2013]; Lü et al. [2015a]. It is a well-established fact that mechanical squeezing, which is one of the key macroscopic quantum effects, can be used for many applications such as improved precision of quantum metrology Safavi-Naeini et al. [2013], measurement of weak classical force Caves et al. [1980], biological measurements Taylor et al. [2013], and quantum-to-classical transitions Hu and Nori [1996]; Wu et al. [1986].

In this context, several schemes have been proposed to generate mechanical squeezing in resonators based on parametric processes, feedback, measurements, and quantum-reservoir engineering Safavi-Naeini et al. [2013]; Mancini and Tombesi [1994]; Wollman et al. [2015]; Gu and Li [2013]; Lü et al. [2015b]; Wang et al. [2016a]; Feng et al. [2018]; Zhang et al. [2018]; Meng et al. [2020]; Mari and Eisert [2009]; Gu et al. [2013]. In a COMS where a movable mirror in its steady state can be regarded as a low-noise Kerr nonlinear medium Mancini and Tombesi [1994], experimental realizations of squeezing in optical fields Purdy et al. [2013]; Safavi-Naeini et al. [2013] and mechanical modes Wollman et al. [2015] have been witnessed. Hybrid optomechanical systems that include atoms have also been proposed to induce mechanical squeezing. For instance, many works have used two-level atom(s) to induce squeezing of the mechanical resonator Wang et al. [2016a]; Zhang and Chen [2020]. It is also found to be interesting to include a correlated emission laser (CEL), which has been studied extensively and the emitted radiation is found to exhibit strong squeezing Kassahun [2016]; Kiffner et al. [2007]; Tesfa [2011].

On the other hand, a mixed quantum state $\hat{\rho}$ of a bipartite system is found to be entangled (inseparable) if and only if

$$\hat{\rho} \neq \sum_i P_i \hat{\rho}_{i1} \otimes \hat{\rho}_{i2}, \tag{2.1}$$

where $\hat{\rho}_{i1}$and $\hat{\rho}_{i2}$ are density operators of mode 1 and 2 with $0 \leq P_i \leq 1$ satisfying

$\sum P_i = 1$.

On the basis of different conditions and assumptions, several inseparability criteria for continuous variable product states have been proposed. One of the mechanism to quantify entanglement is using quadrature variances in terms of the sum of variances of EPR-like operators and product of variances of EPR-like operators that correspond to the Duan et al. [2000] and the Mancini et al. [2002] entanglement criteria; while the quantum entropy measure is another measure which consists the logarithmic negativity entanglement criteria.

Recently, significant effort have been put forward to generate entangled states in COMS that offers a rich avenue for experimenting on recent quantum technologies, improving our understanding of quantum optics in macroscopic regime and at fundamental quantum physics level, and implementing for various applications Aspelmeyer et al. [2014]; Agarwal [2012]; Meystre [2013]. These states have been detected in two-mode cavity radiations Yang et al. [2017], cavity mode and mechanical mode Vitali et al. [2007]; Paternostro et al. [2007], and two mechanical modes Li et al. [2015]; Neveu et al. [2021] using the logarithmic negativity.

Further studies have also addressed on entangled states of hybrid modes as in two-level atom Genes et al. [2008]; Rogers et al. [2012]; He and Ficek [2014] and three-level atom Ge et al. [2013]; Sete and Eleuch [2015]; Zhou et al. [2011] optomechanical systems. It is also well-established that the simultaneously emitted correlated photons with different frequencies as in a cascade three-level atomic system can be a source of robust entanglement in a resonant cavity due to the inherent atomic coherence in the upper and lower energy levels induced by initial preparation of coherent superposition and/or pumping by strong coherent laser Ansari [1993]; Xiong et al. [2005]; Tesfa [2006, 2009, 2008].

It has also been investigated that a bichromatic cavity driving laser can be employed for the generation of entanglement in various configurations in some theoretical proposals Giovannetti et al. [2001]; Giovannetti and Vitali [2001]; Wipf et al. [2008] and experimental realization utilized for cooling a macroscopically heavy movable mirror Corbitt et al. [2007].

Quantum information can also be perceived as the interpretation of quantum process from thermodynamic point of view; and expected to lead to a wider conceptual analysis of quantum phenomena such as quantum decoherence, entanglement, quantum discord and EPR steering.

The notion of entropy in quantum statistical mechanics expressed in von Neumann can be extended to the quantum domain by means of the density matrix. In information theory, entropy is a measure of the efficiency of a system in transmitting a signal or the loss of information in a transmitted signal.

Suppose we have two random variables A and B whose ignorance is described by the Shannon entropy. The correlations between the two random variables of classical systems in information theory are quantized by the mutual information which can be defined as

$$I(A:B) = H(A) + H(B) - H(A,B), \tag{2.2}$$

where $H(\cdot)$ stands for the ignorance about a random variable A or B Shannon entropy, while $H(\cdot,\cdot)$ represents the Shannon entropy of the joint probability distribution. Note that the mutual information measures the average decrease of entropy on A when B is found out.

A different way of writing this quantity by re-defining I and J for a pair of quantum systems is using conditional entropy. The classically equivalent expression for the mutual information using the Baye's rule takes the form

$$J(A:B) = H(A) - H(A|B), \tag{2.3}$$

where $H(A|B) = H(A,B) - H(B)$.

For the quantum systems A and B, all the components involved in the definition of I are easily generalized and what we need to do is use the von Neumann entropy $S(.)$

instead of the Shannon entropy $H(.)$, and replace the classical probability distributions by the appropriate density matrices ρ_A, ρ_B, and ρ_{AB}. Here, ρ_{AB} is the density matrix of the whole system AB. Hence, the quantum mutual information is defined as

$$I_Q(A:B) = S(\rho_A) + S(\rho_B) - S(\rho_{A,B}), \tag{2.4}$$

where $S(\rho_A) = -\mathrm{Tr}(\rho_A \log \rho_A)$ and the subscript 'Q' just indicates that this is a quantum measure. In this formula, $S(\rho_A) + S(\rho_B)$ represents the uncertainty of ρ_A and ρ_B treated separately, and $S(\rho_{A,B})$ is the uncertainty about the combined system described by $\rho_{A,B}$.

The second expression to the right side of equal sign in Eq. (2.4) for the mutual information involving the conditional entropy is harder to upgrade to quantum physics. The reason is that if we do the same substitution of the Shannon with the von Neumann entropy, the resulting entity $S(A,B) - S(B)$ can actually be negative for bipartite quantum systems. Thus, the generalization of $J(A:B)$ is not as automatic as for $I(A:B)$ for quantum systems, since the conditional entropy $S(\rho_{A|B})$ requires us to specify the state of A given the state of B. Such statement in quantum theory is ambiguous until the to-be-measured set of states B is selected.

Consider the total correlations of composite system ρ_{AB} defined in the Hilbert space as quantified by quantum mutual information Groisman et al. [2005]:

$$J(A:B) = S(\rho_A) + S(\rho_B) - S(\rho_{AB}) = S(\rho_A) - S(\rho_{A|B}), \tag{2.5}$$

where $S(\rho)$ is the von Neumann entropy and $\rho_{A,B} = \mathrm{Tr}_{B,A}(\rho)$ are reduced density matrices.

Focusing on perfect measurements of B defined by a set of one-dimensional projectors Π_j^B where the label j distinguishes different outcomes of this measurement. The quantum generalization of J that represents the information gained about the system

A as a result of the measurement Π_j^B can be expressed as:

$$J(A:B)_{\Pi_B^j} = S(A) - S(\rho_{A|\Pi_B^j}) = S(A) - \sum_j p_j S\big(\rho_{A|\Pi_B^j}\big), \tag{2.6}$$

where $S(\rho_{A|\Pi_B^j}) = \sum_j p_j S\big(\rho_{A|\Pi_B^j}\big)$ is the missing information about A that is represented by the entropies, and the state of A after the outcome corresponding to Π_B^j has been detected is $\rho_{A|\Pi_B^j} = \frac{\Pi_B^j \rho_{A,B} \Pi_B^j}{Tr_{A,B} \Pi_B^j \rho_{A,B}}$ with probability $p_j = Tr_{A,B} \Pi_B^j \rho_{A,B} \Pi_B^j$.

By optimizing over all possible measurements in B, we define an alternative version of the mutual information as

$$J(A:B) = S(\rho_A) - \min_{\{\Pi_j\}} \left[\sum_j p_j S_{\rho_{A|j}} \right], \tag{2.7}$$

where $\{\Pi_j\}$ is a positive operator-valued measure (POVM) corresponding to a measurement in subsystem B. On the other hand, the process of minimizing the discord over the possible measurement on apparatus amounts to finding the measurement that disturbs the overall quantum state, and at the same time allows one to extract the most available information about the system.

The two classically identical expressions for the mutual information, Eqs. (2.4) and (2.7), differ in a quantum case Zurek [2000]. Therefore, the discrepancy between the two measures of information defines the quantum discord as Wilde [2013]:

$$D_A(A:B) = I(A:B) - J(A:B), \ \ \text{Or}$$

$$D_B(B:A) = I(B:A) - J(B:A), \tag{2.8}$$

which can also be written, depending on both $\rho_{A,B}$ and the projectors Π_j^B, as

$$D(A:B) = S(\rho_B) - S(\rho_{AB}) + \min_{\{\Pi_j\}} \left[\sum_j p_j S_{\rho_{A|j}} \right]. \tag{2.9}$$

The quantum discord is asymmetric under the change $A \leftrightarrow B$ as the definition of the conditional entropy $S(\rho_{A|\Pi_B^j})$ involves a measurement on one end (in our case the apparatus B) that allows the observer to infer the state of A. This typically involves an increase of entropy. Hence $S(\rho_{A|\Pi_B^j}) \geq S(A, B) - S(A)$, which implies that for any measurement Π_j^B Ollivier and Zurek [2001]

$$D(A : B)_{\Pi_j^B} \geq 0. \tag{2.10}$$

The discord is always non-negative Adesso et al. [2004a] and reaches zero for the classically correlated states Kogias et al. [2015]. It is noted also that discord is not a symmetric quantity i.e. $D_A(\rho) \neq D_B(\rho)$ and D_A refers to the "left" discord, while D_B refers to the "right" discord.

Note that D_A large represents the situation in which a lot of information is missed: destroyed by the measurement on the apparatus alone. However, D_A small can be taken as almost all information about the system that exists in the system-apparatus correlations can be locally recoverable from the state of the apparatus. With this general perception, quantum discord can be taken as a measure of the information that cannot be extracted by reading the state of the apparatus alone.

In light of this, quantum discord is believed to be a good indicator of the quantum nature of the correlations. Even then, despite increasing evidence for the relevance of quantum discord in describing nonclassical resources in information processing, there is no as such a direct criterion to verify the presence of discord for a given quantum state since optimization of the conditional entropy is required due to the involved local measurement process. Fortunately, under restricted Gaussian measurements, a closed analytical relation that can be utilized to quantify the quantum discord for the two-mode Gaussian states can be outlined.

Motivated by the importance and potential of Gaussian states that exhibits quantum discord in emerging technology, it turns out to be imperative investigating quantum discord in CV systems. For continuous variable systems there is only an approximation to the quantum discord, called Gaussian quantum discord, developed by Adesso and

Datta Adesso and Datta [2010] and simultaneously by Giorda and Paris Giorda and Paris [2010]. The main restriction of this approximation is that the optimization over all the measurements over one single mode is restricted to the set of Gaussian measurements, or generalized Gaussian POVMs. For this reason the Gaussian quantum discord provides only an upper bound for the unrestricted quantum discord (except for a family of states, for which Gaussian measurements are known to be optimal). In the following we briefly review the main points needed to evaluate the Gaussian quantum discord of a two-mode Gaussian state.

The means of quantifying the degree of the measure of quantumness in terms of the quantum discord for Gaussian states would be formulated by employing the optimization procedure specialized for CV Gaussian state. In doing so, one needs to brave the involved challenge in the hope that a two-mode CV states can have central importance in area of quantum optics and quantum information processing can exhibit interesting quantum features that can be captured by quantum discord. Notably, existing experience shows that CV Gaussian state can be completely described by first and second order moments of the quadrature operators as depicted in the covariance matrix.

Considering a generic Gaussian $(n+m)$-mode state ρ_{AB} of the bipartite system composed of subsystem A of n-modes and subsystem B of m-modes, we can outline the criteria for Gaussian quantum discord. For each mode j belonging to $A(B)$, the phase-space quadrature operators $\hat{x}_j^{A(B)}$, $\hat{p}_j^{A(B)}$ can be grouped into the vector as

$$\hat{R} = \left(\hat{x}_1^A, \hat{p}_1^A, ..., \hat{x}_n^A, \hat{p}_n^A, \hat{x}_1^B, \hat{p}_1^B, ..., \hat{x}_m^B, \hat{p}_m^B\right)^T. \tag{2.11}$$

Note that each pair satisfies the usual canonical commutation relations can compactly be written as

$$[\hat{R}_k, \hat{R}_l] = i\Omega_{kl}, \tag{2.12}$$

where Ω_{kl} is a constant that can be expressed in the symplectic form as

$$\Omega = \bigoplus_{k,l=1}^{n+m} \begin{pmatrix} 0 & 1 \\ -1 & 0 \end{pmatrix}, \tag{2.13}$$

where $\bigoplus$ is the direct sum.

Any Gaussian state ρ_{AB} is fully specified, up to local displacements, by its covariance matrix (CM),

$$V = \begin{pmatrix} V_A & V_C \\ V_C^T & V_B \end{pmatrix}, \tag{2.14}$$

with V_A, V_B, and V_C represented as

$$V_A = \mathrm{diag}(V_{11}, V_{22}), \;\; V_B = \mathrm{diag}(V_{33}, V_{44}), \;\; \text{and} \;\; V_C = \begin{pmatrix} V_{13} & V_{14} \\ V_{23} & V_{24} \end{pmatrix}. \tag{2.15}$$

Here, $\mathrm{V_A}$ and $\mathrm{V_B}$ are the 2×2 block form of covariance matrices that describe each of the mechanical modes separately; while $\mathrm{V_C}$ represents the 2×2 matrix of correlations between the mechanical modes. The elements of CM V_{ij} in Eq. (2.15) for $\mathrm{i}, \mathrm{j} = 1, ..., 4$ can be obtained by using

$$V_{ij} = Tr[\{\hat{R}_i, \hat{R}_j\}_+ \rho_{AB}] = \frac{1}{2}\big[\langle \hat{R}_i \hat{R}_j + \hat{R}_j \hat{R}_i \rangle\big] - \langle \hat{R}_i \rangle \langle \hat{R}_j \rangle. \tag{2.16}$$

where $\hat{R}_{i,j}$ stand for the real phase-space operators. Mark that the off diagonal elements of this matrix represents intermodal correlations and the sub matrices α and β (the diagonal elements) are the CMs corresponding to the reduced states of two subsystems A and B which represents the inter-correlations associated with energy (more specifically; mean photon numbers).

It is noted that every CMs, V, that corresponds to a physical quantum state has to satisfy the bona fide condition,

$$V + i(\Omega_A \oplus \Omega_B) \geq 0. \tag{2.17}$$

On the other hand, Gaussian variable is usually designated as symplectic if there is a linear transformation S that preserves the symplectic form of Ω, that is,

$$S^T \Omega S = \Omega. \tag{2.18}$$

The symplectic spectrum $\nu = \{\nu_1, ..., \nu_n\}$ of an arbitrary correlation matrix σ can be calculated by finding the (standard) eigenvalues of the matrix $|i\Omega\sigma|$, where Ω defines the symplectic form and is given by Weedbrook et al. [2012]

$$\Omega = \bigoplus_{i}^{n} \begin{pmatrix} 0 & 1 \\ -1 & 0 \end{pmatrix}. \tag{2.19}$$

Here $\bigoplus$ is the direct sum indicating adding matrices on the block diagonal.

For two-mode Gaussian states, we then consider dimensionless two mode quadrature operators $\hat{R} = \left(\hat{x}_1, \hat{p}_1, \hat{x}_2, \hat{p}_2\right)$, i.e. $\hat{x}_i = \frac{1}{\sqrt{2}}(\delta\tilde{b}_i + \delta\tilde{b}_i^\dagger)$ and $\hat{p}_i = \frac{i}{\sqrt{2}}(\delta\tilde{b}_i^\dagger - \delta\tilde{b}_i)$ where $\delta\tilde{b}_i(\delta\tilde{b}_i^\dagger)$ is the annihilation(creation) operator of each mode of a quantum harmonically oscillating mirror. Noting that the Gaussian approximation to the quantum discord applies to two-mode Gaussian states, these are completely described (within local displacements) by the 4×4 covariance matrix as in Eq. (2.14).

In reality, any measure of correlations must be invariant under local unitary operations. If these operations are also Gaussian, they correspond to local symplectic operations at the phase-space level. Therefore, the only quantities one needs to know to evaluate measures of correlations like the mutual information or logarithmic negativity are the local symplectic invariants of the covariance matrix. These invariants are simply the determinants of each 2×2 block and the determinant of the entire CM. The local symplectic invariants of V admit this compact form:

$$X = \det(V_A), \quad Y = \det(V_B), \quad C = \det(V_C), \quad D = \det(V). \tag{2.20}$$

Moreover, by means of a symplectic operation (generally global), any Gaussian state can be transformed in another Gaussian state with CM of the form $V = \mathrm{diag}(\nu_+, \nu_+, \nu_-, \nu_-)$. The symplectic eigenvalues ν_+ and ν_- are invariants under symplectic transformations and can be calculated as

$$v_{\pm} = \left(\frac{\Xi \pm \left(\Xi^2 - 4D\right)^{\frac{1}{2}}}{2} \right)^{1/2}, \tag{2.21}$$

with

$$\Xi = X + Y + 2C. \tag{2.22}$$

In evaluating the expression in Eq. (2.9) for quantum discord, the only nontrivial point for a two-mode Gaussian state is the optimization of the last term over all the possible measurement on the second quantum state (mode 2 or quantum state B). The approach of Refs. Adesso and Datta [2010]; Giorda and Paris [2010] consists in restricting the optimization to the set of Gaussian POVMs Holevo and Werner [2001].

Numerous recent researches have been carried out on quantum discord in various optomechanical systems Chakraborty and Sarma [2017]; Amazioug et al. [2018a, 2020c,a, 2018b, 2020b]. In this regard, the Gaussian quantum discord (GQD) becomes more robust and survives up to a high thermal bath temperature as compared to the optomechanical entanglement in presence of cross-Kerr nonlinearity Chakraborty and Sarma [2017] or in two spatially separated Fabry-Pérot cavities Amazioug et al. [2018a].

It has already been observed that the increase of squeeze parameter in an optomechanical system with two spatially separated Fabry-Pérot cavities enhance the GQD but it decreases with the increase of thermal effects Amazioug et al. [2018a, 2020c,a] whereas purity and quantum discord remain nonzero when entanglement between the mechanical modes and optical modes vanishes under thermal effect Amazioug et al. [2020b].

Steering is another quantum mechanical phenomenon for mixed states of composite quantum systems that allows one party, for instance A (Alice), to change (i.e., to "steer") the state of a distant party, B (Bob), by exploiting their shared entanglement. This phenomenon, fascinatingly discussed by Schrödinger Schrödinger [1935b,a], was already noted by EPR in their famous 1935 paper Einstein et al. [1935]. There it was argued that steering implied an unacceptable "action at a distance", which led EPR to claim the incompleteness of quantum theory. The EPR expectations for local realism were mostly extinguished by Bell's theorems Bell [1964a, 1975], which showed that no locally causal theory can reproduce all the correlations observed in nature Aspect et al. [1982].

The first experimental criterion for the demonstration of the EPR paradox, i.e., for the detection of quantum steering, was later proposed by Reid Reid [1989], but it was not until 2007 that the particular type of nonlocality captured by the concept of steering Einstein et al. [1935]; Schrödinger [1935b,a] was in fact formalized Wiseman et al. [2007]; Jones et al. [2007].

From a quantum information perspective Wiseman et al. [2007], steering corresponds to the task of verifiable entanglement distribution by an untrusted party. If Alice and Bob share a state which is steerable in one way, say from Alice to Bob, then Alice is able to convince Bob (who does not trust Alice) that their shared state is entangled, by performing LOCC Wiseman et al. [2007].

Notice that steering, unlike entanglement, is an asymmetric property: a quantum state may be steerable from Alice to Bob, but not vice versa. On the operational side, it has been recently realized that steering provides security in one-sided device-independent quantum key distribution (QKD) Branciard et al. [2012], where the measurement apparatus of one party only is untrusted. EPR steering also plays an operative role in channel discrimination Piani and Watrous [2015] and tele-amplification He et al. [2014].

Several experiments have been already performed, demonstrating steering and its asymmetry Wittmann et al. [2012]; Vallone [2013]; Saunders et al. [2010]; Eberle et al. [2011]; Händchen et al. [2012]; Bennet et al. [2012]; Smith et al. [2012]; Steinlechner et al. [2013]; Sun et al. [2014], and a number of recent studies have been devoted to improving our understanding of quantum steerability, ranging from the development of better criteria to detect steerable states Cavalcanti et al. [2009]; Walborn et al. [2011]; Schneeloch et al. [2013]; Cavalcanti et al. [2013]; Pramanik et al. [2014], to the analysis of the distribution of steering among multiple parties Bowles et al. [2014]; Midgley et al. [2010]; He and Reid [2013]; Reid [2013b]. However, unlike entanglement, for which a variety of operationally motivated measures exist Horodecki et al. [2009]; Plenio and Virmani [2007], there is still a surprisingly scarce literature addressing the fundamental question of quantifying how steerable a given quantum state is Piani and Watrous [2015]; Skrzypczyk et al. [2014]; Costa et al. [2016].

Focusing on a fully Gaussian scenario: namely, we consider generally mixed multimode bipartite Gaussian states, that constitute a distinctive corner of the infinite-dimensional Hilbert space Weedbrook et al. [2012,?]; Adesso et al. [2014], and study their steerability under Gaussian measurements Eisert et al. [2002]; Fiurášek [2002].

By analyzing the degree of violation of a necessary and sufficient criterion for Gaussian steerability Wiseman et al. [2007]; Jones et al. [2007], we obtain a computable measure of Gaussian steering, and we investigate its properties. In the special case of two-mode Gaussian states, we characterize the maximum allowed steering asymmetry. And it has been shown that the Gaussian steering degree is upper bounded by the Gaussian Rényi-2 entanglement Adesso et al. [2012], with equality on pure states.

To discuss the steerability of bipartite CV systems, we strictly focus on the mixed multi-mode bipartite Gaussian states since Gaussian states and operations play a central role in the analysis and implementation of CV quantum technologies Weedbrook et al. [2012].

To define steerability formally, under a set of measurements $\mathcal{M}_A$ on Alice, a bipartite physical quantum state ρ_{AB} is $A \to B$ steerable - i.e., Alice can steer Bob's variable - if and only if it is not possible for every pair of local observables $R_A \in \mathcal{M}_A$ on A and R_B (arbitrary) on B, with respective outcomes r_A and r_B, to express the joint probability as

Wiseman et al. [2007]

$$P\big(r_A, r_B|R_A, R_B, \rho_{AB}\big) = \sum_j \wp_j \wp(r_A|R_A, j) P(r_B|R_B, \rho_j). \tag{2.23}$$

Here $\wp_j$ and $\wp(r_A|R_A, j)$ are arbitrary probability distributions and $P(r_B|R_B, \rho_j)$ is a probability distribution subject to the extra condition of being evaluated on a quantum state ρ_j, meaning that a complete knowledge of Bob's devices (but not of Alice's ones) is required to formulate the steering condition.

It is good to note that to witness the steerability, at least one measurement pair R_A and R_B must violate the expression in Eq. (2.23) when $\wp_j$ is fixed across all measurements. On account of this, the measure (degree) of quantum steerability should quantify how much the correlations of a given quantum state depart from this condition.

In light of this, since the manifestation of these correlations is expected to be observed by the violation of suitable EPR steering criteria, one can get a quantitative estimation of the degree of steerability by evaluating the maximum violation of the chosen steering criterion as revealed by the pertinent optimal measurements.

In the fully Gaussian scenario, where ρ_{AB} is a Gaussian state described by the CMs σ, we will focus on Alice's measurement set $\mathcal{M}_A$ to be Gaussian (i.e., Gaussian states are mapped into Gaussian states). A Gaussian measurement Fiurášek [2002], which is generally implemented via symplectic transformations followed by balanced homodyne detection, can be described by a positive operator with a CM T^{R_A}, satisfying '$T^{R_A} + i\Omega_A \geq 0$'. Every time Alice makes a measurement R_A and gets an outcome r_A, Bob's conditioned state state $\rho_B^{r_A|R_A}$ is Gaussian with a CM given by

$$Y^{R_A} = Y - C(T^{R_A} + X)^{-1} C^T, \tag{2.24}$$

independent of Alice's outcome.

On the other hand, one can argue Wiseman et al. [2007] that a general $(n+m)$-mode Gaussian state describable by density operator $\hat{\rho}_{AB}$ is $A \rightarrow B$ steerable by Alice's

Gaussian measurement if and only if the condition in Eq. (2.17) is violated.

Writing this in matrix form as in Eq. (2.14), the non steerability inequality $V + i(\Omega_A \oplus \Omega_B) \geq 0$ is equivalent to two simultaneous conditions:

(i). $X > 0$,

(ii). $M_\sigma^B + i\Omega_B \geq 0$,

where $M_\sigma^B = Y - C^T X^{-1} C$ is the Schur complement of X in the covariance matrix V.

Condition (i) is always verified since V_A is a physical CM. Therefore, V is $A \to B$ steerable if and only if the symmetric and positive definite $2\mathrm{m} \times 2\mathrm{m}$ matrix M_σ^B is not a bona fide CM, i.e., if condition (ii) is violated Adesso and Datta [2010]; Giorda and Paris [2010].

By Williamson's theorem Williamson [1936], M_σ^B can be diagonalize by a symplectic transformation S_B such that $S_B M_\sigma^B S_B^T = \mathrm{diag}(\bar{v}_1^B, \bar{v}_2^B, ..., \bar{v}_m^B)$, where $\{\bar{v}_m^B\}$ are simplectic eigenvalues M_σ^B, which can be determined by m local symplectic invariants Serafini [2006]; alternatively, they can be computed as the orthogonal eigenvalues of the matrix $\mid i\Omega_B M_\sigma^B \mid$. The nonsteerability condition (bona fide condition) is thus equivalent to $\bar{v}_j^B \geq 1$ for all $j = 1, ..., m$.

We then propose to quantify how much a bipartite $(\mathrm{m} + \mathrm{n})$ - mode Gaussian state with covariance matrices V is steerable (by Gaussian measurements on Alice's side) via the following quantity:

$$G^{A \to B}(V) := \max\left\{0, -\sum_{j:\bar{v}_j^B < 1} \ln\left(\bar{v}_j^B\right)\right\}. \tag{2.25}$$

This quantity, hereby defined as Gaussian $A \to B$ steerability, is invariant under local unitaries (symplectic operations at the CM level), it vanishes if and only if the state described by V is nonsteerable by Gaussian measurements, and it generally quantifies the amount by which condition $V + i(\Omega_A \oplus \Omega_B) \geq 0$ fails to be fulfilled.

Clearly, the corresponding measure of Gaussian $B \to A$ steerability can be obtained by swapping the roles of A and B, resulting in the above Equation, in which the symplectic eigenvalues of the $2\mathrm{n} \times 2\mathrm{n}$ Schur complement of V_B, $M_\sigma^A = X - C\,Y^{-1}\,C^T$ appear instead.

Highlighting the formal similarity with the formula for the logarithmic negativity Horodecki et al. [2009]; Plenio and Virmani [2007]; Vidal and Werner [2002]; Plenio [2005] - an entanglement measure which quantifies how much the positivity of the partial transpose condition for separability is violated Duan et al. [2000]; Peres [1996]; Horodecki et al. [1996]; Werner and Wolf [2001]-for Gaussian states; in the latter case, however, the symplectic eigenvalues of the partially transposed CM are considered Weedbrook et al. [2012]; Plenio and Virmani [2007]; Vidal and Werner [2002]; Adesso et al. [2004b].

The proposed measure of steering is easily computable for bipartite Gaussian states of an arbitrary number of modes. When the steered party, e.g., Bob in Eq. (2.25), has one mode only $(m = 1)$, the Gaussian steerability acquires a particularly simple form. Indeed, in such a case, M_σ^B has a single symplectic eigenvalue, $\bar{v}^B = \sqrt{\det M_\sigma^B}$; recalling that, by definition of Schur complement, $\det(V) = \det(V_A)\,\det(M_\sigma^B)$, we have

$$G^{A\to B}(V) = \max\left\{0, \frac{1}{2}\ln\left(\frac{\det(V_A)}{\det(V)}\right)\right\}$$

$$= \max\left\{0, \mathcal{S}(A) - \mathcal{S}(\sigma_{AB})\right\} \tag{2.26}$$

where we have introduced the Rényi-2 entropy $\mathcal{S}$, which for a Gaussian state with CM V reads $\mathcal{S}(V) = \frac{1}{2}\ln\left[\det(V)\right]$ Adesso et al. [2012].

In the case of two-mode Gaussian states $(n = m = 1)$, for which the degree of steering in both ways can be easily measured according to our definition of the second line of Eq. (2.26) and its vice versa. Qualification and quantification of steering in two-mode Gaussian states thus reduces entirely to an interplay between the global purity μ and the two marginal purities $\mu_{A(B)}$

$$\mu = \frac{1}{\sqrt{\det V}}, \quad \mu_{A(B)} = \frac{1}{\sqrt{\det V_A(V_B)}}. \tag{2.27}$$

Introducing the ratio $\eta = \frac{\mu_A \mu_B}{\mu}$, all physical two-mode Gaussian states live in the region $\eta_0 \leq \eta \leq 1$ where $\eta_0 = \mu_A\mu_B + \mid \mu_A - \mu_B \mid$ Adesso et al. [2004b]. Therefore,

(i). states with $\eta_0 \leq \eta \leq \eta_e$ are necessarily entangled with $\eta = \sqrt{\mu_A^2 + \mu_B^2 - \mu_A^2\mu_B^2}$,

(ii). states with $\eta \geq \{\mu_A, \mu_B\}$ are non steerable,

(iii). states with $\eta < \mu_B$ are $A \to B$ steerable where the steerable one can also be written as;

$$S^{A\to B} = \sqrt{\frac{\det V}{\det V_A}} < 1 \quad \text{Or} \quad G^{A\to B} > 0, \tag{2.28}$$

(iv). states with $\eta < \mu_A$ are $B \to A$ steerable steerable, which can also be rewritten as Serafini [2006];

$$S^{B\to A} = \sqrt{\frac{\det V}{\det V_B}} < 1 \quad \text{Or} \quad G^{B\to A} > 0. \tag{2.29}$$

Moreover, several other schemes have also been proposed to quantify steering in optomechanical systems Tan et al. [2015]; Gebremariam et al. [2019], and experimental realizations of conversion between microwave and optical light, and generation of steering in opto-electro-mechanical systems have been demonstrated in Refs. Bochmann et al. [2013]; Bagci et al. [2014]; Černotík and Hammerer [2016].

Furthermore, J. E. Qars et al. proposed a scheme to generate dynamical Gaussian steering via a quantum fluctuations transfer from squeezed light to the mechanical modes, and by an appropriate choice of the environmental parameters, one-way steering can be observed in different scenarios El Qars et al. [2017]. On the other hand, the directionality and extent of the steering can be readily controlled for output modes using a nondegenerate parametric oscillator with an injected signal field. The two down-converted modes, which exhibit the greater violations of the steering inequalities, can also be controlled to exhibit asymmetric steering in some regimes Olsen [2017].

3

Materials and Methods

3.1 Materials

The system under consideration is shown in Fig. 3.1; it comprises three-level atoms in a cascade configuration, an external laser pumping these atoms, two harmonically oscillating mirrors, a pumping bichromatic laser, a beam splitter, a two-mode squeezed vacuum reservoir coupled to two-mode cavity radiations, and thermal baths coupled to mechanical modes.

3.2 Methods

3.2.1 System and Hamiltonian

Here, we denote the top, intermediate, and bottom energy levels of a three-level atom by $|a\rangle$, $|b\rangle$, and $|c\rangle$, respectively. Transitions between levels $|a\rangle$ and $|b\rangle$, and between $|b\rangle$ and $|c\rangle$ are considered to be dipole allowed whereas direct transition between levels $|a\rangle$ and $|c\rangle$ is taken to be dipole forbidden. When a three-level cascade atom decays from the top level to the bottom level via the intermediate level, two photon modes, $\hat{a}_1$ and $\hat{a}_2$ of frequencies ω_1 and ω_2 are emitted where these cavity radiation modes are at resonance with transitions $|a\rangle$ to $|b\rangle$ and $|b\rangle$ to $|c\rangle$, respectively. Then, these atoms are injected at a constant rate r_a into a doubly resonant cavity. Injected atoms, which are removed after a time longer than the spontaneous emission time, are presumed to

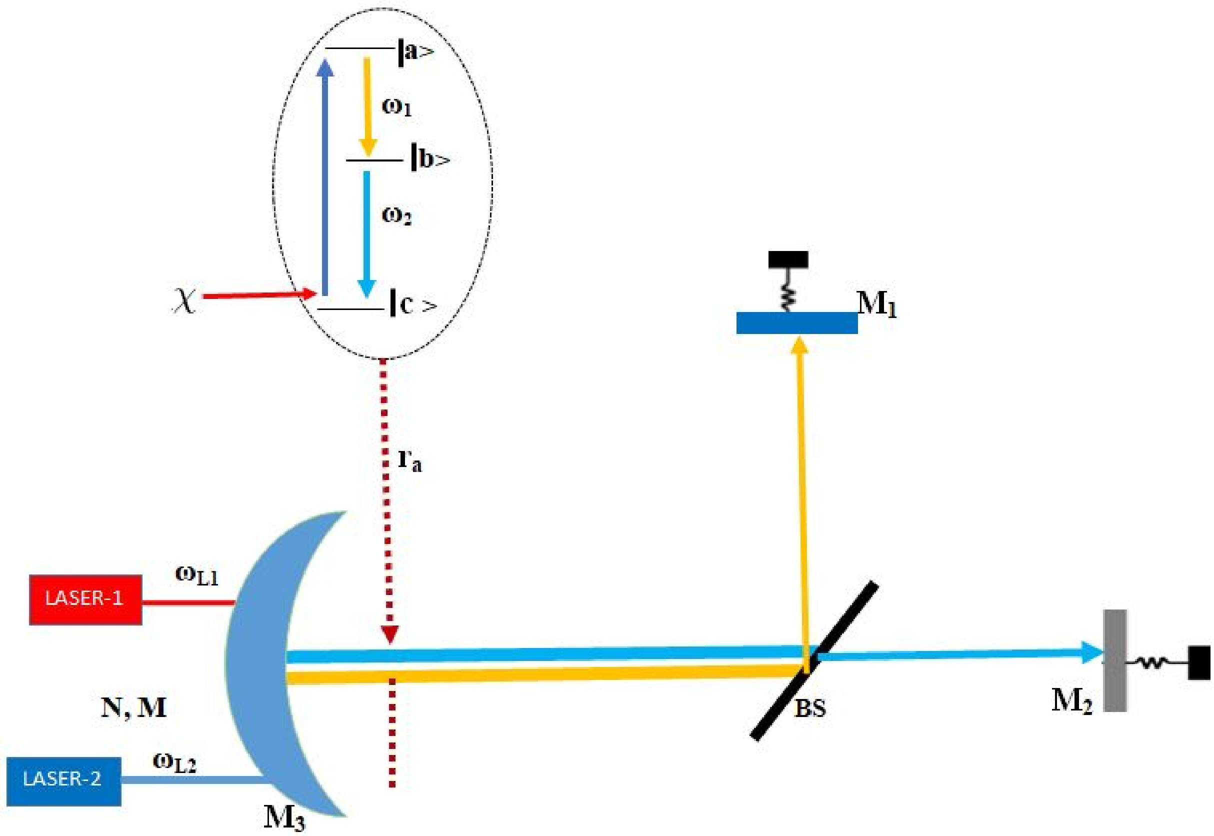

Figure 3.1: Schematic representation of injected three level atoms being pumped by a strong coherent radiation of amplitude χ so that two-mode correlated emission laser is generated. The cavity is driven by a bichromatic laser of frequencies ω_{L_1} and ω_{L_2} via port mirror M_3 and the two-mode cavity radiation is coupled to two-mode squeezed vacuum reservoir having parameters of mean photon number (N) and correlations of these two modes (M). The cavity radiation fields with frequencies ω_1 and ω_2 are then filtered by a beam splitter (BS) and coupled to two movable mirrors (M_1 and M_2) via radiation pressure.

interact nonresonantly with the two cavity modes.

To establish a coherent superposition in the upper and lower energy atomic states, the atoms are assumed to be driven by a strong coherent laser field of amplitude χ and frequency ω_p. These atomic levels are also prepared initially in coherent superposition of upper and lower energy levels to establish additional coherence. The cavity on the other hand is driven by two coherent lasers (a bichromatic laser) of frequencies ω_{L_1} and ω_{L_2}, and the two cavity radiations that are split by a beam splitter (BS) in the cavity are coupled to their respective movable mirrors via radiation pressure.

In this setting, the movable mirrors M_1 and M_2 are treated as quantum-mechanical harmonic oscillators with effective masses m_j and frequencies $\omega_{m_j}(j = 1, 2)$. On the other hand, to include the influence of external noise on the quantum behaviors of mechanical oscillation modes, we assume that the cavity modes in a cavity is coupled to squeezed vacuum reservoir via a port mirror M_3 whereas the modes of oscillating mirrors are coupled to two separate thermal baths.

These mechanical quantum harmonic oscillators could thus be modeled with their respective thermal baths at equilibrium with temperatures T_1 and T_2 having the annihilation (creation) operator of each vibrational mode $\hat{b}_j$ ($\hat{b}_j^\dagger$) satisfying the relation $[\hat{b}_j, \hat{b}_j^\dagger] = 1$ with $j = 1, 2$. In this regard, the movable mirrors are expected to undergo quantum harmonic oscillations resulting in nonclassical correlations when the emerging coherent correlation in CEL can be transferred to the mechanical oscillations via the force electromagnetic radiation exerts on a material surface, where the light's momentum causes fluctuations in the mirror's position, yielding phase noise in the electromagnetic wave.

The Hamiltonian describing the coupling of the upper and bottom levels by coherent radiation can be expressed as Sete and Eleuch [2015]

$$\hat{H}_1 = i\frac{\chi}{2}\left(e^{-i\omega_p t}|a\rangle\langle c| - e^{i\omega_p t}|c\rangle\langle a|\right), \tag{3.1}$$

and the Hamiltonian of bichromatic lasers driving laser in the cavity can be described by Sete and Eleuch [2015]

$$\hat{H}_2 = i\sum_{k=1}^{2}\left(\epsilon_k \hat{a}_k^\dagger e^{-i\omega_{L_k} t} - \epsilon_k^* \hat{a}_k e^{i\omega_{L_k} t}\right), \tag{3.2}$$

where $|\epsilon_k| = \sqrt{\frac{\kappa_k P_k}{\hbar\omega_{L_k}}}$ are the amplitudes of the lasers that drive the cavity, with κ_k, P_k, and ω_{L_k} being the damping rates of cavities, the power and the frequencies of the pump lasers, respectively. In addition, the interaction of a three-level cascade atom with a two-mode cavity radiation can be described in the interaction picture by the Hamiltonian

Tesfa [2021]; Kassahun [2016]; Sete and Eleuch [2015]

$$\hat{H}_3 = ig_1\left(|a\rangle\langle b|\hat{a}_1 - \hat{a}_1^\dagger|b\rangle\langle a|\right) + ig_2\left(|b\rangle\langle c|\hat{a}_2 - \hat{a}_2^\dagger|c\rangle\langle b|\right), \tag{3.3}$$

where $g_1(g_2)$ is the coupling strength between the cavity modes and the atomic transition $|a\rangle \rightarrow |b\rangle$ ($|b\rangle \rightarrow |c\rangle$), and $\hat{a}_k(\hat{a}_k^\dagger)$ is the annihilation(creation) operators for the kth cavity mode with $k = 1, 2$.

On the other hand, the free Hamiltonian of the atoms, the cavity modes and the modes of quantum harmonically oscillating mirrors are described respectively by

$$\hat{H}_3 = \sum_{r=a,b,c} \omega_r |r\rangle\langle r|, \tag{3.4}$$

$$\hat{H}_4 = \sum_{k=1}^{2} \omega_k \hat{a}_k^\dagger \hat{a}_k, \tag{3.5}$$

$$\hat{H}_5 = \sum_{k=1}^{2} \omega_{m_k} \hat{b}_k^\dagger \hat{b}_k, \tag{3.6}$$

where $\omega_r (r = a, b, c)$ are the frequency of the rth atomic level, ω_k is the frequency of the kth cavity mode, and ω_{m_k} are the mechanical oscillator mode frequency while $\hat{b}_k(\hat{b}_k^\dagger)$ are the annihilation (creation) operators of the kth mechanical modes. Moreover, the interaction Hamiltonian of the two cavity modes explicitly with two mechanical modes is expressed as Aspelmeyer et al. [2014]; Sete and Eleuch [2015]

$$\hat{H}_6 = \sum_{k=1}^{2} G_{0_k} \hat{a}_k^\dagger \hat{a}_k \left(\hat{b}_k^\dagger + \hat{b}_k\right), \tag{3.7}$$

where $G_{0_k} = (\omega_k/L_k)\sqrt{\hbar/(m_k\omega_{m_k})}$ $(k = 1, 2)$ denotes the optomechanical coupling strength between the mechanical and cavity modes. With L_k, and m_k being the initial lengths and effective masses of the movable mirrors, respectively.

On the basis of Eqs. (3.1)-(3.7), the total Hamiltonian in the interaction of a three-level cascade atom, whose top and bottom levels are initially prepared in an arbitrary coherent superposition and also coupled by external coherent laser, with two-mode cavity radiation, and the interaction of the two cavity modes with two-modes of vibrating mirrors in a doubly resonant cavity where the cavity is driven by a strong bichromatic laser can be described as

$$\begin{aligned}\hat{H} = &\sum_{r=a,b,c} \omega_r |r\rangle\langle r| + \sum_{k=1}^{2} \omega_k \hat{a}_k^\dagger \hat{a}_k + ig_1 \Big(|a\rangle\langle b|\hat{a}_1 - \hat{a}_1^\dagger |b\rangle\langle a|\Big) + ig_2 \Big(|b\rangle\langle c|\hat{a}_2 - \hat{a}_2^\dagger |c\rangle\langle b|\Big) \\ &+ i\frac{\chi}{2}\left(e^{-i\omega_p t}|a\rangle\langle c| - e^{i\omega_p t}|c\rangle\langle a|\right) + i\sum_{k=1}^{2}\Big(\epsilon_k \hat{a}_k^\dagger e^{-i\omega_{L_k} t} - \epsilon_k^* \hat{a}_k e^{i\omega_{L_k} t}\Big) \\ &+ \sum_{k=1}^{2}\Big[\omega_{m_k}\hat{b}_k^\dagger \hat{b}_k + G_{0_k}\hat{a}_k^\dagger \hat{a}_k(\hat{b}_k^\dagger + \hat{b}_k)\Big]. \end{aligned} \tag{3.8}$$

Considering the fact that $|a\rangle\langle a| + |b\rangle\langle b| + |c\rangle\langle c| = 1$ and employing Eqs. (3.4) and (3.5) the free Hamiltonian for the atom and cavity modes by omitting the constant $\hbar\omega_c$ can be written as

$$\hat{H}_{fr} = (\omega_a - \omega_c)|a\rangle\langle a| + (\omega_b - \omega_c)|b\rangle\langle b| + \omega_1 \hat{a}_1^\dagger \hat{a}_1 + \omega_2 \hat{a}_2^\dagger \hat{a}_2. \tag{3.9}$$

In view of (3.9), the total Hamiltonian, $\hat{H}$, in Eq. (3.8) can be rearranged as

$$\hat{H} = \hat{H}_0 + \hat{H}_X, \tag{3.10}$$

with

$$\hat{H}_0 = \big(\Omega_1 + \Omega_2\big)|a\rangle\langle a| + \Omega_2|b\rangle\langle b| + \Omega_1 \hat{a}_1^\dagger \hat{a}_1 + \Omega_2 \hat{a}_2^\dagger \hat{a}_2, \tag{3.11}$$

$$\begin{aligned}\hat{H}_X = &\big(\xi_1 + \xi_2\big)|a\rangle\langle a| + \xi_2|b\rangle\langle b| + \delta\omega_1 \hat{a}_1^\dagger \hat{a}_1 + \delta\omega_2 \hat{a}_2^\dagger \hat{a}_2 + ig_1\Big(|a\rangle\langle b|\hat{a}_1 - \hat{a}_1^\dagger|b\rangle\langle a|\Big) \\ &+ ig_2\Big(|b\rangle\langle c|\hat{a}_2 - \hat{a}_2^\dagger|c\rangle\langle b|\Big) + i\frac{\chi}{2}\left(e^{-i\omega_p t}|a\rangle\langle c| - e^{i\omega_p t}|c\rangle\langle a|\right) \\ &+ i\sum_{k=1}^{2}\Big(\epsilon_k \hat{a}_k^\dagger e^{-i\omega_{L_k} t} - \epsilon_k^* \hat{a}_k e^{i\omega_{L_k} t}\Big) + \sum_{k=1}^{2}\Big[\omega_{m_k}\hat{b}_k^\dagger \hat{b}_k + G_{0_k}\hat{a}_k^\dagger \hat{a}_k(\hat{b}_k^\dagger + \hat{b}_k)\Big], \end{aligned} \tag{3.12}$$

where $\xi_1 = \omega_{ab} - \Omega_1,\ \omega_{ab} = \omega_a - \omega_b,\ \ \xi_2 = \omega_{bc} - \Omega_2,\ \omega_{bc} = \omega_b - \omega_c,\ \Omega_j = \omega_j - \delta\omega_j$. Note also that Ω_j is the shifted cavity frequency and $\delta\omega_j = G_{0_j}\langle\hat{b}_j^\dagger + \hat{b}_j\rangle$ is the frequency shift due to radiation pressure.

Taking into account of Eq. (3.9), Eq. (3.11) can be rewritten as

$$\hat{H}_0 = \hat{H}_{fr} - \big(\xi_1 + \xi_2\big)|a\rangle\langle a| - \xi_2|b\rangle\langle b| - \delta\omega_1\hat{a}_1^\dagger\hat{a}_1 - \delta\omega_2\hat{a}_2^\dagger\hat{a}_2, \tag{3.13}$$

and hence the interaction Hamiltonian can be derived in the rotating wave approximation i.e. (using a unitary transformation) as

$$\hat{H}_I = e^{i\hat{H}_0 t}\hat{H}_X e^{-i\hat{H}_0 t} = \hat{H}_I^{af} + \hat{H}_I^{fm}, \tag{3.14}$$

with

$$\begin{aligned}\hat{H}_I^{af} =& \left(\xi_1 + \xi_2\right)|a\rangle\langle a| + \xi_2|b\rangle\langle b| + i\frac{\chi}{2}\left(|a\rangle\langle c| - |c\rangle\langle a|\right) + ig_1\Big(|a\rangle\langle b|\hat{a}_1 - \hat{a}_1^\dagger|b\rangle\langle a|\Big)\\ &+ ig_2\Big(|b\rangle\langle c|\hat{a}_2 - \hat{a}_2^\dagger|c\rangle\langle b|\Big),\end{aligned} \tag{3.15}$$

$$\hat{H}_I^{fm} = \sum_{k=1}^{2}\Big[\delta\omega_k\hat{a}_k^\dagger\hat{a}_k + i\big(\epsilon_k\hat{a}_k^\dagger e^{i\delta\omega_k t} - \epsilon_k^*\hat{a}_k e^{-i\delta\omega_k t}\big) + \omega_{m_k}\hat{b}_k^\dagger\hat{b}_k + G_{0_k}\hat{a}_k^\dagger\hat{a}_k\big(\hat{b}_k^\dagger + \hat{b}_k\big)\Big], \tag{3.16}$$

where, $\delta_j = \Omega_j - \omega_{L_j}$, $\delta_{0_j} = \omega_j - \omega_{L_j}$, and the assumed two-photon resonance condition $\omega_p = \Omega_1 + \Omega_2$. In Eq. (3.15), we represent all the terms that involve the atomic operators by $\hat{H}_I^{af}$ that will be used to derive the master equation for the laser system, and the rest of the terms by $\hat{H}_I^{fm}$. As a result, it will be preferable to obtain the master equation for the cavity modes only by tracing out the atomic states.

3.2.2 Master equation

The master equation corresponding to the Hamiltonian in (3.15) can be obtained by applying the standard approach introduced to study a two-mode three-level laser Tesfa [2021]; Kassahun [2016]. Also, the baths that the mechanical oscillators coupled with are considered to be Markovian with a high-Q factor Aspelmeyer et al. [2014]; Agarwal [2012]. With these considerations, the master equation for the cavity modes coupled to the squeezed vacuum reservoir and the two mechanical oscillator modes coupled to their respective thermal environments can be determined as follows.

3.2.2.1 Master Equation for the two - mode laser

Considering that the three-level atoms injected into the cavity are initially in the state $|\psi_A(0)\rangle$ which is a coherent superposition of the upper and the lower atomic energy levels

$$|\psi_A(0)\rangle = C_a(0)|a\rangle + C_c(0)|c\rangle, \tag{3.17}$$

where $C_a(0) = \langle a|\psi_A(0)\rangle$ and $C_c(0) = \langle c|\psi_A(0)\rangle$ are probability amplitudes for the atom to be initially in the upper and lower levels, respectively.

The corresponding initial density operator of the atom can be written as;

$$\hat{\rho}_A(0) = \rho_{aa}^{(0)}|a\rangle\langle a| + \rho_{ac}^{(0)}|a\rangle\langle c| + \rho_{ca}^{(0)}|c\rangle\langle a| + \rho_{cc}^{(0)}|c\rangle\langle c|, \tag{3.18}$$

where $\rho_{aa}^{(0)} = |C_a(0)|^2,\ \ \rho_{cc}^{(0)} = |C_c(0)|^2$ are respectively the probabilities for the atom to be initially in the upper and the lower levels, and $\rho_{ac}^{(0)} = C_a(0)C_c^*(0)$ with its conjugate represents the two-photon atomic coherence at the initial time. We also note that $|\rho_{ac}^{(0)}|^2 = \rho_{aa}^{(0)}\rho_{cc}^{(0)}$. It proves to be convenient to introduce a parameter ι that describes the initial preparation of a three-level atom as

$$\rho_{aa}^{(0)} = \frac{1-\iota}{2}, \tag{3.19}$$

where ι represents the difference between the probabilities of the atom to be at the lower and upper energy levels.

Employing the fact that

$$\rho_{aa}^{(0)} + \rho_{cc}^{(0)} = 1, \tag{3.20}$$

together with the probabilities for the atom to be initially in the upper and the lower levels, one can easily obtain

$$\rho_{cc}^{(0)} = \frac{1+\iota}{2}, \tag{3.21}$$

and

$$|\rho_{ac}^{(0)}| = \frac{1}{2}\sqrt{1-\iota^2}. \tag{3.22}$$

Now, upon setting $\rho_{ac}^{(0)} = |\rho_{ac}^{(0)}|e^{i\theta}$ and considering Eqs. (3.19) - (3.22), Eq. (3.18) can be put in the form

$$\hat{\rho}_A(0) = (\frac{1-\iota}{2})|a\rangle\langle a| + \frac{1}{2}\sqrt{1-\iota^2}e^{i\theta}|a\rangle\langle c| + \frac{1}{2}\sqrt{1-\iota^2}e^{-i\theta}|c\rangle\langle a| + (\frac{1+\iota}{2})|c\rangle\langle c|. \tag{3.23}$$

Considering the case in which the pumped three-level atoms in a cascade configuration and initially prepared in a coherent superposition of the top and bottom levels are injected into a cavity at constant rate r_a and removed after sometime τ, which is long enough for the atoms to spontaneously decay to levels other than the middle or the bottom level, we derive the master equation for the cavity fields using the Hamiltonian in Eq. (3.15) and employing the procedure outlined in Ref. Scully.

Suppose that $\hat{\rho}_{AR}(t, t_j)$ is the density operator for single atom injected into the cavity plus the cavity mode at time t_j, in which $(t-\tau) \leq t_j \leq t$. The density operator for an ensemble of atoms in the cavity plus the two-mode cavity field at time t can then be written as

$$\hat{\rho}_{AR}(t) = r_a \sum_j \hat{\rho}_{AR}(t, t_j)\Delta t_j, \tag{3.24}$$

where $r_a \Delta t_j$ represents the number of atoms injected into cavity in a small time interval Δt_j. Assuming that the atoms are continuously injected into the cavity and taking the limit that $\Delta t_j \to 0$, the summation over j can be converted into integration with respect to t':

$$\hat{\rho}_{AR}(t) = r_a \int_{t-\tau}^{t} \hat{\rho}_{AR}(t, t')dt^{'}. \tag{3.25}$$

Differentiating Eq. (3.25) with respect to t and taking into account the Leibnitz' rule

$$\frac{d}{dx}\int_{u(x)}^{v(x)} f(x,x')dx' = f(x,v)\frac{dv(x)}{dx} - f(x,u)\frac{du(x)}{dx} + \int_{u(x)}^{v(x)} \frac{\partial}{\partial x} f(x,x')dx', \tag{3.26}$$

we obtain

$$\frac{d}{dt}\hat{\rho}_{AR}(t) = r_a[\hat{\rho}_{AR}(t,t) - \hat{\rho}_{AR}(t,t-\tau)] + r_a\int_{t-\tau}^{t} \frac{\partial}{\partial t}\hat{\rho}_{AR}(t,t')dt'. \tag{3.27}$$

We remark that $\hat{\rho}_{AR}(t,t)$ is the density operator for an atom plus the cavity modes at a time when the atom is injected into the cavity, while $\hat{\rho}_{AR}(t,t-\tau)$ represents the density operator for an atom when the atom is removed from the cavity. Assuming that atomic and radiation variables are uncorrelated at the instant the atom is injected into the cavity, the density operator for each atom-field pair can be written as

$$\hat{\rho}_{AR}(t,t) = \hat{\rho}_A(0)\hat{\rho}(t), \tag{3.28}$$

with

$$\hat{\rho}_A(0) = \hat{\rho}_A(t), \tag{3.29}$$

where $\hat{\rho}(t)$ is density operator for the cavity modes alone and $\hat{\rho}_A(0)$ is the initial density operator for each atom.

We also assume that the states of atomic and cavity modes are uncorrelated just after the atom is removed from the cavity, which leads us to write

$$\hat{\rho}_{AR}(t,t-\tau) = \hat{\rho}_A(t-\tau)\hat{\rho}(t), \tag{3.30}$$

where $\hat{\rho}_A(t-\tau)$ is the density operator at time t for an atom injected at $t-\tau$.
In view of Eqs. (3.28) and (3.30), Eq. (3.27) can also be written as

$$\frac{d}{dt}\hat{\rho}_{AR}(t) = r_a\left[\hat{\rho}_A(0) - \hat{\rho}_A(t-\tau)\right]\hat{\rho}(t) + r_a\int_{t-\tau}^{t} \frac{\partial}{\partial t}\hat{\rho}_{AR}(t,t')dt'. \tag{3.31}$$

Besides, the density operator $\hat{\rho}_{AR}(t,t')$ evolves in time according to

$$\frac{\partial}{\partial t}\hat{\rho}_{AR}(t,t') = -i[\hat{H}_I^{af}, \hat{\rho}_{AR}(t,t')]. \tag{3.32}$$

With the aid of Eqs. (3.25) and (3.32), Eq. (3.31) takes the form

$$\frac{d}{dt}\hat{\rho}_{AR}(t) = r_a\left[\hat{\rho}_A(0) - \hat{\rho}_A(t-\tau)\right]\hat{\rho}(t) - i[\hat{H}_I^{af}, \hat{\rho}_{AR}(t)]. \tag{3.33}$$

Tracing over the atomic variables and using the fact that

$$Tr_A(\hat{\rho}_A(0)) = Tr_A(\hat{\rho}_A(t-\tau)) = 1, \tag{3.34}$$

Eq. (3.33) takes the form

$$\frac{d}{dt}\hat{\rho}(t) = -\, iTr_A[\hat{H}_I^{af}, \hat{\rho}_{AR}(t)]. \tag{3.35}$$

Employing Eqs. (3.15) and (3.35), and performing trace operation, the time evolution of the reduced density operator for radiation modes in atom-field interaction is found to be

$$\frac{d}{dt}\hat{\rho}(t) = g_1\big(\hat{a}_1\hat{\rho}_{ba} - \hat{\rho}_{ba}\hat{a}_1 - \hat{a}_1^\dagger\hat{\rho}_{ab} + \hat{\rho}_{ab}\hat{a}_1^\dagger\big) + g_2\big(\hat{a}_2\hat{\rho}_{cb} - \hat{\rho}_{cb}\hat{a}_2 - \hat{a}_2^\dagger\hat{\rho}_{bc} + \hat{\rho}_{bc}\hat{a}_2^\dagger\big), \tag{3.36}$$

in which the matrix element $\hat{\rho}_{mn}$ is defined by

$$\hat{\rho}_{mn} = \langle m|\hat{\rho}_{AB}|n\rangle, \tag{3.37}$$

with m, n = a, b, c.

The next step in the derivation of master equation is to obtain the conditioned density operators, $\hat{\rho}_{ab} = \langle a|\hat{\rho}_{AR}|b\rangle$ and $\hat{\rho}_{bc} = \langle b|\hat{\rho}_{AR}|c\rangle$, and their complex conjugates that appear in Eq. (3.36). To this end, we return to Eq. (3.33) and solve for these elements.

Now multiplying Eq. (3.33) on the left by $\langle m|$ and on the right by $|n\rangle$, we see that

$$\frac{d}{dt}\hat{\rho}_{mn} = \left[r_a\langle m|\hat{\rho}_A(0)|n\rangle - r_a\langle m|\hat{\rho}_A(t-\tau)|n\rangle\right]\hat{\rho}(t) - i[\langle m|\hat{H}_I^{af}\hat{\rho}_{AR}(t)|n\rangle] + i[\langle m|\hat{\rho}_{AR}(t)\hat{H}_I^{af}|n\rangle] - \gamma_{mn}\hat{\rho}_{mn}. \tag{3.38}$$

Assuming that the atom decays to energy levels other than the three lasing levels when it leaves the cavity, i.e.

$$\langle m|\hat{\rho}_A(t-\tau)|n\rangle = 0, \tag{3.39}$$

and employing Eq. (3.37) into (3.33), we obtain

$$\frac{d}{dt}\hat{\rho}_{mn}(t) = r_a\hat{\rho}_{mn}^{(0)}\hat{\rho}(t) - i[\langle m|\hat{H}_I^{af}\hat{\rho}_{AR}(t)|n\rangle] + i[\langle m|\hat{\rho}_{AR}(t)\hat{H}_I^{af}|n\rangle] - \gamma_{mn}\hat{\rho}_{mn}, \tag{3.40}$$

We included the last term to account for the spontaneous emission and dephasing processes. The $\gamma_m \equiv \gamma_{mm}$ are the atomic spontaneous emission rates, and $\gamma_{mn}(m \neq n)$ are the dephasing rates.

With the aid of Eq. (3.40) and taking into account of Eqs. (3.15) and (3.23) one readily obtains

$$\frac{d}{dt}\hat{\rho}_{ab} = -\left(\gamma_{ab} + i\xi_1\right)\hat{\rho}_{ab} - g_1(\hat{\rho}_{aa}\hat{a}_1 - \hat{a}_1\hat{\rho}_{bb}) + g_2\hat{\rho}_{ac}\hat{a}_2^\dagger + \frac{\chi}{2}\hat{\rho}_{cb}, \tag{3.41}$$

$$\frac{d}{dt}\hat{\rho}_{bc} = -\left(\gamma_{bc} + i\xi_2\right)\hat{\rho}_{bc} - g_2(\hat{\rho}_{bb}\hat{a}_2 - \hat{a}_2\hat{\rho}_{cc}) - g_1\hat{a}_1^\dagger\hat{\rho}_{ac} - \frac{\chi}{2}\hat{\rho}_{ba}, \tag{3.42}$$

$$\frac{d}{dt}\hat{\rho}_{aa} = \frac{r_a}{2}(1-\iota)\hat{\rho}(t) + g_1(\hat{a}_1\hat{\rho}_{ba} + \hat{\rho}_{ab}\hat{a}_1^\dagger) + \frac{\chi}{2}(\hat{\rho}_{ca} + \hat{\rho}_{ac}) - \gamma_a\hat{\rho}_{aa}, \tag{3.43}$$

$$\frac{d}{dt}\hat{\rho}_{cc} = \frac{r_a}{2}(1+\iota)\hat{\rho}(t) - g_2(\hat{a}_2^\dagger\hat{\rho}_{bc} + \hat{\rho}_{cb}\hat{a}_2) - \frac{\chi}{2}(\hat{\rho}_{ca} + \hat{\rho}_{ac}) - \gamma_c\hat{\rho}_{cc}, \tag{3.44}$$

$$\frac{d}{dt}\hat{\rho}_{bb} = -g_1(\hat{a}_1^\dagger\hat{\rho}_{ab} + \hat{\rho}_{ba}\hat{a}_1) + g_2(\hat{a}_2\hat{\rho}_{cb} + \hat{\rho}_{bc}\hat{a}_2^\dagger) - \gamma_b\hat{\rho}_{bb}, \tag{3.45}$$

$$\frac{d}{dt}\hat{\rho}_{ac} = \frac{r_a}{2}\sqrt{1-\iota^2}e^{i\theta}\hat{\rho}(t) - \left(\gamma_{ac} + i(\xi_1+\xi_2)\right)\hat{\rho}_{ac} + g_1\hat{a}_1\hat{\rho}_{bc} - g_2\hat{\rho}_{ab}\hat{a}_2 + \frac{\chi}{2}\left(\hat{\rho}_{cc} - \hat{\rho}_{aa}\right), \tag{3.46}$$

Confining ourselves to linear analysis which amounts to keeping terms only up to the second order in the coupling strength, g_j, in the master equation that can be achieved by dropping the $g_j, (j = 1, 2)$ terms in Eqs. (3.43) - (3.46). It then follows that

$$\frac{d}{dt}\hat{\rho}_{aa} = \frac{r_a}{2}(1-\iota)\hat{\rho}(t) + \frac{\chi}{2}(\hat{\rho}_{ca} + \hat{\rho}_{ac}) - \gamma_a\hat{\rho}_{aa}, \tag{3.47}$$

$$\frac{d}{dt}\hat{\rho}_{cc} = \frac{r_a}{2}(1+\iota)\hat{\rho}(t) - \frac{\chi}{2}(\hat{\rho}_{ca} + \hat{\rho}_{ac}) - \gamma_c\hat{\rho}_{cc}, \tag{3.48}$$

$$\frac{d}{dt}\hat{\rho}_{bb} = -\gamma_b\hat{\rho}_{bb}, \tag{3.49}$$

$$\frac{d}{dt}\hat{\rho}_{ac} = \frac{r_a}{2}\sqrt{1-\iota^2}e^{i\theta}\hat{\rho}(t) - \left(\gamma_{ac} + i(\xi_1 + \xi_2)\right)\hat{\rho}_{ac} + \frac{\chi}{2}(\hat{\rho}_{cc} - \hat{\rho}_{aa}), \tag{3.50}$$

where $\gamma_j (j = a, b, c)$ are the jth atomic level spontaneous decay rates, γ_{ac} is the two-photon dephasing rate, and γ_{ab} and γ_{bc} are the dephasing rates for single-photon "coherences" for $\hat{\rho}_{ab}$ and $\hat{\rho}_{bc}$, respectively.

We next apply the good-cavity limit approximation, where the cavity damping rates κ_j are much smaller than the spontaneous emission rates γ_j, $\kappa_j \ll \gamma_j$. We also assume that $\kappa_j < r_a$. In this limit, the cavity modes vary more slowly than the atomic states, and thus the atomic states reach steady state in a short time. The time derivatives of such states can be set to zero while keeping the cavity - mode states time dependent, which is frequently called the large time adiabatic approximation scheme.

Setting the time derivatives in Eqs. (3.47) - (3.51) approximately to zero, we obtain

$$\hat{\rho}_{aa} = \frac{r_a(1-\iota)}{2\gamma_a}\hat{\rho} + \frac{\chi}{2\gamma_a}(\hat{\rho}_{ca} + \hat{\rho}_{ac}), \tag{3.51}$$

$$\hat{\rho}_{cc} = \frac{r_a(1+\iota)}{2\gamma_c}\hat{\rho} - \frac{\chi}{2\gamma_c}(\hat{\rho}_{ca} + \hat{\rho}_{ac}), \tag{3.52}$$

$$\hat{\rho}_{ac} = \frac{r_a\sqrt{1-\iota^2}e^{i\theta}}{2\big(\gamma_{ac} + i(\xi_1 + \xi_2)\big)}\hat{\rho} + \frac{\chi}{2\big(\gamma_{ac} + i(\xi_1 + \xi_2)\big)}(\hat{\rho}_{cc} - \hat{\rho}_{aa}), \tag{3.53}$$

$$\hat{\rho}_{bb} = 0. \tag{3.54}$$

With the aid of Eq. (3.53) along with its complex conjugate, we easily find

$$\hat{\rho}_{ca} + \hat{\rho}_{ac} = \frac{r_a\sqrt{1-\iota^2}}{\gamma_{ac}^2 + (\xi_1+\xi_2)^2}\left(\gamma_{ac}\cos\theta + (\xi_1+\xi_2)\sin\theta\right)\hat{\rho} + \frac{\chi\gamma_{ac}}{\gamma_{ac}^2 + (\xi_1+\xi_2)^2}(\hat{\rho}_{cc} - \hat{\rho}_{aa}). \quad (3.55)$$

On account of Eq. (3.55), Eqs. (3.51) and (3.52) can also take the forms

$$\hat{\rho}_{aa} = \frac{r_a\big[(1-\iota)\left(\gamma_{ac}^2 + (\xi_1+\xi_2)^2\right) + \chi\sqrt{1-\iota^2}\left(\gamma_{ac}\cos\theta + (\xi_1+\xi_2)\sin\theta\right)\big]\hat{\rho} + \chi^2\gamma_{ac}\hat{\rho}_{cc}}{\chi^2\gamma_{ac} + 2\gamma_a\left(\gamma_{ac}^2 + (\xi_1+\xi_2)^2\right)}, \quad (3.56)$$

$$\hat{\rho}_{cc} = \frac{r_a\big[(1+\iota)\left(\gamma_{ac}^2 + (\xi_1+\xi_2)^2\right) - \chi\sqrt{1-\iota^2}\left(\gamma_{ac}\cos\theta + (\xi_1+\xi_2)\sin\theta\right)\big]\hat{\rho} + \chi^2\gamma_{ac}\hat{\rho}_{aa}}{\chi^2\gamma_{ac} + 2\gamma_c\left(\gamma_{ac}^2 + (\xi_1+\xi_2)^2\right)}. \quad (3.57)$$

Substitution of (3.56) and (3.57) interchangeably results in

$$\hat{\rho}_{aa} = \frac{r_a\hat{\rho}}{D_2}T_{aa}, \quad (3.58)$$

$$\hat{\rho}_{cc} = \frac{r_a\hat{\rho}}{D_2}T_{cc}, \quad (3.59)$$

where

$$T_{aa} = \frac{1}{2}\left[(1-\iota)\gamma_c D_1 + \chi^2\gamma_{ac} + \chi\gamma_c\sqrt{1-\iota^2}D_3\right], \quad (3.60)$$

$$T_{cc} = \frac{1}{2}\left[(1+\iota)\gamma_a D_1 + \chi^2\gamma_{ac} - \chi\gamma_a\sqrt{1-\iota^2}D_3\right], \quad (3.61)$$

with

$$D_1 = \gamma_{ac}^2 + (\xi_1+\xi_2)^2, \quad (3.62)$$

$$D_2 = \chi^2\gamma_{ac}\frac{(\gamma_a+\gamma_c)}{2} + \gamma_a\gamma_c\left(\gamma_{ac}^2 + (\xi_1+\xi_2)^2\right), \quad (3.63)$$

$$D_3 = \gamma_{ac}\cos\theta + (\xi_1+\xi_2)\sin\theta. \quad (3.64)$$

Employing Eqs. (3.58) - (3.61) into Eq. (3.53) yields

$$\hat{\rho}_{ac} = \frac{r_a \hat{\rho}}{D_1} T_{ac}, \tag{3.65}$$

where

$$T_{ac} = \frac{1}{2}\left[\sqrt{1-\iota^2} D_3 + \frac{\chi\gamma_{ac}}{D_2}\big(T_{cc} - T_{aa}\big)\right] + \frac{i}{2}\left[\sqrt{1-\iota^2} D_4 - \frac{\chi(\xi_1+\xi_2)}{D_2}\big(T_{cc} - T_{aa}\big)\right], \tag{3.66}$$

$$D_4 = \gamma_{ac}\sin\theta - (\xi_1 + \xi_2)\cos\theta. \tag{3.67}$$

Making use of Eqs. (3.41), (3.42), (3.54) and applying the large time approximation scheme, we see that

$$\hat{\rho}_{ab} = -\frac{g_1}{\gamma_{ab} + i\xi_1}\hat{\rho}_{aa}\hat{a}_1 + \frac{g_2}{\gamma_{ab} + i\xi_1}\hat{\rho}_{ac}\hat{a}_2^\dagger + \frac{\chi}{\gamma_{ab} + i\xi_1}\hat{\rho}_{cb}, \tag{3.68}$$

$$\hat{\rho}_{bc} = \frac{g_2}{\gamma_{bc} + i\xi_2}\hat{a}_2\hat{\rho}_{cc} - \frac{g_1}{\gamma_{bc} + i\xi_2}\hat{a}_1^\dagger\hat{\rho}_{ac} - \frac{\chi}{\gamma_{bc} + i\xi_2}\hat{\rho}_{ba}. \tag{3.69}$$

Substitution of the complex conjugate of one into the other of (3.68) and (3.69), and on account of the resulting equations along with Eqs. (3.58), (3.59), (3.65) and its complex conjugate, we obtain

$$\hat{\rho}_{ab} = -\frac{g_1 r_a}{\mathcal{F}}\left((\gamma_{bc} - i\xi_2)\frac{T_{aa}}{D_2} - \frac{\chi}{2}\frac{T_{ac}^*}{D_1}\right)\hat{\rho}\hat{a}_1 + \frac{g_2 r_a}{\mathcal{F}}\left((\gamma_{bc} - i\xi_2)\frac{T_{ac}}{D_1} + \frac{\chi}{2}\frac{T_{cc}}{D_2}\right)\hat{\rho}\hat{a}_2^\dagger, \tag{3.70}$$

$$\hat{\rho}_{bc} = \frac{g_2 r_a}{\mathcal{F}}\left((\gamma_{ab} - i\xi_1)\frac{T_{cc}}{D_2} - \frac{\chi}{2}\frac{T_{ac}^*}{D_1}\right)\hat{a}_2\hat{\rho} - \frac{g_1 r_a}{\mathcal{F}}\left((\gamma_{ab} - i\xi_1)\frac{T_{ac}}{D_1} - \frac{\chi}{2}\frac{T_{aa}}{D_2}\right)\hat{a}_1^\dagger\hat{\rho}, \tag{3.71}$$

in which

$$\mathcal{F} = \frac{\chi^4}{4} + (\gamma_{ab} + i\xi_1)(\gamma_{bc} - i\xi_2). \tag{3.72}$$

Multiplying Eqs. (3.70) and (3.71) by g_1 and g_2 respectively, we obtain

$$g_1\hat{\rho}_{ab} = \alpha_{11}\hat{\rho}\hat{a}_1 + \alpha_{12}\hat{\rho}\hat{a}_2^\dagger, \tag{3.73}$$

$$g_2\hat{\rho}_{bc} = \alpha_{22}\hat{a}_2\hat{\rho} + \alpha_{21}\hat{a}_1^\dagger\hat{\rho}, \tag{3.74}$$

where

$$\alpha_{11} = -\frac{g_1^2 r_a}{\mathcal{F}}\left((\gamma_{bc} - i\xi_2)\frac{T_{aa}}{D_2} - \frac{\chi}{2}\frac{T_{ac}^*}{D_1}\right), \tag{3.75}$$

$$\alpha_{12} = \frac{g_1 g_2 r_a}{\mathcal{F}}\left((\gamma_{bc} - i\xi_2)\frac{T_{ac}}{D_1} + \frac{\chi}{2}\frac{T_{cc}}{D_2}\right), \tag{3.76}$$

$$\alpha_{22} = \frac{g_2^2 r_a}{\mathcal{F}}\left((\gamma_{ab} - i\xi_1)\frac{T_{cc}}{D_2} - \frac{\chi}{2}\frac{T_{ac}^*}{D_1}\right), \tag{3.77}$$

$$\alpha_{21} = -\frac{g_1 g_2 r_a}{\mathcal{F}}\left((\gamma_{ab} - i\xi_1)\frac{T_{ac}}{D_1} - \frac{\chi}{2}\frac{T_{aa}}{D_2}\right). \tag{3.78}$$

On account of Eqs. (3.73) and (3.74) along with their complex conjugates, the equation of evolution of the density operator for the cavity interacted with the atom, Eq. (3.36) turns out to be

$$\begin{aligned}\frac{d}{dt}\hat{\rho}(t) =& \alpha_{11}(\hat{\rho}\hat{a}_1\hat{a}_1^\dagger - \hat{a}_1^\dagger\hat{\rho}\hat{a}_1) + \alpha_{11}^*(\hat{a}_1\hat{a}_1^\dagger\hat{\rho} - \hat{a}_1^\dagger\hat{\rho}\hat{a}_1)\\ &+ \alpha_{22}(\hat{a}_2\hat{\rho}\hat{a}_2^\dagger - \hat{a}_2^\dagger\hat{a}_2\hat{\rho}) + \alpha_{22}^*(\hat{a}_2\hat{\rho}\hat{a}_2^\dagger - \hat{\rho}\hat{a}_2^\dagger\hat{a}_2)\\ &+ \alpha_{12}(\hat{\rho}\hat{a}_2^\dagger\hat{a}_1^\dagger - \hat{a}_1^\dagger\hat{\rho}\hat{a}_2^\dagger) + \alpha_{12}^*(\hat{a}_1\hat{a}_2\hat{\rho} - \hat{a}_2\hat{\rho}\hat{a}_1)\\ &+ \alpha_{21}(\hat{a}_1^\dagger\hat{\rho}\hat{a}_2^\dagger - \hat{a}_2^\dagger\hat{a}_1^\dagger\hat{\rho}) + \alpha_{21}^*(\hat{a}_2\hat{\rho}\hat{a}_1 - \hat{\rho}\hat{a}_1\hat{a}_2).\end{aligned} \tag{3.79}$$

Note that the terms proportional to $\mathrm{Re}(\alpha_{11})$ give rise to gain for the first cavity mode, while $\mathrm{Im}(\alpha_{11})$ yields a frequency shift; whereas the terms proportional to $\mathrm{Re}(\alpha_{22})$ result in loss of the second cavity mode but $\mathrm{Im}(\alpha_{22})$ produces a frequency shift. Also, the terms proportional to α_{12} and α_{21} represent the correlation between the two cavity modes.

3.2.2.2 Interaction between cavity modes and squeezed vacuum reservoir

To include the effect of two-mode squeezed vacuum reservoir coupled to two-mode cavity radiation via the lossy and stationary port mirror M_3, on the master equation, the Hamiltonian owing to this interaction can be described by

$$\hat{H} = \hat{H}_S + \hat{H}_{SR}, \tag{3.80}$$

where $\hat{H}_S$ is the Hamiltonian of the system describing the interaction in the cavity and $\hat{H}_{SR}$ represents the Hamiltonian that describes the interaction between the cavity and the reservoir modes.

Let $\hat{\rho}_{SR}$ be the density operator for the system plus the reservoir in the interaction picture . We can then write the time evolution of this operator as

$$\frac{d\hat{\rho}_{SR}(t)}{dt} = -i[\hat{H}_S(t) + \hat{H}_{SR}(t), \hat{\rho}_{SR(t)]}.\text{(3.81)}$$

So as to obtain the time evolution of the system alone, which we are interested in, we trace $\hat{\rho}_{SR}(t)$ over the reservoir variables, hence the density operator for the system resulting from the coupling becomes $\hat{\rho}(t) = Tr_R(\hat{\rho}_{SR}(t))$. In view of this, Eq. (3.81) takes the form

$$\frac{d\hat{\rho}(t)}{dt} = -i[\hat{H}_S(t), \hat{\rho}(t)] - iTr_R[\hat{H}_{SR}(t), \hat{\rho}_{SR}(t)]. \tag{3.82}$$

The formal solution to Eq. (3.81) can be written as

$$\hat{\rho}_{SR}(t) = \hat{\rho}_{SR}(0) - i\int_0^t \left[\hat{H}_S(t') + \hat{H}_{SR}(t'), \hat{\rho}_{SR}(t')\right] dt'. \tag{3.83}$$

To proceed further, we assume that there is a weak interaction between the cavity mode and reservoir (as the reservoir which is so large compared to the system is not substantially affected by the interaction). So that applying the Born approximation, we can write the valid relation

$$\hat{\rho}_{SR}(t') = \hat{\rho}(t')\hat{R}, \tag{3.84}$$

where $\hat{R}$ is the density operator for the reservoir assumed to be constant in time. With the aid of Eq. (3.84), we rewrite Eq. (3.83) as

$$\hat{\rho}_{SR}(t) = \hat{\rho}(0)\hat{R} - i\int_0^t \left[\hat{H}_S(t') + \hat{H}_{SR}(t'), \hat{\rho}(t')\hat{R}\right] dt'. \tag{3.85}$$

Substituting (3.85) into (3.82), we obtain the time evolution of the reduced density operator for the cavity radiation coupled to a reservoir as

$$\begin{aligned}\frac{d\hat{\rho}(t)}{dt} =& -i\left[\hat{H}_S(t),\hat{\rho}(t)\right] - i\left[\langle\hat{H}_{SR}(t)\rangle_R,\hat{\rho}(0)\right]\\ &-\int_0^t\left[\langle\hat{H}_{SR}(t)\rangle_R,[\hat{H}_S(t'),\hat{\rho}(t')]\right]dt'\\ &-\int_0^t Tr_R\left[\hat{H}_{SR}(t),[\hat{H}_{SR}(t'),\hat{\rho}(t')\hat{R}]\right]dt',\end{aligned} \tag{3.86}$$

Consider a two-mode squeezed vacuum reservoir interacting with two cavity modes; this interaction can be described in the interaction picture by the Hamiltonian

$$\begin{aligned}\hat{H}_{SR}(t) =& i\sum_l \lambda_l(\hat{a}_1^\dagger\hat{C}_l e^{i(\omega_1-\omega_l)t} - \hat{a}_1\hat{C}_l^\dagger e^{-i(\omega_1-\omega_l)t})\\ &+ i\sum_n \lambda_n(\hat{a}_2^\dagger\hat{D}_n e^{i(\omega_2-\omega_n)t} - \hat{a}_2\hat{D}_n^\dagger e^{-i(\omega_2-\omega_n)t}),\end{aligned} \tag{3.87}$$

in which $\hat{a}_1$ and $\hat{a}_2$ are annihilation operators for the cavity modes with frequencies ω_1 and ω_2, while $\hat{C}_l$ and $\hat{D}_n$ are annihilation operators for the reservoir sub-modes having frequencies ω_l and ω_n, and λ_l and λ_n are the coupling constants between the cavity modes and the reservoir modes.

One can also see that the two-mode squeezed vacuum reservoir operators satisfy the following properties:

$$\langle\hat{C}_l\rangle_R = \langle\hat{D}_n\rangle_R = 0, \tag{3.88}$$

$$\langle\hat{C}_l^\dagger\hat{C}_n\rangle_R = \langle\hat{D}_l^\dagger\hat{D}_n\rangle_R = N\delta_{ln}, \tag{3.89}$$

$$\langle\hat{C}_l\hat{C}_n^\dagger\rangle_R = \langle\hat{D}_l\hat{D}_n^\dagger\rangle_R = (N+1)\delta_{ln}, \tag{3.90}$$

$$\langle\hat{C}_l\hat{C}_n\rangle_R = \langle\hat{C}_l^\dagger\hat{C}_n^\dagger\rangle_R = 0, \tag{3.91}$$

$$\langle\hat{D}_l\hat{D}_n\rangle_R = \langle\hat{D}_l^\dagger\hat{D}_n^\dagger\rangle_R = 0, \tag{3.92}$$

$$\langle\hat{C}_l\hat{D}_n\rangle_R = M\delta_{l,2no-n:}\ \ \langle\hat{C}_l^\dagger\hat{D}_n^\dagger\rangle_R = M^*\delta_{l,2no-n}, \tag{3.93}$$

$$\langle\hat{C}_l\hat{D}_n^\dagger\rangle_R = \langle\hat{C}_l^\dagger\hat{D}_n\rangle_R = 0, \tag{3.94}$$

where N and M characterize the two-mode squeezed vacuum, such that the correlation between the reservoir modes is described by $|M|^2 \leq N(N+1)$, and N represents the mean photon number of each squeezed vacuum reservoir. The equality $|M|^2 = N(N+1)$ holds for minimum uncertainty squeezed states, which is the case considered in this dissertation.

On account of Eq. (3.88), we easily see that $\langle \hat{H}_{SR(t)\rangle_{R=0}}$, and therefore

$$[\langle \hat{H}_{SR}(t)\rangle_R, \hat{\rho}(0)] = [\langle \hat{H}_{SR}(t)\rangle_R, [\hat{H}(t'), \hat{\rho}(t')]] = 0.$$

In view of these results, Eq. (3.86) reduces to

$$\begin{aligned}\frac{d\hat{\rho}(t)}{dt} =& -i[\hat{H}_S(t), \hat{\rho}(t)] - \int_0^t Tr_R\big(\hat{H}_{SR}(t)\hat{H}_{SR}(t')\hat{R}\big)\hat{\rho}(t')dt' - \int_0^t \hat{\rho}(t')Tr_R\big(\hat{R}\hat{H}_{SR}(t')\hat{H}_{SR}(t)\big)dt' \\ &+ \int_0^t Tr_R\big(\hat{H}_{SR}(t)\hat{\rho}(t')\hat{R}\hat{H}_{SR}(t')\big)dt' + \int_0^t Tr_R\big(\hat{H}_{SR}(t)\hat{R}\hat{\rho}(t')\hat{H}_{SR}(t')\big)dt'. \qquad (3.95)\end{aligned}$$

By employing the Hamiltonian in Eq. (3.87), and properties in Eqs. (3.89) - (3.94), we readily obtain

$$\begin{aligned}Tr_R\left(\hat{R}\hat{H}_{SR}(t)\hat{H}_{SR}(t')\right) =& \big[p_1\hat{a}_1\hat{a}_1^\dagger + p_2\hat{a}_1^\dagger\hat{a}_1 + p_3\hat{a}_2\hat{a}_2^\dagger + p_4\hat{a}_2^\dagger\hat{a}_2 \\ &+ p_5\hat{a}_1^\dagger\hat{a}_2^\dagger + p_6\hat{a}_1\hat{a}_2 + p_7\hat{a}_2^\dagger\hat{a}_1^\dagger + p_8\hat{a}_2\hat{a}_1\big], \qquad (3.96)\end{aligned}$$

where

$$p_1 = N\sum_l \lambda_l^2 e^{i(\omega_1-\omega_l)(t-t')}, \qquad (3.97)$$

$$p_2 = (N+1)\sum_l \lambda_l^2 e^{-i(\omega_1-\omega_l)(t-t')}, \qquad (3.98)$$

$$p_3 = N\sum_n \lambda_n^2 e^{i(\omega_2-\omega_n)(t-t')}, \qquad (3.99)$$

$$p_4 = (N+1)\sum_n \lambda_n^2 e^{-i(\omega_2-\omega_n)(t-t')}, \qquad (3.100)$$

$$p_5 = -M\sum_n \lambda_n\lambda_{2n_a-n} e^{i(\omega_1-\omega_l)t'+i(\omega_2-\omega_{2n_a-n})t}, \qquad (3.101)$$

$$p_6 = -M^* \sum_l \lambda_l \lambda_{2l_a - l} e^{-i(\omega_1 - \omega_l)t' - i(\omega_2 - \omega_{2l_a - l})t}, \tag{3.102}$$

$$p_7 = -M \sum_n \lambda_n \lambda_{2n_a - n} e^{i(\omega_2 - \omega_n)t' + i(\omega_1 - \omega_{2n_a - n})t}, \tag{3.103}$$

$$p_8 = -M^* \sum_l \lambda_l \lambda_{2l_a - l} e^{-i(\omega_2 - \omega_n)t' - i(\omega_1 - \omega_{2l_a - l})t}. \tag{3.104}$$

Assuming that the frequencies of the reservoir modes (ω_l's) are closely spaced, the summation over l can be changed to integration over frequency (ω). In view of this fact, one can write

$$\sum_l \lambda_l^2 e^{\pm i(\omega_1 - \omega_l)(t-t')} = \int_0^\infty g(\omega)\lambda^2(\omega) e^{\pm i(\omega_1 - \omega)(t-t')} d\omega, \tag{3.105}$$

where $g(\omega)$ is the density of the modes for which the frequency lies between ω and $\omega + d\omega$. On the other hand, assuming that ω varies very little around ω_1, we can replace $g(\omega)$ by $g(\omega_1)$ and $\lambda^2(\omega)$ by $\lambda^2(\omega_1)$, and extend the lower limit of the integration to $-\infty$. Consequently, we have

$$\sum_l \lambda_l^2 e^{\pm i(\omega_1 - \omega_l)(t-t')} = g(\omega_1)\lambda^2(\omega_1) \int_{-\infty}^\infty e^{\pm i(\omega_1 - \omega)(t-t')} d\omega. \tag{3.106}$$

Upon setting $\omega' = \omega - \omega_1$, we notice that

$$\sum_l \lambda_l^2 e^{\pm i(\omega_1 - \omega_l)(t-t')} = g(\omega_1)\lambda^2(\omega_1) \int_{-\infty}^\infty e^{\mp i\omega'(t-t')} d\omega'. \tag{3.107}$$

It then follows that,

$$\sum_l \lambda_l^2 e^{\pm i(\omega_1 - \omega_l)(t-t')} = \kappa_1 \delta(t - t'), \tag{3.108}$$

in which $\kappa_1 = 2\pi g(\omega_1)\lambda^2(\omega_1)$ is defined to be the damping constant for cavity mode $\hat{a}_1$ with $g(\omega_1)$ being the density operator for the reservoir modes which is assumed to be at resonance with the cavity mode $\hat{a}_1$. In line with this, one can readily obtain,

$$\sum_n \lambda_n^2 e^{\pm i(\omega_2 - \omega_n)(t-t')} = \kappa_2 \delta(t - t'), \tag{3.109}$$

where $\kappa_2 = 2\pi g(\omega_2)\lambda^2(\omega_2)$ is defined to be the damping constant for cavity mode $\hat{a}_2$ with $g(\omega_2)$ being the density operator for the reservoir modes which is assumed to be at resonance with the cavity mode $\hat{a}_2$.

Following similar procedures, it is possible to obtain

$$\sum_n \lambda_n \lambda_{n_{a_1}+n_{a_2}-n} e^{i(\omega_1-\omega_l)t'+i(\omega_2-\omega_{n_{a_1}+n_{a_2}-n})t} = \sqrt{\kappa_2\kappa_1}\delta(t-t'), \tag{3.110}$$

$$\sum_l \lambda_l \lambda_{l_{a_1}+l_{a_2}-l} e^{-i(\omega_1-\omega_l)t'-i(\omega_2-\omega_{l_{a_1}+l_{a_2}-l})t} = \sqrt{\kappa_1\kappa_2}\delta(t-t'). \tag{3.111}$$

With the aid of Eqs. (3.108) - (3.111), one can put Eqs. (3.97) - (3.104) in the form

$$p_1 = N\kappa_1\delta(t-t'), \tag{3.112}$$

$$p_2 = (N+1)\kappa_1\delta(t-t'), \tag{3.113}$$

$$p_3 = N\kappa_2\delta(t-t'), \tag{3.114}$$

$$p_4 = (N+1)\kappa_2\delta(t-t'), \tag{3.115}$$

$$p_5 = p_7 = -M\sqrt{\kappa_2\kappa_1}\delta(t-t'), \tag{3.116}$$

$$p_6 = p_8 = -M^*\sqrt{\kappa_1\kappa_2}\delta(t-t'). \tag{3.117}$$

By applying Eqs. (3.112) - (3.117), Eq. (3.96) takes the form

$$\begin{aligned} Tr_R\big(\hat{R}\hat{H}_{SR}(t)\hat{H}_{SR}(t')\big) =& \big[\kappa_1 N\hat{a}_1\hat{a}_1^\dagger + \kappa_1(N+1)\hat{a}_1^\dagger\hat{a}_1 + \kappa_2 N\hat{a}_2\hat{a}_2^\dagger + \kappa_2(N+1)\hat{a}_2^\dagger\hat{a}_2 \\ & - \sqrt{\kappa_2\kappa_1}M\big(\hat{a}_1^\dagger\hat{a}_2^\dagger + \hat{a}_2^\dagger\hat{a}_1^\dagger\big)\sqrt{\kappa_1\kappa_2}M^*\big(\hat{a}_1\hat{a}_2 + \hat{a}_2\hat{a}_1\big)\big]\delta(t-t'). \end{aligned} \tag{3.118}$$

Employing the Markov's approximation, $\hat{\rho}(t') = \hat{\rho}(t)$, Gerry and Knight [2005] together with Eq. (3.118), we can express the term on the second line of Eq. (3.95) as

$$\begin{aligned}\int_0^t \hat{\rho}(t')Tr_R\bigg(\hat{R}\hat{H}_{SR}(t')\hat{H}_{SR}(t)\bigg)dt' =&\frac{\kappa_1}{2}N\hat{\rho}\hat{a}_1\hat{a}_1^\dagger + \frac{\kappa_1}{2}(N+1)\hat{\rho}\hat{a}_1^\dagger\hat{a}_1 + \frac{\kappa_2}{2}N\hat{\rho}\hat{a}_2\hat{a}_2^\dagger\\ &+ \frac{\kappa_2}{2}(N+1)\hat{\rho}\hat{a}_2^\dagger\hat{a}_2 - \frac{\sqrt{\kappa_2\kappa_1}}{2}M\big(\hat{\rho}\hat{a}_1^\dagger\hat{a}_2^\dagger + \hat{\rho}\hat{a}_2^\dagger\hat{a}_1^\dagger\big)\\ &- \frac{\sqrt{\kappa_1\kappa_2}}{2}M^*\big(\hat{\rho}\hat{a}_1\hat{a}_2 + \hat{\rho}\hat{a}_2\hat{a}_1\big).\end{aligned} \tag{3.119}$$

We also see that

$$\begin{aligned}\int_0^t Tr_R\left(\hat{H}_{SR}(t)\hat{H}_{SR}(t')\hat{R}\right)\hat{\rho}(t')dt' =&\frac{\kappa_1}{2}N\hat{a}_1\hat{a}_1^\dagger\hat{\rho} + \frac{\kappa_1}{2}(N+1)\hat{a}_1^\dagger\hat{a}_1\hat{\rho} + \frac{\kappa_2}{2}N\hat{a}_2\hat{a}_2^\dagger\hat{\rho}\\ &+ \frac{\kappa_2}{2}(N+1)\hat{a}_2^\dagger\hat{a}_2\hat{\rho} - \frac{\sqrt{\kappa_2\kappa_1}}{2}M\big(\hat{a}_1^\dagger\hat{a}_2^\dagger\hat{\rho} + \hat{a}_2^\dagger\hat{a}_1^\dagger\hat{\rho}\big)\\ &- \frac{\sqrt{\kappa_1\kappa_2}}{2}M^*\big(\hat{a}_1\hat{a}_2\hat{\rho} + \hat{a}_2\hat{a}_1\hat{\rho}\big).\end{aligned} \tag{3.120}$$

With the help of the Hamiltonian in Eq. (3.87) and the cyclic property of the trace operation, we readily get

$$\begin{aligned}Tr_R\left(\hat{H}_{SR}(t)\hat{\rho}(t')\hat{R}\hat{H}_{SR}(t)\right) =&p_1\hat{a}_1\hat{\rho}(t')\hat{a}_1^\dagger + p_2\hat{a}_1^\dagger\hat{\rho}(t')\hat{a}_1 + p_3\hat{a}_2\hat{\rho}(t')\hat{a}_2^\dagger + p_4\hat{a}_2^\dagger\hat{\rho}(t')\hat{a}_2\\ &+ p_5\hat{a}_1^\dagger\hat{\rho}(t')\hat{a}_2^\dagger + p_6\hat{a}_1\hat{\rho}(t')\hat{a}_2 + p_7\hat{a}_2^\dagger\hat{\rho}(t')\hat{a}_1^\dagger + p_8\hat{a}_2\hat{\rho}(t')\hat{a}_1.\end{aligned} \tag{3.121}$$

Considering the Markov's approximation and Eqs. (3.112)- (3.117), we find

$$\begin{aligned}\int_0^t Tr_R\left(\hat{H}_{SR}(t)\hat{\rho}(t')\hat{R}\hat{H}_{SR}(t)\right)dt' =&\frac{\kappa_1}{2}\Big[(N+1)\hat{a}_1\hat{\rho}\hat{a}_1^\dagger + N\hat{a}_1^\dagger\hat{\rho}\hat{a}_1\Big] + \frac{\kappa_2}{2}\Big[(N+1)\hat{a}_2\hat{\rho}\hat{a}_2^\dagger + \hat{a}_2^\dagger\hat{\rho}\hat{a}_2\Big]\\ &- \frac{\sqrt{\kappa_1\kappa_2}}{2}\Big[M(\hat{a}_2^\dagger\hat{\rho}\hat{a}_1^\dagger + \hat{a}_1^\dagger\hat{\rho}\hat{a}_2^\dagger) + M^*(\hat{a}_2\hat{\rho}\hat{a}_1 + \hat{a}_1\hat{\rho}\hat{a}_2)\Big].\end{aligned} \tag{3.122}$$

It can also be established in a similar way that

$$\begin{aligned}\int_0^t Tr_R\big(\hat{H}_{SR}(t)\hat{R}\hat{\rho}(t')\hat{H}_{SR}(t')\big)dt' =&\frac{\kappa_1}{2}\Big[(N+1)\hat{a}_1\hat{\rho}\hat{a}_1^\dagger + N\hat{a}_1^\dagger\hat{\rho}\hat{a}_1\Big] + \frac{\kappa_2}{2}\Big[(N+1)\hat{a}_2\hat{\rho}\hat{a}_2^\dagger + \hat{a}_2^\dagger\hat{\rho}\hat{a}_2\Big]\\ &- \frac{\sqrt{\kappa_1\kappa_2}}{2}\Big[M(\hat{a}_2^\dagger\hat{\rho}\hat{a}_1^\dagger + \hat{a}_1^\dagger\hat{\rho}\hat{a}_2^\dagger) + M^*\left(\hat{a}_2\hat{\rho}\hat{a}_1 + \hat{a}_1\hat{\rho}\hat{a}_2\right)\Big].\end{aligned} \tag{3.123}$$

Substitution of Eqs. (3.119), (3.120), (3.122) and (3.123) into Eq. (3.95), results in the master equation as a result of the coupling between the two-modes of a doubly resonant cavity to the two-mode squeezed vacuum reservoir

$$\begin{aligned}\frac{d\hat{\rho}}{dt} =& - i[\hat{H}_S(t), \hat{\rho}(t)] + \frac{k_1(N+1)}{2}\left(2\hat{a}_1\hat{\rho}\hat{a}_1^\dagger - \hat{a}_1^\dagger\hat{a}_1\hat{\rho} - \hat{\rho}\hat{a}_1^\dagger\hat{a}_1\right) + \frac{k_1 N}{2}\left(2\hat{a}_1^\dagger\hat{\rho}\hat{a}_1 - \hat{a}_1\hat{a}_1^\dagger\hat{\rho} - \hat{\rho}\hat{a}_1\hat{a}_1^\dagger\right)\\ &+ \frac{k_2(N+1)}{2}\left(2\hat{a}_2\hat{\rho}\hat{a}_2^\dagger - \hat{a}_2^\dagger\hat{a}_2\hat{\rho} - \hat{\rho}\hat{a}_2^\dagger\hat{a}_2\right) + \frac{k_2 N}{2}\left(2\hat{a}_2^\dagger\hat{\rho}\hat{a}_2 - \hat{a}_2\hat{a}_2^\dagger\hat{\rho} - \hat{\rho}\hat{a}_2\hat{a}_2^\dagger\right)\\ &+ \frac{\sqrt{k_1k_2}}{2}M\left(2\hat{a}_1^\dagger\hat{\rho}\hat{a}_2^\dagger + 2\hat{a}_2^\dagger\hat{\rho}\hat{a}_1^\dagger - \hat{a}_1^\dagger\hat{a}_2^\dagger\hat{\rho} - \hat{a}_2^\dagger\hat{a}_1^\dagger\hat{\rho} - \hat{\rho}\hat{a}_1^\dagger\hat{a}_2^\dagger - \hat{\rho}\hat{a}_2^\dagger\hat{a}_1^\dagger\right)\\ &+ \frac{\sqrt{k_1k_2}}{2}M^*\left(2\hat{a}_1\hat{\rho}\hat{a}_2 + 2\hat{a}_2\hat{\rho}\hat{a}_1 - \hat{a}_1\hat{a}_2\hat{\rho} - \hat{a}_2\hat{a}_1\hat{\rho} - \hat{\rho}\hat{a}_1\hat{a}_2 - \hat{\rho}\hat{a}_2\hat{a}_1\right). \end{aligned} \tag{3.124}$$

3.2.2.3 Master Equation for damped mechanical oscillator

The quantum mechanical description of a mechanical oscillator taken to be part of an optomechanical device cannot be considered as a Brownian particle, but rather as a mesoscopic mechanical system, such as a movable mirror mounted on a vibrating structure Dirac [1927]. With this consideration, we seek to present a quantum description of master equation for two modes of the mechanical oscillators coupled to two separate thermal baths with all the natural physical requirement. Having a unique equilibrium state the structure of the mechanical oscillator is further determined by suitable symmetry requirements and by physical constraints on the behavior of the mean values of position and momentum. Since the focus is on quantum effects, the theoretical models must be fully consistent with quantum mechanics. Actually the correct quantum description of a mesoscopic mechanical oscillator and of the dissipative effects (thermal noises) due to the interaction with vibrational modes is not a trivial task, and there is not a unique accepted model for them Lindblad [1976]; Leggett [1984,?]; Vacchini [2002].

It is noted that the quantum master equation often used for open quantum systems that relies on the Born-Markov approximation is valid for weak coupling. Within the context of the model studied here, the weak coupling condition is equivalent to the situation where the damping rate is much smaller than the (renormalized) oscillation frequency. Therefore, the quantum master equation in the interaction picture is obtained as, wherein the full density matrix $\hat{\rho}_I(t)$ obeys

$$\frac{d\hat{\rho}_I(t)}{dt} = -i[\hat{H}_I(t), \rho_I(t)], \tag{3.125}$$

with $\hat{H}_I = \hat{H}_{SB}(t)$ and $\hat{H}_{SB}$ is given by considering a system oscillator of effective mass m coupled to a bath of oscillators of effective mass M. The total Hamiltonian of a harmonically oscillating mirror can be described as

$$\hat{H} = \hat{H}_S + \hat{H}_B + \hat{H}_{SB}, \tag{3.126}$$

where

$$\hat{H}_S = \frac{\hat{p}^2}{2m} + \frac{m\omega_m^2}{2}\hat{q}^2, \tag{3.127}$$

$$\hat{H}_B = \sum_k \left[\frac{\hat{P}_k^2}{2M} + \frac{M\omega_k^2}{2}\hat{Q}_k^2\right], \tag{3.128}$$

describing the Hamiltonian of quantum harmonically oscillating mirror and the Hamiltonian of a bath of harmonic oscillators to be taken in thermal equilibrium at temperature T. For unity masses ($m = M = 1$) the system-bath coupling is taken to be

$$\hat{H}_{SB} = -q\sum_k \hat{C}_k\hat{Q}_k, \tag{3.129}$$

and the equations of motion are

$$\ddot{\hat{q}} + \omega_m^2\hat{q} = \sum_k \hat{C}_k\hat{Q}_k, \tag{3.130}$$

$$\ddot{\hat{Q}}_k + \omega_k^2\hat{Q}_k = \hat{C}_k\hat{q}(t). \tag{3.131}$$

We will solve the dynamics as an initial condition problem, setting up initial conditions at time $t = 0$. This allows us to understand the transient evolution of correlation functions and the approach to an asymptotic stationary state.

We proceed by solving Eq. (3.131), the equations of motion for the bath variables, and inserting the solution into the equations of motion for the system coordinate, namely

$$\hat{Q}_k(t) = \hat{Q}_k^{(0)}(t) + C_k \int_0^t \frac{sin[\omega_k(t-t')]}{\omega_k} q(t')dt', \tag{3.132}$$

where

$$\hat{Q}_k^{(0)}(t) = \frac{1}{\sqrt{2\omega_k}} \left[\hat{r}_k e^{-i\omega_k t} + \hat{r}_k^\dagger e^{i\omega_k t} \right], \tag{3.133}$$

is the operator solution of the homogeneous equation in terms of independent annihilation ($\hat{r}_k$) and creation ($\hat{r}_k^\dagger$) bath operators. A thermal bath which is assumed to be in thermal equilibrium at temperature T is found to take statistical average over the bath variables as

$$\langle \hat{n} \rangle = \langle \langle \hat{r}_k^\dagger \hat{r}_k \rangle \rangle = (e^{\frac{\hbar\omega_k}{k_B T}} - 1)^{-1}. \tag{3.134}$$

We note that our doubly resonant optomechanical system contains one fixed, heavy port mirror M_3 and two movable, totally reflecting as well as light-weight mirrors, M_1 and M_2. Here, the movable mirrors are modeled as a quantum harmonic oscillator with effective mass m_j, angular frequency ω_{m_j} (typically in the micro or nanogram range) and momentum decay rate γ_{m_j} for $j = 1, 2$ as shown in Fig. (3.1). Optomechanical coupling between the oscillating-mirror modes and the cavity fields is realized by the radiation pressure. The system is driven by external lasers at frequencies ω_{L_j} and two-mode cavity radiations are generated due to CEL, then the circulating photons in the doubly resonant cavity of lengths L_j bounce off the movable mirrors and exert radiation pressure forces on the surfaces of the movable mirrors, proportional to the instantaneous photon number in the cavity, due to momentum transfer from the intracavity photons to the movable mirrors. The motion of the movable mirrors induced by the radiation pressure changes the cavity's length, and alters the intensity of the cavity field, which in turn modifies the radiation pressure force itself. It is noted that the interaction of the cavity field with the movable mirrors through the radiation pressure is a nonlinear effect. In addition, the damping effects of the modes of movable mirrors are considered by coupling them with thermal bath environments at equilibrium with respective temperatures T_1 and T_2 Huang and Agarwal [2009].

As pointed out by Dirac, vibrational modes (phonon states) of a single mode mechanical oscillator are mathematically identical to photon states of a single mode of an electric field Dirac [1927]. However, there are several key differences between quantum optical and mechanical system; the most important being the fact that mechanical systems are massive, while photons are mass less. Moreover, assuming that the mechanical oscillator modes are in adiabatic regime, $\omega_{m_j} \ll \omega_j$ for $(j = 1, 2)$, Law [1995] the generated photons behaviour are found to show neglection of; the retardation effect Aguirregabiria and Bel [1987], the photon creation in the cavity with moving boundaries due to the Casimir effect Calucci [1992], the Doppler effect Karrai et al. [2008], thus the radiation pressure force does not depend on the velocity of the movable mirrors.

As the investigation of various nonclassical correlations of mechanical modes resulted from the induced coherence of two-mode cavity radiation that can be transferred to the movable mirrors are sought for, we consider the dynamics of the field modes in the Markovian regime under which $\kappa_j \gg \gamma_{m_j}$ Sete and Eleuch [2015]; Pinard et al. [2005] that is the case for mirrors with a high mechanical Q-factor and weak effective optomechanical coupling. Now, if Φ is the transmissivity of the partially transmitting fixed mirror and F is the cavity finesse then the photon decay rate due to the partial transmission of the fixed mirror is defined as Svelto and Svelto [1998]

$$\kappa = \frac{\pi c}{2FL}, \quad \text{with} \quad F = \frac{\pi(1-\Phi)^{1/4}}{1-(1-\Phi)^{1/2}}. \tag{3.135}$$

Previous work Leggett [1984] has shown that while using careful approximations a positive Markovian dynamics can be obtained in this framework but the final results are valid only from medium to high temperatures of the thermal bath. In the construction of models of optomechanical systems in the quantum regime at low temperatures other than the medium and high temperatures, we consider the reduced dynamics of a massive open-micro mechanical oscillator. In this context, the Markovian master equation for the harmonic oscillator can be derived from effective environmental models of bosonic oscillators using a standard approach is usually considered Caldeira and Leggett [1983]; Ford et al. [1988]; Xiong et al. [2010]; Zhang et al. [2012]; Yang et al. [2013].

On the other hand, the requirement that the equilibrium state should be the canonical thermal state determined by the standard Hamiltonian of a harmonic oscillator is known to be incompatible with positivity and translational invariance Lindblad [1976]. This incompatibility induced some authors to rebut to translational invariance Săndulescu and Scutaru [1987] or to accept non-positive dynamical equations and to give more relevance to obtaining time evolutions very close to the classical ones Caldeira and Leggett [1983]. A non-positive dynamics can be satisfactory when the system is near the classical regime, but this approach becomes questionable when quantum effects are searched for Giovannetti and Vitali [2001]; Jacobs et al. [1999]. The positivity and translational invariance can be maintained by weakening the requests on the equilibrium state i.e. a weak formulation of energy equipartition at equilibrium. The result is therefore to single out from the many proposals appearing in the literature a unique consistent dynamics in the Markov approximation. With our formulated assumptions that the quantum mechanically oscillating mirrors in the existence of a well defined positive Markovian dynamics, under damped (not overdamped) oscillations and translationally invariant apart from the harmonic potential, a weak equipartition condition and the existence of a unique stationary state in Gibbs form can essentially fix the structure of the reduced dynamics Barchielli and Vacchini [2015]. For two quantum harmonically oscillating mirrors being coupled to their respective thermal environments at equilibrium can thus be written as

$$\frac{d\hat{\rho}_m}{dt} = -i\left[\hat{H}_m, \hat{\rho}\right] + \frac{\gamma_{m_1}}{2}(n_1+1)\left(2\hat{b}_1\hat{\rho}\hat{b}_1^\dagger - \hat{b}_1^\dagger\hat{b}_1\hat{\rho} - \hat{\rho}\hat{b}_1^\dagger\hat{b}_1\right) + \frac{\gamma_{m_1}}{2}n_1\left(2\hat{b}_1^\dagger\hat{\rho}\hat{b}_1 - \hat{b}_1\hat{b}_1^\dagger\hat{\rho} - \hat{\rho}\hat{b}_1\hat{b}_1^\dagger\right)$$
$$+ \frac{\gamma_{m_2}}{2}(n_2+1)\left(2\hat{b}_2\hat{\rho}\hat{b}_2^\dagger - \hat{b}_2^\dagger\hat{b}_2\hat{\rho} - \hat{\rho}\hat{b}_2^\dagger\hat{b}_2\right) + \frac{\gamma_{m_2}}{2}n_2\left(2\hat{b}_2^\dagger\hat{\rho}\hat{b}_2 - \hat{b}_2\hat{b}_2^\dagger\hat{\rho} - \hat{\rho}\hat{b}_2\hat{b}_2^\dagger\right), \tag{3.136}$$

where $\hat{H}_m = \hat{H}_{m_1} + \hat{H}_{m_2}$ describes the sum of Hamiltonian of the two quantum harmonically oscillating mirrors, γ_{m_j} are damping rates of the mechanical oscillators, and n_j are the thermal phonon number at mechanical bath temperatures T_j for $j = 1, 2$.

On account of Eqs. (3.79), (3.124) and (3.136) the master equation for a nondegenerate three-level laser coupled to two-mode squeezed vacuum reservoir, and two quantum harmonically oscillating mirrors coupled to thermal baths in equilibrium at temperatures T_1 and T_2 can be written as

$$\frac{d}{dt}\hat{\rho}(t) = -i[\hat{H}_I(t), \hat{\rho}(t)] + \alpha_{11}(\hat{\rho}\hat{a}_1\hat{a}_1^\dagger - \hat{a}_1^\dagger\hat{\rho}\hat{a}_1) + \alpha_{11}^*(\hat{a}_1\hat{a}_1^\dagger\hat{\rho} - \hat{a}_1^\dagger\hat{\rho}\hat{a}_1)$$
$$+ \alpha_{22}(\hat{a}_2\hat{\rho}\hat{a}_2^\dagger - \hat{a}_2^\dagger\hat{a}_2\hat{\rho}) + \alpha_{22}^*(\hat{a}_2\hat{\rho}\hat{a}_2^\dagger - \hat{\rho}\hat{a}_2^\dagger\hat{a}_2) + \alpha_{12}(\hat{\rho}\hat{a}_2^\dagger\hat{a}_1^\dagger - \hat{a}_1^\dagger\hat{\rho}\hat{a}_2^\dagger)$$
$$+ \alpha_{12}^*(\hat{a}_1\hat{a}_2\hat{\rho} - \hat{a}_2\hat{\rho}\hat{a}_1) + \alpha_{21}(\hat{a}_1^\dagger\hat{\rho}\hat{a}_2^\dagger - \hat{a}_2^\dagger\hat{a}_1^\dagger\hat{\rho}) + \alpha_{21}^*(\hat{a}_2\hat{\rho}\hat{a}_1 - \hat{\rho}\hat{a}_1\hat{a}_2)$$
$$+ \sum_{j=1}^{2}\left[\frac{k_j(N+1)}{2}(2\hat{a}_j\hat{\rho}\hat{a}_j^\dagger - \hat{a}_j^\dagger\hat{a}_j\hat{\rho} - \hat{\rho}\hat{a}_j^\dagger\hat{a}_j) + \frac{k_jN}{2}(2\hat{a}_j^\dagger\hat{\rho}\hat{a}_j - \hat{a}_j\hat{a}_j^\dagger\hat{\rho} - \hat{\rho}\hat{a}_j\hat{a}_j^\dagger)\right]$$
$$+ \frac{\sqrt{k_1k_2}}{2}M\left(2\hat{a}_1^\dagger\hat{\rho}\hat{a}_2^\dagger + 2\hat{a}_2^\dagger\hat{\rho}\hat{a}_1^\dagger - \hat{a}_1^\dagger\hat{a}_2^\dagger\hat{\rho} - \hat{a}_2^\dagger\hat{a}_1^\dagger\hat{\rho} - \hat{\rho}\hat{a}_1^\dagger\hat{a}_2^\dagger - \hat{\rho}\hat{a}_2^\dagger\hat{a}_1^\dagger\right)$$
$$+ \frac{\sqrt{k_1k_2}}{2}M^*\left(2\hat{a}_1\hat{\rho}\hat{a}_2 + 2\hat{a}_2\hat{\rho}\hat{a}_1 - \hat{a}_1\hat{a}_2\hat{\rho} - \hat{a}_2\hat{a}_1\hat{\rho} - \hat{\rho}\hat{a}_1\hat{a}_2 - \hat{\rho}\hat{a}_2\hat{a}_1\right)$$
$$+ \sum_{j=1}^{2}\left[\frac{\gamma_{m_j}}{2}(n_j+1)\left(2\hat{b}_j\hat{\rho}\hat{b}_j^\dagger - \hat{b}_j^\dagger\hat{b}_j\hat{\rho} - \hat{\rho}\hat{b}_j^\dagger\hat{b}_j\right) + \frac{\gamma_{m_j}}{2}n_j\left(2\hat{b}_j^\dagger\hat{\rho}\hat{b}_j - \hat{b}_j\hat{b}_j^\dagger\hat{\rho} - \hat{\rho}\hat{b}_j\hat{b}_j^\dagger\right)\right], \tag{3.137}$$

in which $\hat{H}_I$ is described by Eq. (3.14).

3.2.3 Quantum Langevin equations

To analyze the various nonclassical features of the two-cavity modes, the cavity-mechanical modes and the two-mechanical modes, it is more convenient to use the quantum Langevin approach in which the master equation is applied to determine the evolution of expectation values of different operators of the cavity, the mechanical and their correlations for the atom-cavity mode and optomechanical system separately. This procedure is justified in the regime where the atom-field coupling turns out to be much stronger than the optomechanical coupling.

With the aid of the master equation (3.137), the field-mirror interaction Hamiltonian (3.16), and making use of the general relation

$$\frac{d}{dt}\langle\hat{O}\rangle = Tr\left(\frac{d\hat{\rho}}{dt}\hat{O}\right), \tag{3.138}$$

together with the cyclic properties of the trace operations, and the commutation relations; the nonlinear quantum Langevin equations are found to be

$$\frac{d}{dt}\langle\hat{a}_j(t)\rangle = -\left(\frac{k_j}{2}+\alpha_{jj}+i\delta\omega_j\right)\langle\hat{a}_j(t)\rangle - \alpha_{jk}\langle\hat{a}_k^\dagger(t)\rangle - iG_{0_j}\langle\hat{a}_j(\hat{b}_j^\dagger+\hat{b}_j)\rangle + \epsilon_j e^{i\delta_j t}, \tag{3.139}$$

$$\frac{d}{dt}\langle\hat{b}_j(t)\rangle = -\left(\frac{\gamma_{m_j}}{2}+i\omega_{m_j}\right)\langle\hat{b}_j(t)\rangle - iG_{0_j}\langle\hat{a}_j^\dagger\hat{a}_j\rangle, \quad (j=1,2), \tag{3.140}$$

$$\begin{aligned}\frac{d}{dt}\langle\hat{a}_j^2(t)\rangle =& -2\left(\frac{k_j}{2}+\alpha_{jj}+i\delta\omega_j\right)\langle\hat{a}_j^2(t)\rangle - 2\alpha_{jk}\langle\hat{a}_j(t)\hat{a}_k^\dagger(t)\rangle \\ &- 2iG_{0_j}\langle\hat{a}_j^2(\hat{b}_j^\dagger+\hat{b}_j)\rangle + 2\epsilon_j e^{i\delta_j t}\langle\hat{a}_j(t)\rangle,\end{aligned} \tag{3.141}$$

$$\frac{d}{dt}\langle\hat{b}_j^2(t)\rangle = -2\left(\frac{\gamma_{m_j}}{2}+i\omega_{m_j}\right)\langle\hat{b}_j^2(t)\rangle - 2iG_{0_j}\langle\hat{b}_j\hat{a}_j^\dagger\hat{a}_j\rangle, \quad (j=1,2), \tag{3.142}$$

$$\begin{aligned}\frac{d}{dt}\langle\hat{a}_1^\dagger\hat{a}_1\rangle =& -(\kappa_1+\alpha_{11}+\alpha_{11}^*)\langle\hat{a}_1^\dagger\hat{a}_1\rangle - \alpha_{12}^*\langle\hat{a}_1\hat{a}_2\rangle - \alpha_{12}\langle\hat{a}_2^\dagger\hat{a}_1^\dagger\rangle + \epsilon_1^* e^{-i\delta_1 t}\langle\hat{a}_1\rangle \\ &+ \epsilon_1 e^{i\delta_1 t}\langle\hat{a}_1^\dagger\rangle + \kappa_1 N - \big(\alpha_{11}+\alpha_{11}^*\big),\end{aligned} \tag{3.143}$$

$$\begin{aligned}\frac{d}{dt}\langle\hat{a}_2^\dagger\hat{a}_2\rangle =& -(\kappa_2+\alpha_{22}+\alpha_{22}^*)\langle\hat{a}_2^\dagger\hat{a}_2\rangle - \alpha_{21}^*\langle\hat{a}_1\hat{a}_2\rangle - \alpha_{21}\langle\hat{a}_2^\dagger\hat{a}_1^\dagger\rangle + \epsilon_2^* e^{-i\delta_2 t}\langle\hat{a}_2\rangle \\ &+ \epsilon_2 e^{i\delta_2 t}\langle\hat{a}_2^\dagger\rangle + \kappa_2 N,\end{aligned} \tag{3.144}$$

$$\frac{d}{dt}\langle \hat{a}_1\hat{a}_1^\dagger\rangle = -\left(\kappa_1+\alpha_{11}+\alpha_{11}^*\right)\langle \hat{a}_1\hat{a}_1^\dagger\rangle - \alpha_{12}\langle \hat{a}_2^\dagger\hat{a}_1^\dagger\rangle - \alpha_{12}^*\langle \hat{a}_1\hat{a}_2\rangle + \epsilon_1^* e^{-i\delta_1 t}\langle \hat{a}_1\rangle + \epsilon_1 e^{i\delta_1 t}\langle \hat{a}_1^\dagger\rangle + \kappa_1(N+1), \tag{3.145}$$

$$\frac{d}{dt}\langle \hat{a}_2\hat{a}_2^\dagger\rangle = -\left(\kappa_2+\alpha_{22}+\alpha_{22}^*\right)\langle \hat{a}_2\hat{a}_2^\dagger\rangle - \alpha_{21}\langle \hat{a}_2^\dagger\hat{a}_1^\dagger\rangle - \alpha_{21}^*\langle \hat{a}_1\hat{a}_2\rangle + \epsilon_2^* e^{-i\delta_2 t}\langle \hat{a}_2\rangle + \epsilon_2 e^{i\delta_2 t}\langle \hat{a}_2^\dagger\rangle + \left(\alpha_{22}+\alpha_{22}^*\right) + \kappa_2(N+1), \tag{3.146}$$

$$\begin{aligned}\frac{d}{dt}\langle \hat{a}_1\hat{a}_2\rangle = &-\left(\frac{(\kappa_1+\kappa_2)}{2}+\alpha_{11}+\alpha_{22}+i\delta\omega_1+i\delta\omega_2\right)\langle \hat{a}_1\hat{a}_2\rangle \\ &-\alpha_{12}\langle \hat{a}_2^\dagger\hat{a}_2\rangle - \alpha_{21}\langle \hat{a}_1\hat{a}_1^\dagger\rangle - iG_{0_1}\big\langle \hat{a}_1\hat{a}_2(\hat{b}_1^\dagger+\hat{b}_1)\big\rangle \\ &- iG_{0_2}\big\langle \hat{a}_1\hat{a}_2(\hat{b}_2^\dagger+\hat{b}_2)\big\rangle + \left(\epsilon_1 e^{i\delta_1 t}\langle \hat{a}_2\rangle + \epsilon_2 e^{i\delta_2 t}\langle \hat{a}_1\rangle\right) - \sqrt{\kappa_1\kappa_2}M,\end{aligned} \tag{3.147}$$

$$\begin{aligned}\frac{d}{dt}\langle \hat{a}_j^\dagger\hat{a}_k\rangle = &-\left(\frac{(\kappa_j+\kappa_k)}{2}+\alpha_{jj}^*+\alpha_{kk}-i\delta\omega_j+i\delta\omega_k\right)\langle \hat{a}_j^\dagger\hat{a}_k\rangle \\ &-\alpha_{jk}^*\langle \hat{a}_k^2\rangle - \alpha_{kj}\langle \hat{a}_j^{\dagger 2}\rangle + iG_{0_j}\big\langle \hat{a}_j^\dagger\hat{a}_k(\hat{b}_j^\dagger+\hat{b}_j)\big\rangle \\ &- iG_{0_k}\big\langle \hat{a}_j^\dagger\hat{a}_k(\hat{b}_k^\dagger+\hat{b}_k)\big\rangle + \left(\epsilon_j^* e^{-i\delta_j t}\langle \hat{a}_k\rangle + \epsilon_k e^{i\delta_k t}\langle \hat{a}_j^\dagger\rangle\right),\end{aligned} \tag{3.148}$$

$$\frac{d}{dt}\langle \hat{b}_j^\dagger\hat{b}_j\rangle = -\gamma_{m_j}\langle \hat{b}_j^\dagger\hat{b}_j\rangle - iG_{0_j}\langle \hat{a}_j^\dagger\hat{a}_j(\hat{b}_j^\dagger-\hat{b}_j)\rangle + \gamma_{m_j}n_j, \tag{3.149}$$

$$\frac{d}{dt}\langle \hat{b}_j\hat{b}_j^\dagger\rangle = -\gamma_{m_j}\langle \hat{b}_j\hat{b}_j^\dagger\rangle - iG_{0_j}\langle \hat{a}_j^\dagger\hat{a}_j(\hat{b}_j^\dagger-\hat{b}_j)\rangle + \gamma_{m_j}\left(n_j+1\right), \tag{3.150}$$

$$\frac{d}{dt}\langle \hat{b}_1\hat{b}_2\rangle = -\left(\frac{\gamma_{m_1}+\gamma_{m_2}}{2}+i(\omega_{m_1}+\omega_{m_2})\right)\langle \hat{b}_1\hat{b}_2\rangle - iG_{0_1}\langle \hat{a}_1^\dagger\hat{a}_1\hat{b}_2\rangle - iG_{0_2}\langle \hat{a}_2^\dagger\hat{a}_2\hat{b}_1\rangle, \tag{3.151}$$

$$\frac{d}{dt}\langle \hat{b}_j^\dagger\hat{b}_k\rangle = -\left(\frac{\gamma_{m_j}+\gamma_{m_k}}{2}+i(\omega_{m_k}-\omega_{m_j})\right)\langle \hat{b}_j^\dagger\hat{b}_k\rangle + iG_{0_j}\langle \hat{a}_j^\dagger\hat{a}_j\hat{b}_k\rangle - iG_{0_k}\langle \hat{a}_k^\dagger\hat{a}_k\hat{b}_j^\dagger\rangle, \tag{3.152}$$

$$\begin{aligned}\frac{d}{dt}\langle \hat{a}_j\hat{b}_j\rangle = &-\left(\frac{\kappa_j}{2}+\frac{\gamma_{m_j}}{2}+i(\omega_{m_j}+\delta\omega_j)+\alpha_{jj}\right)\langle \hat{a}_j\hat{b}_j\rangle - \alpha_{jk}\langle \hat{a}_k^\dagger\hat{b}_j\rangle \\ &- iG_{0_j}\left[\langle \hat{a}_j^\dagger\hat{a}_j\hat{a}_j\rangle + \langle \hat{a}_j\hat{b}_j(\hat{b}_j^\dagger+\hat{b}_j)\rangle\right] + \epsilon_j e^{i\delta_j t}\langle \hat{b}_j\rangle,\end{aligned} \tag{3.153}$$

$$\begin{aligned}\frac{d}{dt}\langle \hat{a}_j^\dagger\hat{b}_j\rangle = &-\left(\frac{\kappa_j}{2}+\frac{\gamma_{m_j}}{2}-i(-\omega_{m_j}+\delta\omega_j)+\alpha_{jj}^*\right)\langle \hat{a}_j^\dagger\hat{b}_j\rangle - \alpha_{jk}^*\langle \hat{a}_k\hat{b}_j\rangle \\ &- iG_{0_j}\left[\langle \hat{a}_j^\dagger\hat{a}_j\hat{a}_j^\dagger\rangle - \langle \hat{a}_j^\dagger\hat{b}_j(\hat{b}_j^\dagger+\hat{b}_j)\rangle\right] + \epsilon_j^* e^{-i\delta_j t}\langle \hat{b}_j\rangle,\end{aligned} \tag{3.154}$$

$$\frac{d}{dt}\langle\hat{a}_j\hat{b}_k\rangle = -\Big(\frac{\kappa_j}{2} + \frac{\gamma_{m_k}}{2} + i(\omega_{m_k} + \delta\omega_j) + \alpha_{jj}\Big)\langle\hat{a}_j\hat{b}_k\rangle - \alpha_{jk}\langle\hat{a}_k^\dagger\hat{b}_k\rangle$$
$$- iG_{0_j}\langle\hat{a}_j\hat{b}_k(\hat{b}_j^\dagger + \hat{b}_j)\rangle - iG_{0_k}\langle\hat{a}_j\hat{a}_k^\dagger\hat{a}_k\rangle + \epsilon_j e^{i\delta_j t}\langle\hat{b}_k\rangle, \tag{3.155}$$

with $j \neq k$. The general equations for evolution of the cavity and mechanical modes together with their conjugates can also be obtained by removing the bracket from Eqs. (3.139) and (3.140) and by adding appropriate noise operators $\hat{F}_j$ and $\hat{f}_j$ with vanishing mean $\langle\hat{F}_j\rangle = \langle\hat{f}_j\rangle = 0$ as follows using the procedure in Tesfa [2021]; Walls and Milburn [2008]; Kassahun [2016]

$$\frac{d\hat{a}_j(t)}{dt} = -\left(\frac{k_j}{2} + \alpha_{jj} + i\delta\omega_j\right)\hat{a}_j(t) - \alpha_{jk}\hat{a}_k^\dagger(t) - iG_{0_j}\hat{a}_j(\hat{b}_j^\dagger + \hat{b}_j) + \epsilon_j e^{i\delta_j t} + \hat{F}_j, \tag{3.156}$$

$$\frac{d\hat{b}_j(t)}{dt} = -\Big(\frac{\gamma_{m_j}}{2} + i\omega_{m_j}\Big)\hat{b}_j(t) - iG_{0_j}\hat{a}_j^\dagger\hat{a}_j + \sqrt{\gamma_{m_j}}\hat{f}_j. \tag{3.157}$$

The noise operator $\hat{F}_j$ is due to the coupling of two-mode squeezed vacuum reservoir with the cavity modes, whereas $\hat{f}_j$ stands for the noise operator corresponding to a thermal reservoir coupled to a mode of mechanical oscillator. Besides, $G_{0_j}\langle\hat{b}_j^\dagger + \hat{b}_j\rangle$ is considered to be the frequency shift due to radiation pressure.

It then follows that the correlation properties of the noise operators can be obtained by using Einstein relations Scully. That is for any operators $\hat{A}$ and $\hat{B}$ and their respective noise operators $\hat{F}_A$ and $\hat{F}_B$

$$2\langle D_{\hat{A}\hat{B}}\rangle = \frac{d}{dt}\big\langle\hat{A}\hat{B}\big\rangle - \big\langle\big(\frac{d\hat{A}}{dt} - \hat{F}_A\big)\hat{B}\big\rangle - \big\langle\hat{A}\big(\frac{d\hat{B}}{dt} - \hat{F}_B\big)\big\rangle, \tag{3.158}$$

where $\langle D_{\hat{A}\hat{B}}\rangle$ is the diffusion coefficient with $\hat{A}$ and $\hat{B} = \hat{a}_j, \hat{b}_j$ for $j = 1, 2$. With the aid of this relation and the equations for second-order moments of the cavity mode operators $\hat{a}_j$ as in Eqs. (3.143) - (3.148), together with the relation

$$\big\langle\hat{F}_{\hat{A}}(t)\hat{F}_{\hat{B}}(t')\big\rangle = 2\langle D_{\hat{A}\hat{B}}\rangle\delta(t - t'), \tag{3.159}$$

the non-zero correlation properties of the cavity mode noise operators are:

$$\left\langle \hat{F}_1^\dagger(t)\hat{F}_1(t')\right\rangle = \left[\kappa_1 N - 2\,\mathrm{Re}(\alpha_{11})\right]\delta(t-t'), \tag{3.160}$$

$$\left\langle \hat{F}_1(t)\hat{F}_1^\dagger(t')\right\rangle = \kappa_1(N+1)\delta(t-t'), \tag{3.161}$$

$$\left\langle \hat{F}_2^\dagger(t)\hat{F}_2(t')\right\rangle = \kappa_2 N\delta(t-t'), \tag{3.162}$$

$$\left\langle \hat{F}_2(t)\hat{F}_2^\dagger(t')\right\rangle = \left[\kappa_2(N+1) + 2\,\mathrm{Re}(\alpha_{22})\right]\delta(t-t'), \tag{3.163}$$

$$\left\langle \hat{F}_1(t)\hat{F}_2(t')\right\rangle = -\sqrt{\kappa_1\kappa_2}M\delta(t-t'), \tag{3.164}$$

$$\left\langle \hat{F}_1^\dagger(t)\hat{F}_2^\dagger(t')\right\rangle = \left(\alpha_{12}^* - \alpha_{21}^* - \sqrt{\kappa_1\kappa_2}M^*\right)\delta(t-t'), \tag{3.165}$$

$$\left\langle \hat{F}_2(t)\hat{F}_1(t')\right\rangle = \left(\alpha_{12} - \alpha_{21} - \sqrt{\kappa_1\kappa_2}M\right)\delta(t-t'), \tag{3.166}$$

$$\left\langle \hat{F}_2^\dagger(t)\hat{F}_1^\dagger(t')\right\rangle = \left(\alpha_{21}^* - \alpha_{12}^* - \sqrt{\kappa_1\kappa_2}M^*\right)\delta(t-t'). \tag{3.167}$$

In addition, with the aid of Eqs. (3.149) - (3.155) and assuming that the mechanical quality factors are large (i.e. $Q = \frac{\omega_{m_j}}{\gamma_{m_j}} \gg 1$) Benguria and Kac [1981] the nonvanishing correlations between the mechanical modes noise operators take the forms

$$\left\langle \hat{f}_j^\dagger(t)\hat{f}_j(t')\right\rangle = n_j\delta(t-t'), \tag{3.168}$$

$$\left\langle \hat{f}_j(t)\hat{f}_j^\dagger(t')\right\rangle = \left(n_j+1\right)\delta(t-t'), \tag{3.169}$$

where $n_j^{-1} = \left(\exp(\frac{\hbar\omega_{m_j}}{k_B T_j}) - 1\right)$ denotes thermal bath's vibrational mode number, k_B is the Boltzmann constant, and T_j is the corresponding temperature of the jth thermal bath.

3.3 Linearization and Covariance Matrix

3.3.1 Linearization of QLE

Due to the nonlinear nature of the radiation pressure, it is not easy to get the rigorous analytical solutions of Eqs. (3.156) and (3.157). To overcome this difficulty, we adopt the linearization approach as discussed in Ref. Walls and Milburn [2008]. In this regard, a reasonable optomechanical interaction can be achieved when the cavity is intensely driven by strong power lasers Mancini and Tombesi [1994]. On the other hand, the optimal transfer of quantum properties from the two cavity fields to the mechanical modes can be achieved in an adiabatic regime Pinard et al. [2005].

With the aid of linearization scheme, the dynamics of small fluctuations around the steady state can be obtained by decomposing each operator into two parts, the sum of its average operator in the steady state and a small fluctuation operator as

$$\hat{a}_j = \langle a\rangle_{j_{ss}} + \delta\hat{a}_j, \;\; \hat{b}_j = \langle b\rangle_{j_{ss}} + \delta\hat{b}_j, \tag{3.170}$$

where the steady state mean value of each bosonic operator is thus taken to be larger when compared to the corresponding quantum fluctuation: $|\langle\hat{a}_j\rangle| = |a_{j_{ss}}| \gg |\delta\hat{a}_j|$ and $|\langle\hat{b}_j\rangle| = |b_{j_{ss}}| \gg |\delta\hat{b}_j|$ for $j = 1, 2$. The mean value of fluctuation operator are $\langle\delta\hat{a}_j\rangle = \langle\delta\hat{b}_j\rangle = 0$, while the mean operator values $\langle a\rangle_{j_{ss}}$ and $\langle b\rangle_{j_{ss}}$ are complex numbers and can be evaluated by setting the time derivatives to zero and factorizing the averages in Eqs. (3.156) and (3.157).

In order to investigate the quantum correlations between the different bipartite modes (two optical modes, optical-mechanical modes and two mechanical modes) in the system, it is more convenient to transform Eqs. (3.156) and (3.157) in terms of the quadrature operators and their corresponding Hermitian input noise operators. These dimensionless quadrature operators are introduced for the optical and mechanical modes as:

$$\delta\hat{X}_j = \frac{1}{\sqrt{2}}\big(\delta\hat{a}_j^\dagger + \delta\hat{a}_j\big), \tag{3.171}$$

$$\delta\hat{Y}_j = \frac{i}{\sqrt{2}}\big(\delta\hat{a}_j^\dagger - \delta\hat{a}_j\big), \tag{3.172}$$

$$\delta\hat{P}_j = \frac{1}{\sqrt{2}}\big(\delta\hat{b}_j^\dagger + \delta\hat{b}_j\big), \tag{3.173}$$

$$\delta\hat{Q}_j = \frac{i}{\sqrt{2}}\big(\delta\hat{b}_j^\dagger - \delta\hat{b}_j\big), \tag{3.174}$$

and the corresponding Hermitian input noise operators

$$\delta\hat{X}_j^{\rm in} = \frac{1}{\sqrt{2}}\big(\delta\hat{a}_j^{\dagger,\rm in} + \delta\hat{a}_j^{\rm in}\big), \tag{3.175}$$

$$\delta \hat{Y}_j^{\rm in} = \frac{i}{\sqrt{2}}\big(\delta \hat{a}_j^{\dagger,{\rm in}} - \delta \hat{a}_j^{\rm in}\big), \tag{3.176}$$

$$\delta \hat{P}_j^{\rm in} = \frac{1}{\sqrt{2}}\big(\delta \hat{b}_j^{\dagger,{\rm in}} + \delta \hat{b}_j^{\rm in}\big), \tag{3.177}$$

$$\delta \hat{Q}_j^{\rm in} = \frac{i}{\sqrt{2}}\big(\delta \hat{b}_j^{\dagger,{\rm in}} - \delta \hat{b}_j^{\rm in}\big), \tag{3.178}$$

with

$$\delta \hat{a}_j^{\rm in}(t) = \frac{1}{\sqrt{\kappa_j}}\hat{F}_j, \tag{3.179}$$

$$\delta \hat{b}_j^{\rm in}(t) = \sqrt{\gamma_{m_j}}\hat{f}_j. \tag{3.180}$$

With the above definitions, the dynamics of fluctuations of the Langevin equations in Eqs. (3.156) and (3.157) can be expressed in a more compact form as

$$\frac{d}{dt}S(t) = B\, S(t) + {\rm u(t)}, \tag{3.181}$$

where $S(t)$ is the column vector of fluctuation modes of mechanical oscillators, $\rm u(t)$ being the column vector of the noise sources, and B is the corresponding 8×8 time-dependent coefficient matrix, which contains information about the mean values of the system. Here the transpose of $S(t)$ and $\rm u(t)$ are described as

$$S(t)^T = \Big(\delta\hat{X}_1, \delta\hat{Y}_1, \delta\hat{X}_2, \delta\hat{Y}_2, \delta\hat{P}_1, \delta\hat{Q}_1, \delta\hat{P}_2, \delta\hat{Q}_2\Big)$$

$${\rm u(t)}^T = \Big(\sqrt{2\kappa_1}\delta\hat{X}_1^{\rm in}, \sqrt{2\kappa_1}\delta\hat{Y}_1^{\rm in}, \sqrt{2\kappa_2}\delta\hat{X}_2^{\rm in}, \sqrt{2\kappa_2}\delta\hat{Y}_2^{\rm in}, \delta\hat{P}_1^{\rm in}, \delta\hat{Q}_1^{\rm in}, \delta\hat{P}_2^{\rm in}, \delta\hat{Q}_2^{\rm in}\Big)\,, \tag{3.182}$$

while B is expressed as

$$B = \begin{pmatrix} -\frac{\kappa_1^{'}}{2} & \Gamma_1 & -\alpha_{12} & 0 & -2G_{0_1}\frac{d_1}{a_1^2+b_1^2} & 0 & 0 & 0 \\ -\Gamma_1 & -\frac{\kappa_1^{'}}{2} & 0 & \alpha_{12} & 2G_{0_1}\frac{c_1}{a_1^2+b_1^2} & 0 & 0 & 0 \\ -\alpha_{21} & 0 & -\frac{\kappa_2^{'}}{2} & \Gamma_2 & 0 & 0 & -2G_{0_2}\frac{d_2}{a_1^2+b_1^2} & 0 \\ 0 & \alpha_{21} & -\Gamma_2 & -\frac{\kappa_2^{'}}{2} & 0 & 0 & 2G_{0_2}\frac{c_2}{a_1^2+b_1^2} & 0 \\ 0 & 0 & 0 & 0 & -\frac{\gamma_{m_1}}{2} & \omega_{m_1} & 0 & 0 \\ 2G_{0_1}\frac{c_1}{a_1^2+b_1^2} & 2G_{0_1}\frac{d_1}{a_1^2+b_1^2} & 0 & 0 & -\omega_{m_1} & -\frac{\gamma_{m_1}}{2} & 0 & 0 \\ 0 & 0 & 0 & 0 & 0 & 0 & -\frac{\gamma_{m_2}}{2} & \omega_{m_2} \\ 0 & 0 & 2G_{0_2}\frac{c_2}{a_1^2+b_1^2} & 2G_{0_2}\frac{d_2}{a_1^2+b_1^2} & 0 & 0 & -\omega_{m_2} & -\frac{\gamma_{m_2}}{2} \end{pmatrix}, \tag{3.183}$$

with

$$\kappa_j^{'} = \kappa_j + 2\alpha_{jj},$$

$$\epsilon_1 = \epsilon_1^*, \;\; \epsilon_2 = \epsilon_2^*,$$

$$\alpha_{11} = \alpha_{11}^*, \;\; \alpha_{22} = \alpha_{22}^*, \;\; \alpha_{12} = \alpha_{12}^*, \;\; \alpha_{21} = \alpha_{21}^*,$$

$$a_1 = a_1^* = \big[\big(\kappa_1/2 + \alpha_{11}\big)\big(\kappa_2/2 + \alpha_{22}^*\big) + \Gamma_1\Gamma_2 - \alpha_{12}\alpha_{21}^*\big],$$

$$b_1 = b_1^* = \big[\Gamma_2\big(\kappa_1/2 + \alpha_{11}\big) - \Gamma_1\big(\kappa_2/2 + \alpha_{22}^*\big)\big],$$

$$c_1 = c_1^* = \big[\big\{-\epsilon_1^*\big(\kappa_2/2 + \alpha_{22}^*\big) + \epsilon_2\alpha_{12}\big\}a_1 - \epsilon_1^*\Gamma_2 b_1\big],$$

$$d_1 = d_1^* = \big[\big\{-\epsilon_1^*\big(\kappa_2/2 + \alpha_{22}^*\big) + \epsilon_2\alpha_{12}\big\}b_1 + \epsilon_1^*\Gamma_2 a_1\big],$$

$$c_2 = c_2^* = \big[\big\{-\epsilon_2^*\big(\kappa_1/2 + \alpha_{11}^*\big) + \epsilon_1\alpha_{21}\big\}a_1^* + \epsilon_2^*\Gamma_1 b_1^*\big],$$

$$d_2 = d_2^* = \big[\epsilon_2^*\Gamma_1 a_1^* - \big\{-\epsilon_2^*\big(\kappa_1/2 + \alpha_{11}^*\big) + \epsilon_1\alpha_{21}\big\}b_1^*\big]. \tag{3.184}$$

Next, the various nonclassical correlations of the two-mechanical modes can be obtained with the aid of the linearized quantum Langevin equation as follows. This study is justified in the regime where the atom-field coupling turns out to be much stronger than the optomechanical coupling. To this end, we apply a transformed frame defined by $\tilde{a}_j = \hat{a}_j \exp(-i\delta_j t)$ and Eq. (3.170) so that the equations for both fluctuations and c-number steady state values have a coupling between the two cavity modes (terms proportional to α_{12} and α_{21}) that contain highly oscillating factor $\exp(-(\delta_1 + \delta_2)t)$. One can still obtain solutions for $\langle\tilde{a}_j\rangle$ in the steady state that amount to dropping the highly oscillating terms completely i.e. applying the rotating-wave approximation, or choosing a condition such that $\delta_2 = -\delta_1$ and retaining the coupling terms. So, one can verify that one can verify that

$$\langle\tilde{a}_j\rangle = \frac{\epsilon_j}{\frac{\kappa_j}{2} + \alpha_{jj} - i\Delta_j}, \tag{3.185}$$

$$\langle\hat{b}_j^\dagger + \hat{b}_j\rangle = -\frac{2\omega_{m_j} G_{0_j}\langle\tilde{a}_j^\dagger\tilde{a}_j\rangle}{\frac{\gamma_{m_j}^2}{4} + \omega_{m_j}^2}, \tag{3.186}$$

where $\Delta_j = \omega_{L_j} - \omega_j - G_{0_j}\langle\hat{b}_j^\dagger + \hat{b}_j\rangle$ denote the cavity-mode detunings.

Upon introducing the slowly varying fluctuation operators $\delta\hat{a}(t) = \delta\tilde{a}(t)\exp(i\delta_j t)$ and $\delta\hat{b}(t) = \delta\tilde{b}(t)\exp(-i\omega_{m_j}t)$ into Eqs. (3.156) and (3.157), the dynamics of the linearized quantum Langevin equations for the fluctuation modes can be written as

$$\frac{d}{dt}\big(\delta\hat{a}_j\big) = -\big(\frac{\kappa_j^{'}}{2} - i\Delta_j\big)\delta\hat{a}_j - \alpha_{jk}\delta\hat{a}_k^\dagger - iG_{0_j}\langle\tilde{a}_j\rangle\big(\delta\tilde{b}_j^\dagger e^{i(\delta_j+\omega_{m_j})t} + \delta\tilde{b}_j e^{i(\delta_j-\omega_{m_j})t}\big) + \hat{F}_j, \tag{3.187}$$

$$\frac{d}{dt}\big(\delta\tilde{b}_j\big) = -\frac{\gamma_{m_j}}{2}\delta\tilde{b}_j - iG_{0_j}\langle\tilde{a}_j^\dagger\rangle\delta\hat{a}_j\ e^{-i(\delta_j-\omega_{m_j})t} - iG_{0_j}\langle\tilde{a}_j\rangle\delta\hat{a}_j^\dagger\ e^{i(\delta_j+\omega_{m_j})t} + \sqrt{\gamma_{m_j}}\tilde{f}_j, \tag{3.188}$$

with $\kappa_j^{'} = \kappa_j + 2\alpha_{jj}$, $\tilde{f}_j = \hat{f}_j\exp(i\omega_{m_j}t)$, $\tilde{F}_j = \hat{F}_j\exp(-i\delta_j t)$, $\delta\hat{a}_j^{\rm in}(t) = \frac{1}{\sqrt{\kappa_j}}\hat{F}_j$, and $\delta\hat{b}_j^{\rm in}(t) = \sqrt{\gamma_{m_j}}\hat{f}_j$. It might not be difficult to verify that the operators $\delta\hat{a}_j$ and $\delta\hat{b}_j$ satisfy the usual boson commutation relations $[\delta\hat{a}_j, \delta\hat{a}_j^\dagger] = [\delta\hat{b}_j, \delta\hat{b}_j^\dagger] = 1$.

Since no rotating-wave approximation has been made in the fluctuation equations, the coupling terms (proportional to α_{12} and α_{21}) induced by the two-photon coherence are kept. For optomechanical coupling, when $\delta_j = \omega_{m_j}$, the interaction describes parametric amplification and can be used to realize optomechanical squeezing Aspelmeyer et al. [2014], whereas when $\delta_j = -\omega_{m_j}$, the interaction is relevant in inducing quantum state transfer and cooling Aspelmeyer et al. [2014]; Sete and Eleuch [2015]; Pinard et al. [2005].

In this work, since we are interested in transferring the non-zero quantum features of the cavity fields to the mechanical modes, we take $\delta_j = -\omega_{m_j}$. We also choose $\omega_{L_j} \approx \omega_j + G_{0_j}\langle \hat{b}_j^\dagger + \hat{b}_j\rangle$ so that α_{jj} and α_{jk} are real. Upon carrying out the adiabatic approximation to Eq. (3.187), we obtain coupled Langevin equations for the modes of mechanical fluctuation operators $\delta\tilde{b}_j$,

$$\delta\dot{\tilde{b}}_1 = -\frac{\Lambda_1}{2}\delta\tilde{b}_1 - G_{12}\delta\tilde{b}_2^\dagger - c_1\hat{F}_1^\dagger + c_2\hat{F}_2 + \sqrt{\gamma_{m_1}}\tilde{f}_1, \tag{3.189}$$

$$\delta\dot{\tilde{b}}_2 = -\frac{\Lambda_2}{2}\delta\tilde{b}_2 - G_{21}\delta\tilde{b}_1^\dagger + d_1\hat{F}_1 - d_2\hat{F}_2^\dagger + \sqrt{\gamma_{m_2}}\tilde{f}_2, \tag{3.190}$$

where $\Lambda_1 = \gamma_{m_1} - \Lambda_{b_1}$, $\Lambda_2 = \gamma_{m_2} - \Lambda_{b_2}$ with $\Lambda_{b_1} = 4G_1G_1^*\kappa_2^{'}/K$, $\Lambda_{b_2} = 4G_2G_2^*\kappa_1^{'}/K$ in which $K = \kappa_1^{'}\kappa_2^{'} - 4\alpha_{12}\alpha_{21}$ denotes the effective damping rate for the mechanical modes induced by the radiation pressure. In the same way, $G_{12} = 4G_1G_2\alpha_{12}^*/K$ and $G_{21} = 4G_1G_2\alpha_{21}^*/K$ are effectively coupled between the two mechanical modes induced by the laser system, whereas $c_1 = 2G_1\kappa_2^{'}/K$, $c_2 = 4G_1\alpha_{12}^*/K$, $d_1 = 4G_2\alpha_{21}^*/K$, and $d_2 = 2G_2\kappa_1^{'}/K$ in which many-photon coupling is denoted by $G_j = iG_{0_j}\langle\tilde{a}_j\rangle$.

3.3.2 Steady state covariance matrix

So as to analyze the detail of the various non-zero quantum features between the mechanical modes, we seek to obtain the covariance matrix (CM) applying the quadrature operators defined as

$$\delta\tilde{H}_j = \frac{1}{\sqrt{2}}\left(\delta\tilde{b}_j^\dagger + \delta\tilde{b}_j\right), \tag{3.191}$$

$$\delta\tilde{L}_j = \frac{i}{\sqrt{2}}\left(\delta\tilde{b}_j^\dagger - \delta\tilde{b}_j\right). \tag{3.192}$$

where the corresponding Hermitian input noise operators are

$$\delta\tilde{H}_j^{\rm in} = \frac{1}{\sqrt{2}}\left(\tilde{F}_{b_j}^\dagger + \tilde{F}_{b_j}\right), \tag{3.193}$$

$$\delta\tilde{L}_j^{\rm in} = \frac{i}{\sqrt{2}}\left(\tilde{F}_{b_j}^\dagger - \tilde{F}_{b_j}\right), \tag{3.194}$$

with $\tilde{F}_{b_1} = -c_1\hat{F}_1^\dagger + c_2\hat{F}_2 + \sqrt{\gamma_{m_1}}\tilde{f}_1$ and $\tilde{F}_{b_2} = d_1\hat{F}_1 - d_2\hat{F}_2^\dagger + \sqrt{\gamma_{m_2}}\tilde{f}_2$.

Once the expressions for these fluctuation operators are attained, we can write a matrix equation of the form

$$\dot{\mathbf{R}}(t) = \mathcal{A}\ \mathbf{R}(t) + \mathbf{v}(t), \tag{3.195}$$

where $\mathbf{R}(t) = \left(\delta\tilde{H}_1, \delta\tilde{L}_1, \delta\tilde{H}_2, \delta\tilde{L}_2\right)^T$, $\mathbf{v}(t) = \left(\delta\hat{H}_1^{\text{in}}, \delta\hat{L}_1^{\text{in}}, \delta\hat{H}_2^{\text{in}}, \delta\hat{L}_2^{\text{in}}\right)^T$,

$$\mathcal{A} = \begin{pmatrix} -\frac{\Lambda_1}{2} & 0 & -G_{12} & 0 \\ 0 & -\frac{\Lambda_1}{2} & 0 & G_{12} \\ -G_{21} & 0 & -\frac{\Lambda_2}{2} & 0 \\ 0 & G_{21} & 0 & -\frac{\Lambda_2}{2} \end{pmatrix}, \tag{3.196}$$

which epitomizes the coupling between the fluctuations and vector $\mathbf{v}(t)$ that contains the noise operators of both cavity and mirrors.

We then attempt to find a stable solution for Eq. (3.195) so that it attains unique steady-state-independent initial conditions. Since the quantum noises $\hat{F}_j$ and $\hat{f}_j$ are taken to be zero-mean Gaussian noises and the dynamics of $\delta\tilde{H}_j$ and $\delta\tilde{L}_j$ is linearized, the steady-state fluctuation becomes a zero-mean Gaussian state that can be fully characterized by the CM of the system. One may note that the system can reach a stable steady-state condition when real parts of the eigenvalues of the drift matrix $\mathcal{A}$ are all negative. The stability condition can then be obtained by using the Routh-Hurwitz criterion Hurwitz et al. [1964]. In this context, the steady-state CM can be found by solving the Lyapunov equation DeJesus and Kaufman [1987]

$$\mathcal{A}\, V + V^T\, \mathcal{A} = -\mathcal{D}, \tag{3.197}$$

where the matrix A is described by Eq. (3.196) and the elements of CM, V_{ij}, are found by applying $V_{ij} = \frac{\left\langle R_{i_{\text{ss}}} R_{j_{\text{ss}}} + R_{j_{\text{ss}}} R_{i_{\text{ss}}} \right\rangle}{2}$ with $i, j = 1, ..., 4$. The diffusion matrix $(\mathcal{D})$ with its entries is obtained by using $\mathcal{D}_{ij}\delta(t - t') = \frac{\left\langle v_i(t) v_j(t') + v_j(t') v_i(t) \right\rangle}{2}$. The stable solutions to Eq. (3.197) are obtained when $\Lambda_1\Lambda_2 > 4G_{12}G_{21}$ with

$$\mathcal{D} = \begin{pmatrix} B_{11} & 0 & B_{13} & B_{14} \\ 0 & B_{11} & B_{14} & -B_{13} \\ B_{13} & B_{14} & B_{33} & 0 \\ B_{14} & -B_{13} & 0 & B_{33} \end{pmatrix}, \tag{3.198}$$

where
$$\begin{aligned} B_{11} =& c_1^2 \left[\frac{\kappa_1(2N+1) - 2\alpha_{11}}{2}\right] - c_1 c_2 \left[\frac{\alpha_{12} - \alpha_{21} - 2\sqrt{\kappa_1\kappa_2}(M^* + M)}{2}\right] \\ &+ c_2^2 \left[\frac{\kappa_2(2N+1) + 2\alpha_{22}}{2}\right] + \gamma_{m_1}\big(\frac{2n_1+1}{2}\big), \end{aligned} \tag{3.199}$$

$$\begin{aligned} B_{13} =& c_1 d_1 \left[\frac{\kappa_1(2N+1) - 2\alpha_{11}}{2}\right] + \frac{(c_1 d_2 + c_2 d_1)}{2} \left[\frac{\alpha_{12} - \alpha_{21} - 2\sqrt{\kappa_1\kappa_2}(M^* + M)}{2}\right] \\ &- c_2 d_2 \left[\frac{\kappa_2(2N+1) + 2\alpha_{22}}{2}\right] + \gamma_{m_1}\big(\frac{2n_1+1}{2}\big), \end{aligned} \tag{3.200}$$

$$B_{14} = i\frac{(c_2 d_1 - c_1 d_2)}{2} \left[\frac{\alpha_{21} - \alpha_{12} - 2\sqrt{\kappa_1\kappa_2}(M^* - M)}{2}\right], \tag{3.201}$$

$$\begin{aligned} B_{33} =& d_1^2 \left[\frac{\kappa_1(2N+1) - 2\alpha_{11}}{2}\right] - d_1 d_2 \left[\frac{\alpha_{12} - \alpha_{21} - 2\sqrt{\kappa_1\kappa_2}(M^* + M)}{2}\right] \\ &+ d_2^2 \left[\frac{\kappa_2(2N+1) + 2\alpha_{22}}{2}\right] + \gamma_{m_2}\big(\frac{2n_2+1}{2}\big), \end{aligned} \tag{3.202}$$

with c_i and d_i being expressed in Eq. (3.184).

In the next sections, the elements of a CM determined from Eq. (3.197) can be applied to study various properties of nonclassical correlations on different basis. For instance; squeezing, entanglement using different criteria, intermodal correlations and correlations of number of mechanical modes, quantum discord, steering, and statistical properties of mechanical modes.

4

Results and Discussions

4.1 Quantum Correlations via quadrature variances

In this section, quantification of quantum correlations between the fluctuations of mechanical modes such as squeezing and entanglement together with effects of parameters of atom, cavity and reservoirs on these properties is investigated on the basis of quadrature variances in relation to the electric and/or magnetic fields.

4.1.1 Quantification of squeezing via quadrature variances

The squeezing properties of the quantum fluctuation of two-mechanical modes can be defined by

$$\delta C_+ = \frac{1}{\sqrt{2}}(\delta\tilde{b}_{1_+} + \delta\tilde{b}_{2_+}), \tag{4.1}$$

$$\delta C_- = \frac{1}{\sqrt{2}}(\delta\tilde{b}_{1_-} + \delta\tilde{b}_{2_-}), \tag{4.2}$$

where $\delta\tilde{b}_{1_+} = (\delta\tilde{b}_1 + \delta\tilde{b}_1^\dagger)$, $\delta\tilde{b}_{1_-} = i(\delta\tilde{b}_1^\dagger - \delta\tilde{b}_1)$, $\delta\tilde{b}_{2_+} = (\delta\tilde{b}_2 + \delta\tilde{b}_2^\dagger)$, and $\delta\tilde{b}_{2_-} = i(\delta\tilde{b}_2^\dagger - \delta\tilde{b}_2)$. The operators δC_+ and δC_- are Hermitian and satisfy the commutation relation $[\delta C_+, \delta C_-] = 2i$.

It might be worth noting that a two-mode Gaussian state is said to be in a squeezed state if the variances of the quadrature fluctuation operators are $\Delta(\delta C_+)^2 < 1$ and $\Delta(\delta C_-)^2 > 1$ or $\Delta(\delta C_-)^2 < 1$ and $\Delta(\delta C_+)^2 > 1$ such that $\Delta(\delta C_+)\Delta(\delta C_-) \geq 1$ Kassahun

[2016]. Meanwhile, a degree of squeezing is considered in the sense that how much it is close to the maximum. With this background, the quadrature variances of the operators δC_+ and δC_- can be expressed as

$$\Delta(\delta C_\pm)^2 = \langle \delta C_\pm^2 \rangle - \langle \delta C_\pm \rangle^2. \tag{4.3}$$

With the aid of the predefined quantum fluctuation operators $\delta \tilde{H}_j$, $\delta \tilde{L}_j$ as in Eqs. (3.191) and (3.192), and considering Eqs. (4.1)-(4.3), we see that the variances of the quadrature fluctuation operators at steady state take the form

$$\Delta(\delta C_+)^2 = \langle \delta \tilde{H}_1 \delta \tilde{H}_1 \rangle + \langle \delta \tilde{H}_1 \delta \tilde{H}_2 \rangle + \langle \delta \tilde{H}_2 \delta \tilde{H}_1 \rangle + \langle \delta \tilde{H}_2 \delta \tilde{H}_2 \rangle, \tag{4.4}$$

$$\Delta(\delta C_-)^2 = \langle \delta \tilde{L}_1 \delta \tilde{L}_1 \rangle + \langle \delta \tilde{L}_1 \delta \tilde{L}_2 \rangle + \langle \delta \tilde{L}_2 \delta \tilde{L}_1 \rangle + \langle \delta \tilde{L}_2 \delta \tilde{L}_2 \rangle. \tag{4.5}$$

The elements of the CM from the solution of the Lyapunov equation (3.197) for the expectation values of Eqs. (4.4) and (4.5) can be applied to obtain the variances of the plus and minus quadratures of mechanical quantum fluctuation operators at steady state as

$$\Delta(\delta C_+)^2 = [V_{11} + V_{33} + 2V_{13}]_{\mathrm{ss}}\,, \tag{4.6}$$

$$\Delta(\delta C_-)^2 = [V_{22} + V_{44} + 2V_{24}.]_{\mathrm{ss}}\,. \tag{4.7}$$

In general, it is perceived that squeezing becomes minimum when the variance of the mechanical quadrature operator is equal to one and maximum when it is zero, and anything in between is considered as a degree of squeezing in the sense that how much it is close to zero.

To demonstrate the induced nonclassical behavior of modes of two harmonically oscillating mirrors at steady state in a doubly resonant cavity when all atoms injected into cavity are initially at the lower-energy level $|\psi(0)\rangle = |c\rangle$, we choose the values of parameters of two mirrors, cavity parameters, atomic energy levels, and two cavity radiations based on recent experiments for an optomechanical system Arcizet et al.

Table 4.1: Experimental values for various parameters of our system as in Refs. Arcizet et al. [2006]; Verhagen et al. [2012]; Gröblacher et al. [2009] to plot Figs. (4.1) - (4.14) in standard case

Parameter	Values and units
Atom-field coupling ($g_1 = g_2$)	$2.0\pi \times 2.50$ MHz
Cavity damping rates	$\kappa_1 = 1.97$ kHz, $\kappa_2 = 2.59$ kHz
Mechanical damping rates ($\gamma_{m_1} = \gamma_{m_2}$)	$2\pi \times 60.00$ Hz
Angular frequencies of movable mirrors ($\omega_{m_1} = \omega_{m_2}$)	$2\pi \times 3.00$ MHz
Masses of the mechanical oscillators ($m_1 = m_2$)	5.00 ng
Initial lengths of a doubly resonant cavity	$L_1 = 1.064$ mm $L_2 = 0.810$ mm
Frequencies of atomic-energy levels	$\omega_a = 66.542$ GHz, $\omega_b = 43.271$ GHz, $\omega_c = 25.555$ GHz
Cavity-modes frequencies	$\omega_1 = 23.27$ GHz, $\omega_2 = 17.71$ GHz
Frequencies of a bichromatic laser driving the cavity	$\omega_{L_1} = 741.0\pi$ THz, $\omega_{L_2} = 564.0\pi$ THz
Rate of atomic injection (r_a)	0.350 MHz
Atomic decay rates ($\gamma_a = \gamma_b$ $= \gamma_c = \gamma_{ab} = \gamma_{bc} = \gamma_{ac} = \gamma$)	11.50 MHz
Powers of input lasers driving the cavity ($P_1 = P_2$)	5.54 μW
Thermal baths temperatures to movable mirrors ($T_1 = T_2$)	5.80 mK
Photon number of squeezed vacuum reservoir (N)	1

[2006]; Verhagen et al. [2012]; Gröblacher et al. [2009] as shown in Table 4.1.

4.1.2 Quantification of entanglement via sum of quadrature variances

Quantification of entanglement in terms of the sum of quadrature variances is one of the approaches used to verify the entanglement between two mechanical modes Duan et al. [2000]. In this respect, a maximally entangled CV states can be expressed as a co-eigenstate of a pair of EPR-like operators $\hat{u}$ and $\hat{v}$, in which these quantum states are found to be entangled provided that the sum of the variances satisfies the inequality Tesfa [2006]

$$\Delta u^2 + \Delta v^2 < 2, \tag{4.8}$$

where

$$\hat{u} = \delta\tilde{H}_1 + \delta\tilde{H}_2, \;\; \hat{v} = \delta\tilde{L}_1 - \delta\tilde{L}_2, \tag{4.9}$$

with $[\delta\tilde{H}_j, \delta\tilde{L}_{j'}] = i\delta_{jj'}$. In the quantification of entanglement using the sum of quadrature variances of EPR-like operators, the entanglement becomes minimum when the sum of variances is respectively equal two, while it is maximum when it is zero. Anything in between is considered as a degree of entanglement in the sense that how much it is close to the maximum.

With the aid of Eqs. (3.191), (3.192), (4.9), and the relation $\langle\delta\tilde{H}_j\rangle = \langle\delta\tilde{L}_j\rangle = 0$, we obtain the sum of the variances of EPR-like operators at steady state as

$$\begin{aligned}\big(\Delta u^2 + \Delta v^2\big) &= \Big(\langle\delta\tilde{H}_1\delta\tilde{H}_1\rangle + \langle\delta\tilde{L}_1\delta\tilde{L}_1\rangle\Big) + \Big(\langle\delta\tilde{H}_2\delta\tilde{H}_2\rangle + \langle\delta\tilde{L}_2\delta\tilde{L}_2\rangle\Big) \\ &+ \Big(\langle\delta\tilde{H}_1\delta\tilde{H}_2\rangle + \langle\delta\tilde{H}_2\delta\tilde{H}_1\rangle - \langle\delta\tilde{L}_1\delta\tilde{L}_2\rangle - \langle\delta\tilde{L}_2\delta\tilde{L}_1\rangle\Big). \end{aligned} \tag{4.10}$$

Upon substituting the elements of CM for the correlations on the right side of Eq. (4.10) from the solution of Eq. (3.197), we obtain

$$\big(\Delta u^2 + \Delta v^2\big)_{\text{ss}} = \big[V_{11} + V_{22} + V_{33} + V_{44} + 2\big(V_{13} - V_{24}\big)\big]_{\text{ss}}. \tag{4.11}$$

4.1.3 Quantification of entanglement via product of quadrature variances

Another sufficient inseparability criterion to quantify the entanglement of two-mechanical modes involves the product of variances of CV operators. In the quantification of entanglement using this technique, the variances of the two CV operators $\hat{u}$ and $\hat{v}$ as described in Eq. (4.9) satisfies the inequality Mancini et al. [2002]

$$\Delta u^2 \Delta v^2 < 1. \tag{4.12}$$

In this context, the product of variances of these pairs of co-eigenstate of EPR-like operators reduces to zero for maximally entangled continuous variable states. But the entanglement in this case takes a value of one for minimal entanglement. Following to the previous detection of entanglement using the sum of variances of EPR-like operators, we employ (3.191) and Eqs. (4.9) once again in Eq. (4.12) so that we obtain the product of variances of quadrature operators as

$$\begin{aligned}\left(\Delta u^2 \Delta v^2\right) &= \Big[\langle\delta\tilde{H}_1\delta\tilde{H}_1\rangle + \langle\delta\tilde{H}_2\delta\tilde{H}_2\rangle + \langle\delta\tilde{H}_1\delta\tilde{H}_2\rangle + \langle\delta\tilde{H}_2\delta\tilde{H}_1\rangle\Big] \\ &\quad \times\Big[\langle\delta\tilde{L}_1\delta\tilde{L}_1\rangle + \langle\delta\tilde{L}_2\delta\tilde{L}_2\rangle - \langle\delta\tilde{L}_1\delta\tilde{L}_2\rangle - \langle\delta\tilde{L}_2\delta\tilde{L}_1\rangle\Big].\end{aligned} \tag{4.13}$$

Up on substituting the elements of CM from the solution of Eq. (3.197), we obtain the simplified steady state product of quadrature variances as

$$\left(\Delta u^2 \Delta v^2\right)_{ss} = \Big[\left(V_{11} + V_{33} + 2V_{13}\right) \times \left(V_{22} + V_{44} - 2V_{24}\right)\Big]_{ss}. \tag{4.14}$$

Noting that the mechanical oscillators in our system were not directly coupled initially, the quantum behavior of the two-mode cavity radiation in CEL emitted from cascade atoms Kiffner et al. [2007]; Tesfa [2011] could be transferred to the quantum harmonically oscillating mirrors due to the emerging optical radiation pressures.

In order to investigate the dependence of quadrature squeezing and entanglement of mechanical modes (modes of quantum harmonically oscillating mirrors) on various atomic, cavity and reservoir parameters such as amplitude of atomic pumping laser (χ), strength of atom-field coupling, rate of atomic injection, atomic decay rates, frequencies of a bichromatic laser, initial lengths of a doubly-resonant cavity, temperature(s) of the reservoir(s) coupled to mechanical modes, and photon numbers of squeezed vacuum reservoir coupled to cavity modes more closely, we plot the plus quadrature variance of fluctuation modes versus the amplitude (χ) of a laser that drive the atom for squeezing;

whereas the entanglement is plotted for the sum and product of EPR-like fluctuation-mode operators versus χ.

Making use of the generated laser, the induced coupling between two-quantum fluctuation modes of the mechanical oscillations shows squeezing and entanglement properties in a wide range of amplitude χ of a laser that drive the atom as indicated in Figs. (4.1)-(4.7). These quantum properties increase for smaller values of amplitude of atomic pumping laser with the highest degree of squeezing 77.750% and entanglement using Duan et al. [2000]. criterion being 77.759%, appearing at around $\chi \approx 4.11\gamma$ for the values given in Table 4.1.

Considering a well-established fact that the external radiation that pumps a three-level atom induces atomic coherent superposition can significantly modify the absorption-emission mechanism of atoms which is essentially responsible for a strong dependence of the nonclassical properties of the radiation on the amplitude of the driving radiation Tesfa [2011, 2008], we extend the exploration of the effect of the strength of a bichromatic laser that drive a doubly resonant cavity with regard to their frequencies so that in Fig. (4.1), the effect of varying the frequencies of the lasers driving the cavity on the degree of squeezing and entanglement of the mechanical modes is found to be investigated.

Table 4.2: Numerical values of the degree of quadrature squeezing and entanglement from Fig. 4.1 for different values of frequencies of a bichromatic cavity driving laser.

Frequencies of a bichromatic laser (THz)	Squeezing (below shot-noise)	Entanglement (below max.)	Occurs at ($\frac{\chi}{\gamma}$)
$\omega_{L_1} = 741.0\pi, \omega_{L_2} = 564.0\pi$	77.75%	77.759%	4.11
$\omega_{L_1} = 741.0\pi, \omega_{L_2} = 741.0\pi$	70.31%	70.31%	4.11
$\omega_{L_1} = 564.0\pi, \omega_{L_2} = 564.0\pi$	54.36%	54.38%	4.11
$\omega_{L_1} = 564.0\pi, \omega_{L_2} = 741.0\pi$	42.60%	42.45%	4.11

To this end, we first observe in this figure that the degree of induced quantum correlations of the mechanical modes at steady state as quantified by quadrature variance of the coupled fluctuation mode $\Delta(\delta C_+)^2$ in the case of squeezing and the sum of vari-

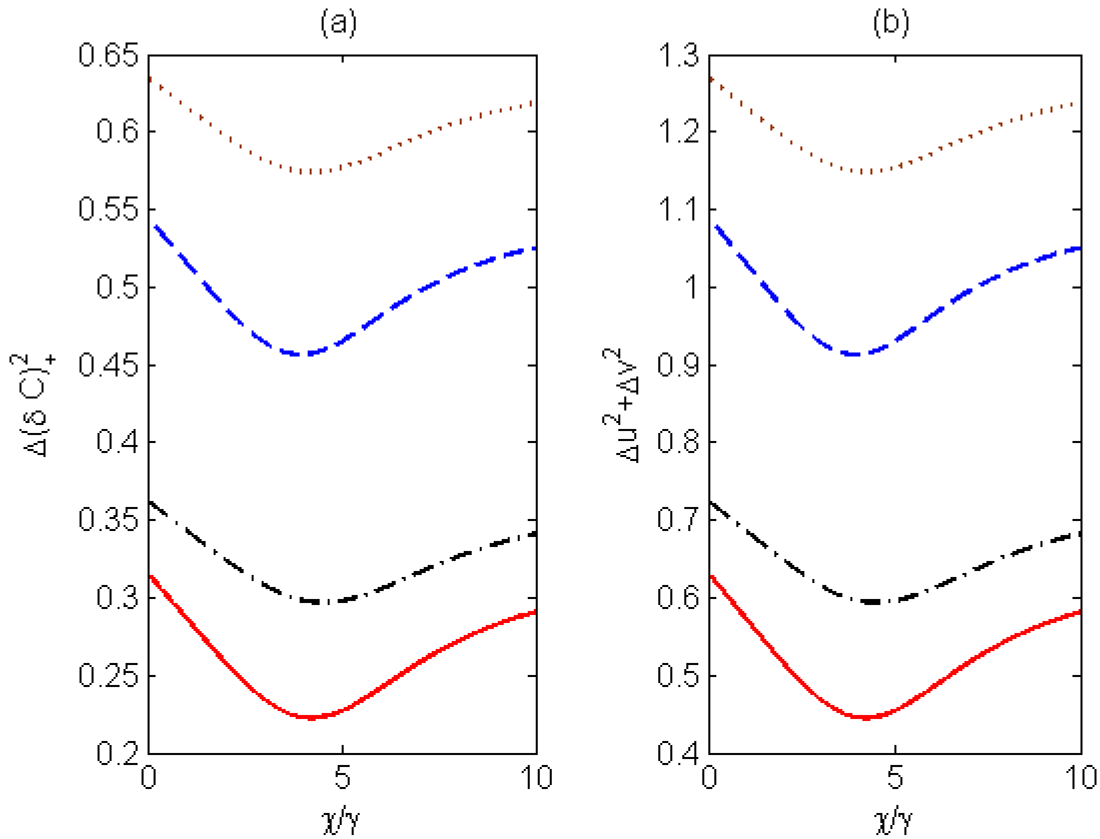

Figure 4.1: Plots of (a) quadrature variance of the two-mechanical oscillator modes $\Delta(\delta C_+)^2$ (Eq. (4.6)) and (b) the sum of quadrature variances of of EPR-like modes of mechanical oscillators $(\Delta u^2 + \Delta v^2)$ (Eq. (4.11)) against $\frac{\chi}{\gamma}$ at steady state for simultaneously applied two-input lasers driving the cavity with frequencies of $\omega_{L_1} = 741.0\pi$ THz and $\omega_{L_2} = 564.0\pi$ THz (red solid curve), $\omega_{L_1} = \omega_{L_2} = 741.0\pi$ THz (black dash-dotted curve), $\omega_{L_1} = \omega_{L_2} = 564.0\pi$ THz (blue dashed curve), and $\omega_{L_1} = 564.0\pi$ THz and $\omega_{L_2} = 741.0\pi$ THz (brown dotted curve). The other parameters are as shown in Table 4.1.
.

ances of EPR-like operators for entanglement $\Delta u^2 + \Delta v^2$ is found to be strongest as depicted in Table 4.2 when the frequency of a bichromatic laser ω_{L_1} is greater than that of ω_{L_2} (i.e. $\omega_{L_1} = 741.0\pi$ THz, $\omega_{L_2} = 564.0\pi$ THz), while the degree of squeezing is found to be weakest when a bichromatic laser's frequency ω_{L_1} is less than ω_{L_2} (i.e. $\omega_{L_1} = 564.0\pi$ THz, $\omega_{L_2} = 741.0\pi$ THz).

The degree of squeezing and entanglement are also enhanced but a little bit weaker than the strongest one for simultaneous input lasers of frequency $\omega_{L_1} = \omega_{L_2} = 741.0\pi$ THz. However, better degree of squeezing and entanglement than the weakest is observed when the frequencies of a bichromatic laser is $\omega_{L_1} = \omega_{L_2} = 564.0\pi$ THz. This can be explained by the fact that the degree of squeezing and entanglement are related directly to the effective couplings between the two-mechanical modes, G_{12} and G_{21}, so that the quadrature squeezing and entanglement can be enhanced as the effective couplings rely directly on the respective coupling terms induced by the two-photon coherence α_{12} and α_{21}, and on the product G_1G_2. Here, the $G_j = iG_{0_j}\langle\tilde{a}_j\rangle$ for $j = 1, 2$ which represents the many-photon coupling depend directly on the amplitude of a bichromatic laser via $\langle\tilde{a}_j\rangle = 2\epsilon_j/(\kappa_j + 2\alpha_{jj} - 2i\Delta_j)$.

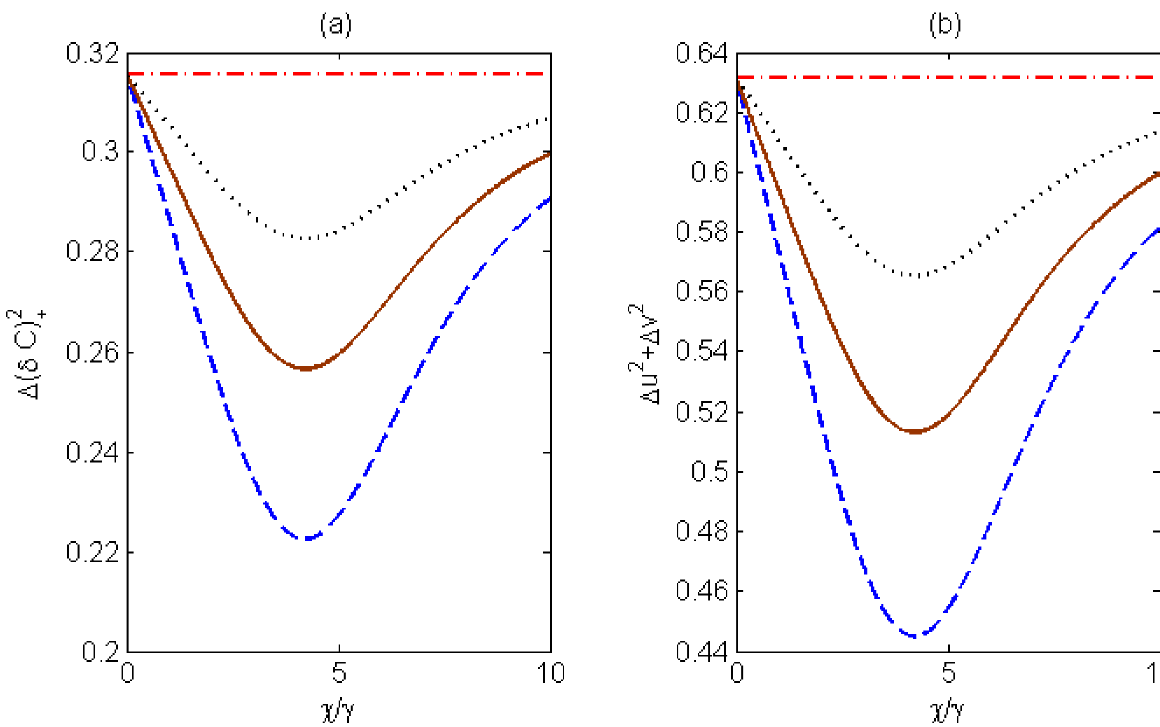

Figure 4.2: Plots of the steady-state (a) quadrature variance of the two-mechanical oscillator modes $\Delta(\delta C_+)^2$ (Eq. (4.6)) and (b) the sum of quadrature variances of EPR-like modes of mechanical oscillators $(\Delta u^2 + \Delta v^2)$ (Eq. (4.11)) against $\frac{\chi}{\gamma}$ for different atom-field coupling strengths $g_1 = g_2 = g = 5.0\pi$ MHz (blue dashed curve), $g = 4.0\pi$ MHz (brown solid curve), $g = 3.0\pi$ MHz (black dotted curve), and $g = 0$ (red dash-dotted curve). The other parameters are as shown in Table 4.1.

We notice in Fig. (4.2) and Table 4.3 that the degree of induced quadrature squeezing and entanglement of mechanical modes is enhanced with increased strength of atom-field coupling. It can also be observed that there is a threshold coupling between the atoms and the fields, $g = 8.92\pi$ MHz, above which the mechanical squeezing and entanglement would not be manifested. On the other hand, the mechanical squeezing

Table 4.3: Numerical value of the degree of quadrature squeezing and entanglement from Fig. 4.2 (a) and (b) for different values of atom-field coupling strength.

Atom - field coupling strength (MHz)	Squeezing (below shot-noise)	Entanglement (below max.)	Occurs at ($\frac{\chi}{\gamma}$)
$g = 5\pi$	77.75%	77.759%	4.11
$g = 4\pi$	74.34%	74.30%	4.11
$g = 3\pi$	71.73%	71.62 %	4.11
$g = 0$	68.43%	68.43%	[0.01, 10]

and entanglement can survive even at greater atom-field coupling strength in the case where the power of the laser driving the cavity is increased. Markedly, appropriate coupling between the atoms and cavity needs to be used to witness a meaningful degree of quadrature squeezing and entanglement.

Table 4.4: Numerical value of the degree of quadrature squeezing and entanglement from Fig. 4.3 (a) and (b) for different values of atomic injection rate.

Atomic - injection rate strength (MHz)	Squeezing (below shot-noise)	Entanglement (below max.)	Occurs at ($\frac{\chi}{\gamma}$)
$r_a = 0.35$	77.75%	77.759 %	4.11
$r_a = 0.25$	75.04%	75.03 %	4.11
$r_a = 0.15$	72.36%	72.36 %	4.11
$r_a = 0$	68.43%	68.43%	[0.01, 10]

In order to enhance and control the degree of squeezing and entanglement of the mechanical modes, we can also use different parameters of three-level atoms such as atomic injection rates and atomic decay rates. It is shown in Fig. (4.3) and Table 4.4 that the degrees of squeezing and entanglement of fluctuation mode of mechanical oscillators would be enhanced with the rate at which atoms are injected into the doubly resonant cavity due to the increase the quantum properties of cavity radiations that can be induced on the modes of mechanical oscillations through the coupling between cavity radiations and modes of movable mirrors. Maximum degrees of squeezing and entanglement is obtained when the atomic injection rates is 1.113 MHz, while deeply

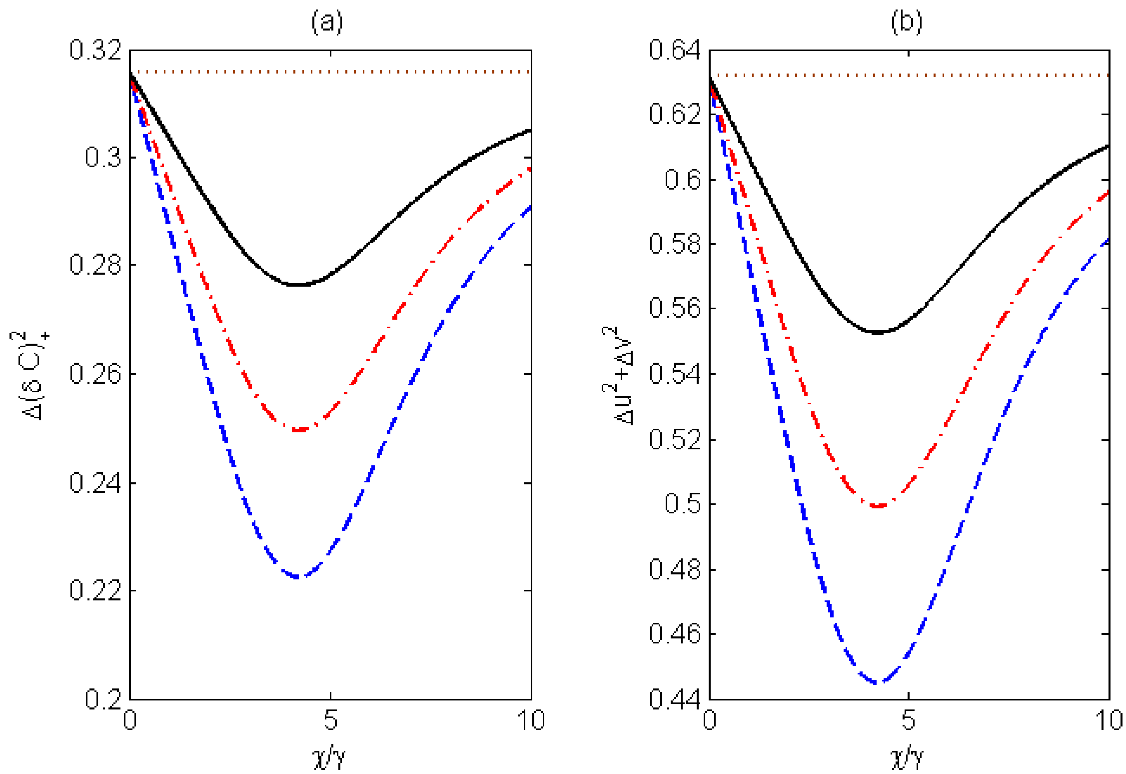

Figure 4.3: Plots of the steady-state (a) quadrature variance of the two-coupled modes of mechanical oscillators $\Delta(\delta C_{+})^2$ (Eq. (4.6)) and (b) the sum of variances of EPR-like modes of mechanical oscillators $(\Delta u^2 + \Delta v^2)$ (Eq. (4.11)) against $\frac{\chi}{\gamma}$ for different rates of atomic injection $r_a = 0.35$ MHz (blue dashed curve), $r_a = 0.25$ MHz (red dash-dotted curve), $r_a = 0.15$ MHz (black solid curve), $r_a = 0.0$ MHz (brown dotted curve). The other parameters are as shown in Table 4.1.

weak degree of these two quantum properties are exhibited when no atoms are injected ($r_a = 0$) into the cavity. On the other hand, squeezing and entanglement of the mechanical-modes can survive even at greater atomic injection rate than 1.113 MHz in the case where the power of the laser driving the cavity is increased. These outcomes indicate that the effect of the rate at which the atoms are injected into the cavity may provide a better control over squeezing and entanglement of mechanical modes.

To see the situation related to atomic parameters more closely, we also studied the dependence of the degree of induced squeezing and entanglement of mechanical modes on the atomic damping rate. As it is seen in Fig. (4.4), the degree of squeezing and entanglement depend on the value of the rate at which atoms are decayed γ.

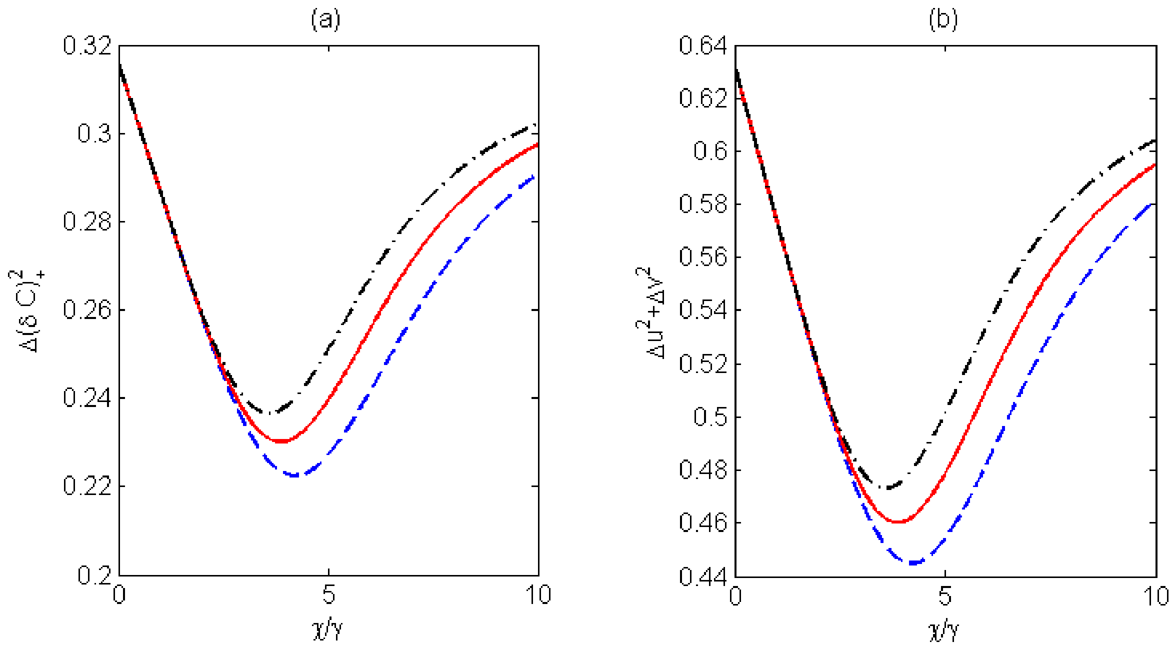

Figure 4.4: Plots of the (a) sum of quadrature variances of EPR-like modes $(\Delta u^2 + \Delta v^2)$ of mechanical oscillators (Eq. (4.11)) (b) quadrature variance of the two-coupled modes of mechanical oscillators $\Delta(\delta C_+)^2$ (Eq. (4.6)) against $\frac{\chi}{\gamma}$ for different atomic decay rates (assuming that the spontaneous and stimulated emission rates are the same) $\gamma = 11.50$ MHz (blue dashed curve), $\gamma = 12.50$ MHz (red solid curve), and $\gamma = 13.50$ MHz (black dashed-dotted curve). The other parameters are as shown in Table 4.1

Accordingly, the degrees of squeezing and entanglement of mechanical modes show overlapping-increase irrespective of the values of atomic decay rates until maximum values of squeezing and entanglement are achieved. Particularly, different atomic decay rates lead to the same mechanical modes squeezing and entanglement for $\chi/\gamma < 2.5$. But the degree of quadrature squeezing and entanglement decrease for larger atomic decay rate after obtaining optimum values of squeezing and entanglement. These results may reveal the effect of the atomic decay rates in increasing the degree of squeezing and entanglement of coupled oscillating mirrors with regards to how rapidly the atoms are removed from the lower-energy level.

We also explore the effect of the photon number of squeezed vacuum reservoir on the degree of induced squeezing and entanglement of mechanical modes.

The degree of squeezing and entanglement of mechanical modes is found to be

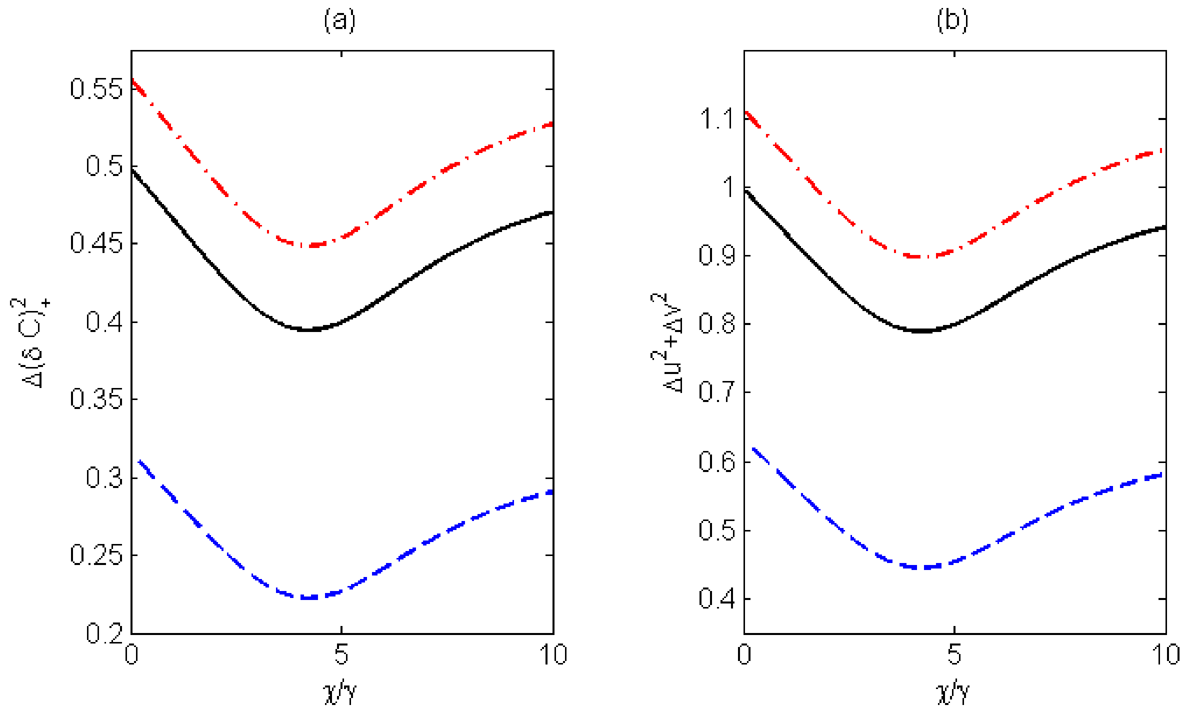

Figure 4.5: Plots of the steady-state (a) quadrature variance of the two-coupled mode mechanical oscillators $\Delta(\delta C_+)^2$ (Eq. (4.6)) and (b) the sum of quadrature variances $(\Delta u^2 + \Delta v^2)$ of EPR-like modes of mechanical oscillators (Eq. (4.11)) against $\frac{\chi}{\gamma}$ for different photon numbers of squeezed vacuum reservoirs coupled to cavity modes $N = 1.00$ (blue dashed curve), $N = 0.75$ (black solid curve), and $N = 0.50$ (red dash-dotted curve). The other parameters are as shown in Table 4.1.

Table 4.5: Numerical value of the degree of quadrature squeezing and entanglement from Fig. 4.4 (a) and (b) for different values of photon number of squeezed vacuum reservoir.

Photon number of squeezed vacuum reservoir	Squeezing (below shot-noise)	Entanglement (below max.)	Occurs at ($\frac{\chi}{\gamma}$)
$N = 1.00$	77.75%	77.759 %	4.11
$N = 0.75$	74.34%	60.55 %	4.11
$N = 0.50$	71.73%	55.073 %	4.11

enhanced with the photon number of squeezed vacuum reservoir or for intense of squeezed vacuum reservoir as shown in Fig. (4.5). From this point of view, it is possible to observe that the presence of squeezed vacuum reservoir is crucial for existence of squeezing of mechanical modes under certain conditions since its effect looks much better transferred to the squeezing property of mechanical oscillators. Very weak squeezing is also signified in the absence of squeezed vacuum reservoir $(N = 0)$ when the power of lasers driving the cavity is found to be higher i.e. $(554$ mW$)$ and when the strength of atom-field coupling gets weak $(1.95\pi$ MHz$)$. In contrary, optimum degree of induced bipartite mechanical-mode entanglement is found to be observed in the absence of squeezed vacuum reservoir $(N = 0)$ as the effect of noise resulting from squeezed vacuum reservoir is neglected. This entails that the induced squeezing and entanglement properties of the two of mechanical modes can also be controlled via the input external squeezed vacuum reservoir coupled to cavity radiations.

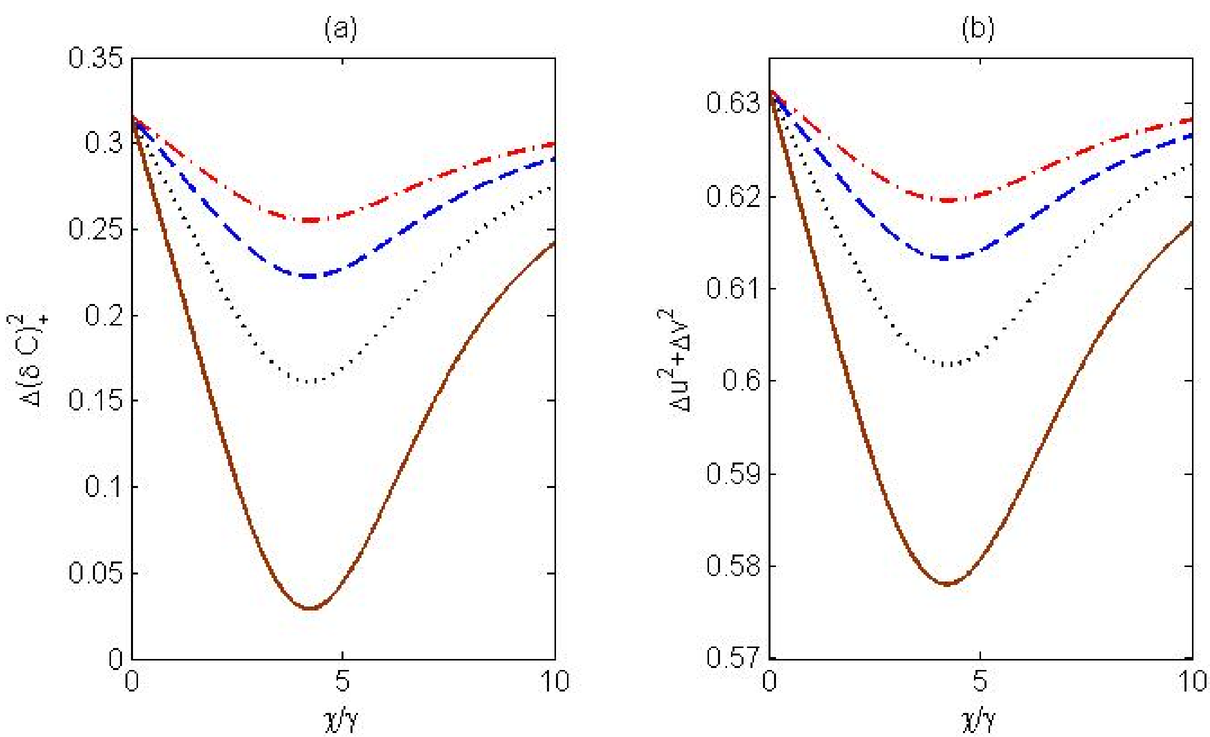

Figure 4.6: Plots of (a) quadrature variance of the two-coupled modes of mechanical oscillators $\Delta(\delta C_+)^2$ (Eq. (4.6)) and (b) the sum of quadrature variances of EPR-like modes of mechanical oscillators $(\Delta u^2 + \Delta v^2)$ (Eq. (4.11)) against $\frac{\chi}{\gamma}$ at steady state for different initial lengths of a doubly resonant cavity $L_1 = 0.7448$ mm and $L_2 = 0.567$ mm (brown solid curve), $L_1 = 0.9044$ mm and $L_2 = 0.6885$ mm (black dotted curve), $L_1 = 1.064$ mm and $L_2 = 0.810$ mm (blue dashed curve), $L_1 = 1.2236$ mm and $L_2 = 0.9315$ mm (red dash-dotted curve). The other parameters are as shown in Table 4.1.

.

According to the plots in Fig. (4.6) and the results depicted in Table4.6), a decrease in the initial lengths of a doubly resonant cavity is found to enhance the degree of squeezing and entanglement of the mechanical modes since it leads to increase the field-mirror coupling, which results in an increase in the effective coupling between mechanical modes that appears in direct relation to the correlations in the CM of a bipartite-mechanical modes. In addition, we see from Table 4.6 that the degree of

Table 4.6: Numerical value of the degree of quadrature squeezing and entanglement from Fig. 4.6 (a) and (b) for different values of initial lengths of a doubly resonant cavity.

Initial lengths of a doubly resonant cavity (mm)	Squeezing (below shot-noise)	Entanglement (below max.)	Occurs at $(\frac{\chi}{\gamma})$
$L_1 = 0.7448$, $L_2 = 0.567$	97.11%	71.09 %	4.11
$L_1 = 0.9044$, $L_2 = 0.6885$	83.85%	69.90 %	4.11
$L_1 = 1.064$, $L_2 = 0.810$	77.75%	69.34 %	4.11
$L_1 = 1.2236$, $L_2 = 0.9315$	74.50%	69.02%	4.11

squeezing shows significant variation for different initial lengths the cavity but the degree of entanglement exhibits insignificant difference for these initial lengths.

We also noted that the threshold initial lengths of the cavity for optimum degree of squeezing is $L_1 = 0.72352$ mm, $L_2 = 0.55080$ mm, but for that of maximum degree of entanglement the corresponding initial length is $L_1 = 0.3358$ mm, $L_2 = 0.25564$ mm. No squeezing and entanglement exists below these specific values of initial lengths for other values given in Table 4.1. This can be described by the fact that the field-mirror couplings, G_{0_1} and G_{0_2}, through which the transfer of quantum properties of the cavity radiation to the mechanical modes has been carried out; depend inversely on the their respective initial lengths of a doubly resonant cavity.

As clearly shown in figure 4.7, the degree of induced quadrature squeezing and entanglement in Duan et al. criterion of the mechanical modes is found to be enhanced for larger temperature(s) of the reservoir(s) coupled to the mechanical modes. The degree of squeezing and entanglement of mechanical modes is found to be maximum at a temperature of 7.50 mK; whereas the degrees of these quantum properties become

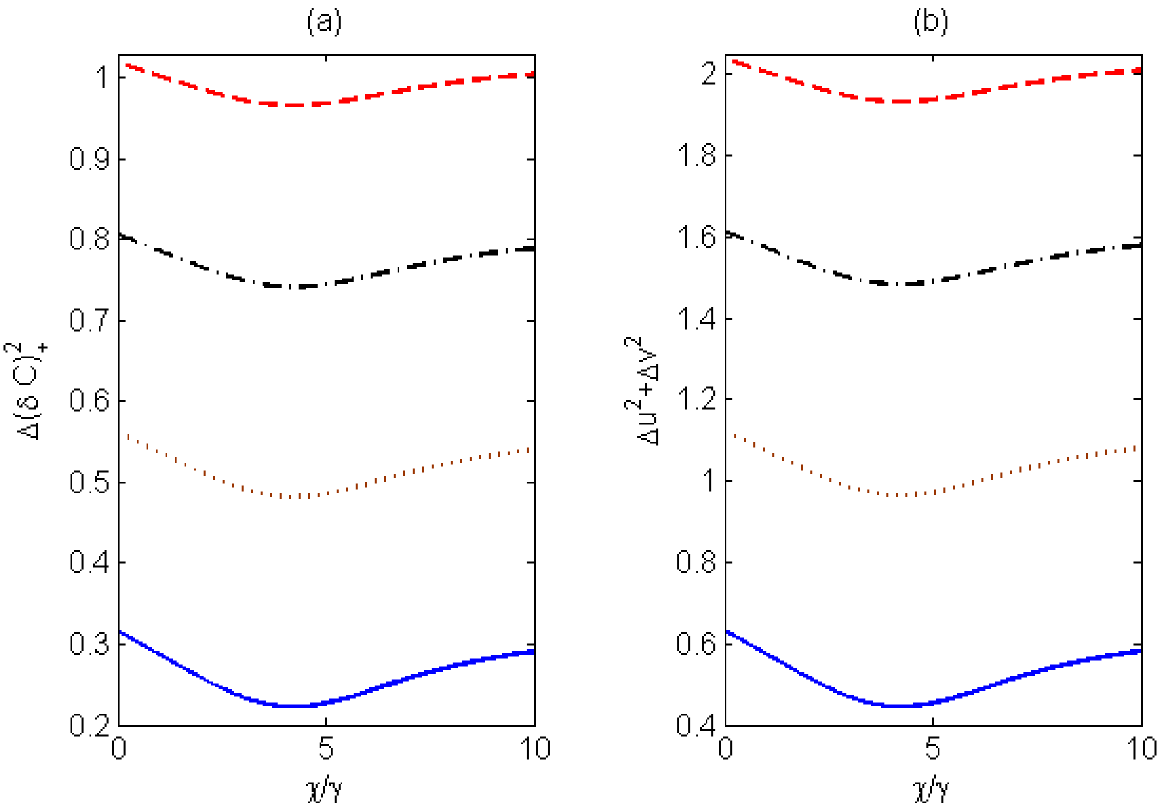

Figure 4.7: Plots of (a) $\Delta(\delta C_+)^2$ (Eq. (4.6)) and (b) $(\Delta u^2 + \Delta v^2)$ (Eq. (4.11)) against $\frac{\chi}{\gamma}$ at steady state for different temperatures of the thermal bath coupled to mechanical-modes $T = 5.8$ m K (blue solid curve), $T = 3.8$ m K (brown dotted curve), $T = 1.8$ m K (black dash-dotted curve), and $T = 0.0$ m K (red dashed curve). The other parameters are as shown in Table 4.1.

.

Table 4.7: Numerical value of the degree of quadrature squeezing and entanglement from Fig. 4.7 (a) and (b) for different values of temperature of a thermal bath coupled to the modes of harmonically oscillating mirrors.

Temperature of a reservoir coupled to mechanical modes	Squeezing (below shot-noise)	Entanglement (below max.)	Occurs at $(\frac{\chi}{\gamma})$
$T = 5.8$mK	77.75 %	77.76%	4.11
$T = 3.8$mK	51.79%	51.97%	4.11
$T = 1.8$mK	25.84%	25.86%	4.11
$T = 0$	3.41%	3.34%	4.11

weakest when the temperature of thermal baths coupled to mechanical modes as shown in Table 4.7 is $T = 0$ K as there exists zero-point energy at this temperature.

This can described by the fact that the lower the temperature of a bath coupled to quantum mechanical oscillators the smaller the oscillation of the movable mirror so that the correlation between the mechanical modes reduces. On the other hand, an increase in the temperature of a thermal bath generally increases the vibration of modes of the mechanical oscillator resulting in an increase in their quantum behaviors such as squeezing and entanglement.

To study the relation among various quantum correlations on the basis of quadrature

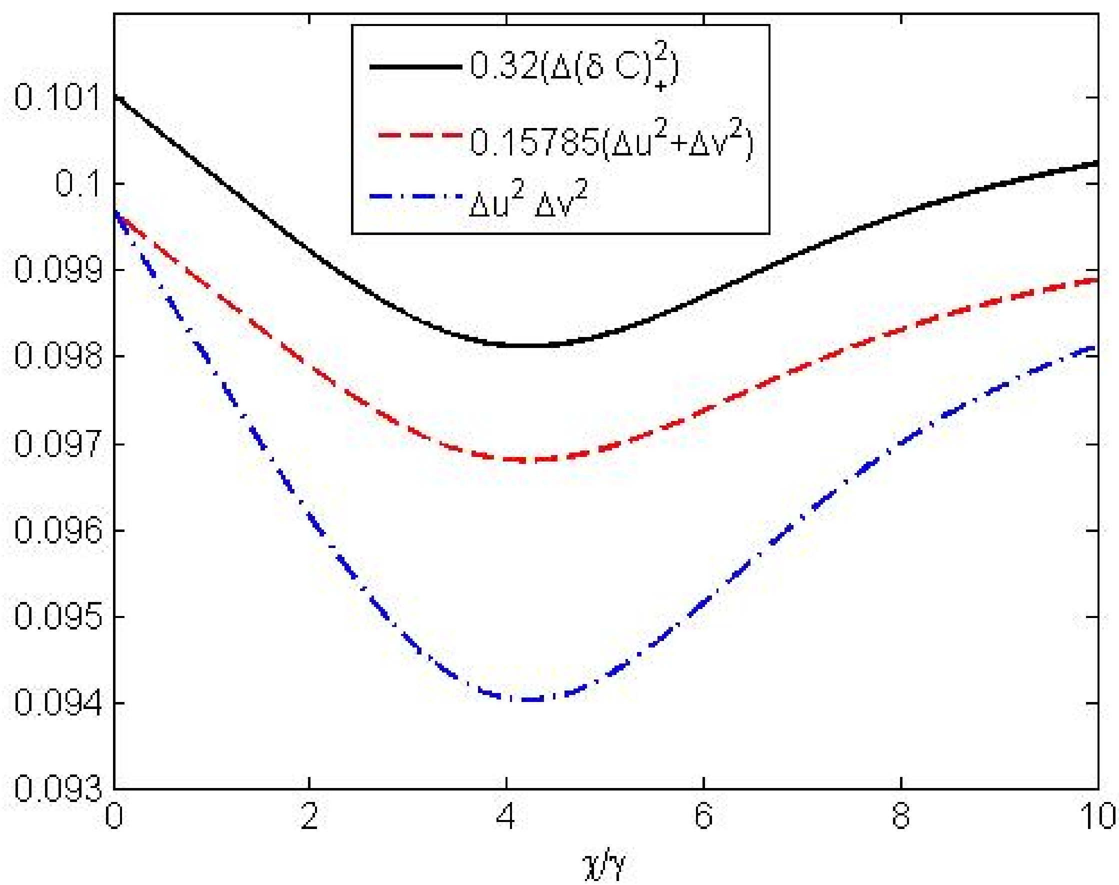

Figure 4.8: Plots of the steady state $\Delta(\delta C_+)^2$ (black solid curve), $(\Delta u^2 + \Delta\nu^2)$ (red dashed curve), and $(\Delta u^2 \Delta\nu^2)$ (blue dash-dotted curve) against χ/γ . The other parameters are as shown in Table 4.1.

.

variances and search for prospective conditions under which this quantum system shows robust movable mirrors squeezing and entanglement of the mechanical modes when optimal quantum state transfer from the two-mode cavity field to the mechanical modes is considered.

It is possible to infer from Fig. (4.8) that the trend of variation in the degree of quadrature squeezing and two different degree of entanglement measures using quadrature variances. Critical observation indicates that the overall tendency of quadrature squeezing follows the same pattern as the entanglement using the sum and product of EPR-like quadrature variances for the values given in Table 4.1 as these quantum behaviours associated with quadrature variances originate from the same source relying on the uncertainty relation. Particularly, the variances of the two-coupled mechanical modes $\Delta(\delta C_+)^2$ and the sum of variances of EPR-like operators $(\Delta u^2 + \Delta \nu^2)$ show perfect overlap for 0.3157 $(\Delta u^2 + \Delta \nu^2)$ and 0.15785 $\Delta(\delta C_+)^2$ which indicates that $(\Delta u^2 + \Delta \nu^2) = 2\,\Delta(\delta C_+)^2$.

Moreover, comparison between the two measures of entanglement at steady state has been carried out as shown in Fig. (4.8) with $\Delta u^2 + \Delta \nu^2$ (red dashed curve), and $\Delta u^2 \Delta \nu^2$ (blue dash-dotted curve) so as to see their interrelation. In this regard, it is noted that the inseparability associated with the product of variances of EPR-like operators $(\Delta u^2 \Delta \nu^2) < 1$ is stronger than that of the sum of variances of EPR-like operators $(\Delta u^2 + \Delta \nu^2) < 2$ with the same initial point which follows from $(\Delta u^2 \Delta \nu^2) \leq \frac{(\Delta u^2 + \Delta \nu^2)}{2}$ Mancini et al. [2002]. Nonetheless the above above two criteria originate from the same source, one can also observe that $(\Delta u^2 \Delta \nu^2)_{\mathrm{ss}}$ overlaps with $(\Delta u^2 + \Delta \nu^2)_{\mathrm{ss}}$ when $(\Delta u^2 \Delta \nu^2)_{\mathrm{ss}} = 0.15785(\Delta u^2 + \Delta \nu^2)_{\mathrm{ss}}$. In these measures optimum degree of entanglement, 69.32% and 70.62%, are achieved for the sum and product of EPR-like operators at the value of $\chi/\gamma = 4.11$, respectively.

4.2 Nonclassical Correlations via entropy measures

In this section, various results of nonclassical correlations between bipartite states other than the quantum features using quadrature variance is noticed in detail in relation to quantum information entropy such as the entanglement using logarithmic negativity measure, quantum discord and steering of the mechanical modes together with the effects of different atomic and cavity parameters on these quantum properties.

4.2.1 Quantification via logarithmic negativity

The prominent logarithmic negativity Vidal and Werner [2002] entanglement measure is based on the positive partial transpose (PPT) Peres [1996]; Horodecki et al. [1996] of a density matrix ρ_{AB}. In general, the PPT criterion is only a necessary but not a sufficient criterion for entanglement, i.e., there might be states that signal a vanishing logarithmic negativity that are, however, not separable. An extensive and instructive account of negativities for Gaussian states based on the well established fact that for the composite state to be separable to its constitute, the product density operator should have a PPT is available in Weedbrook et al. [2012].

Notably, the logarithmic negativity for CV is defined as

$$E_N = \max\left[0, -\ln(2\mathrm{V_s})\right], \tag{4.15}$$

where $\mathrm{V_s}$ is the smallest eigenvalue of the symplectic matrix Adesso et al. [2004b]. In line with this, the two mechanical modes are said to be entangled if and only if $\mathrm{E_N} > 0$ or $\mathrm{V_s} < \frac{1}{2}$. In this regard, the smallest symplectic eigenvalue $\mathrm{V_s}$ of the partial transpose of the 4×4 correlation matrix is found to have a form

$$\mathrm{V_s} = \left(\frac{\sigma - \left(\sigma^2 - 4\det V\right)^{\frac{1}{2}}}{2}\right)^{1/2}, \tag{4.16}$$

where

$$\sigma = \det V_A + \det V_B - 2\det V_C, \tag{4.17}$$

with V, V_A, V_B, and V_C expressed as in Eqs. (2.14) and (2.15).

4.2.2 Gaussian quantum discord

Despite increasing evidence for the relevance of quantum discord in describing non-classical resources in information processing, there is no direct criterion to verify the presence of discord in a given quantum state. Its evaluation involves optimization procedure, and analytical results are known only in a few cases Ollivier and Zurek [2001]; Luo [2008a]. A necessary and sufficient condition for the existence of nonzero quantum discord for any dimensional bipartite states have been obtained Wilde [2013]; Cover [1999]; Cerf and Adami [1997]. This condition is easily experimentally implementable Dakić et al. [2010].

The von Neumann entropy of n-mode Gaussian state with a covariance matrix (V) can be expressed as

$$S(\rho) = \sum_{i}^{N} f(v_i), \tag{4.18}$$

where $v_i's$ are the symplectic eigenvalues and

$$f(x) = \left(\frac{x+1}{2}\right)\ln\left(\frac{x+1}{2}\right) - \left(\frac{x-1}{2}\right)\ln\left(\frac{x-1}{2}\right). \tag{4.19}$$

Accordingly, the minimization relying on different approaches for a general two-mode Gaussian states σ leads to the two-mode Gaussian quantum discord of the form

$$D_{A|B} = D(\rho_{12}) = f(\sqrt{Y}) - f(v_-) - f(v_+) + f(\sqrt{E_{\min}}), \tag{4.20}$$

where $E_{\min}$ is given by

$$E_{\min} = \min_{\sigma_0} \det(\varepsilon) = \begin{cases} \frac{2C^2+(\frac{1}{4}-Y)(X-4D)+2|C|\sqrt{C^2+(\frac{1}{4}-Y)(X-4D)}}{4(\frac{1}{4}-Y)^2}, & \text{if } g \le 0; \\ \\ \frac{XY-C^2+D-\sqrt{C^4+(D-XY)^2-2C^2(XY+D)}}{2Y}, & \text{if } g > 0. \end{cases} \tag{4.21}$$

where σ_0 is the CM of the state ρ_0 that defines the POVM Holevo and Werner [2001] and the terms X, Y, C and D are described in Eq. (2.20).

The quantity g that discriminates the two cases in Eq. (4.21) is

$$g = (D - XY)^2 - (\frac{1}{4} + Y)C^2(X + 4D). \tag{4.22}$$

The case $g > 0$ corresponds to states for which the Gaussian discord is optimized by homodyne measurements. On the other hand, $g \leq 0$ corresponds to heterodyne measurements.

In the Gaussian scenario, it follows that the two-mode Gaussian states with zero Gaussian quantum discord are product states with no correlations at all. Note that correlated two-mode Gaussian states can exhibit nonclassical correlations certified by a nonzero quantum discord.

4.2.3 Gaussian Steering

Upon defining the CM and its elements as in Eqs. (2.14) and (2.15), the measure of steerability for continuous variable Gaussian state, in general, is found to be

$$G^{\{A\to B\}(\{B\to A\})} = -\ln\left(\sqrt{\frac{\det V}{\det V_A(V_B)}}\right). \tag{4.23}$$

Steerability exists for $G > 0$. The measure of Gaussian $B \to A$ steerability can be obtained by swapping the roles of A with B. Note that the higher degree of steerability amounts to the possibility of altering the state of the remote system without necessarily interacting with it; which might be handy to teleport quantum information reliably.

In order to investigate the various quantum properties in relation to entropy measures, we use the correlations in elements of CM which can be obtained from solution of Eq. (3.197). By applying these correlations into Eqs. (4.15) and (4.16) for entanglement, into Eqs. (4.20) - (4.22) for Gaussian quantum discord, and into Eqs. (2.28)-(4.23) for Gaussian steering; we plot various graphs where the entanglement is quantified with the aid of logarithmic negativity, and the other measures of nonclassical correlations using quantum discord and steering in the absence of squeezed vacuum reservoir ($N = M = 0$) which is in particular different from a value given, $N = 1$, in Table 4.1. In addition, we also see the effects of different atomic, cavity and reservoir parameters on these nonclassical properties with regard to entropy measures.

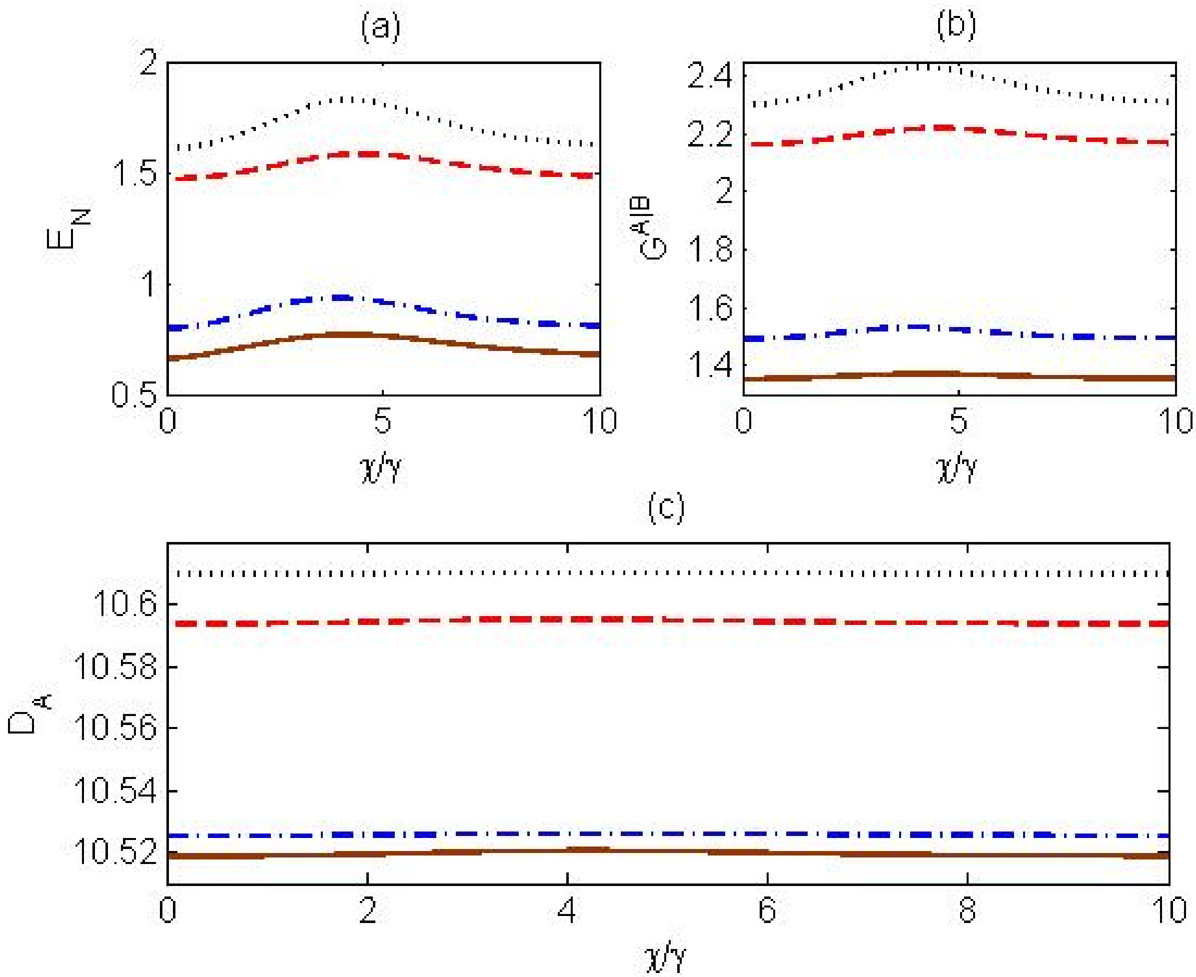

Figure 4.9: Plots of (a) entanglement using logarithmic negativity of the two-mechanical oscillator modes E_N (Eq. (4.15)) (b) steering $G^{A|B}$ of modes of mechanical oscillators (Eq. (4.23)), and (c) quantum discord D_A (Eq. (4.20)) against $\frac{\chi}{\gamma}$ at steady state for simultaneously applied two-input lasers driving the cavity with frequencies of $\omega_{L_1} = 741.0\pi$ THz and $\omega_{L_2} = 564.0\pi$ THz (brown solid curve), $\omega_{L_1} = \omega_{L_2} = 741.0\pi$ THz (blue dash-dotted curve), $\omega_{L_1} = \omega_{L_2} = 564.0\pi$ THz (red dashed curve), and $\omega_{L_1} = 564.0\pi$ THz and $\omega_{L_2} = 741.0\pi$ THz (black dotted curve). The other parameters are as shown in Table 4.1.
.

It has been demonstrated in previous chapter that the quantum behavior of the two-mode laser in CEL could be transferred to the modes of oscillations of the mov-

Table 4.8: Numerical values of optimum degrees of entanglement using logarithmic negativity (E_N) all occurring at $\chi/\gamma = 4.11$, Gaussian steering ($G^{(A|B)}$) all appearing at $\chi/\gamma = 4.11$ and Gaussian discord (D_A) taken place in all the ranges of χ/γ starting from 0.01 as indicated in Fig. 4.9 (a), (b) and (c) for different values of frequencies of a bichromatic cavity driving laser.

Frequencies of a bichromatic laser (THz)	E_N	$G^{(A\|B)}$	D_A
$\omega_{L_1} = 741.0\pi, \omega_{L_2} = 564.0\pi$	1.826	2.430	10.61
$\omega_{L_1} = 741.0\pi, \omega_{L_2} = 741.0\pi$	1.580	2.217	10.60
$\omega_{L_1} = 564.0\pi, \omega_{L_2} = 564.0\pi$	0.9329	1.530	10.53
$\omega_{L_1} = 564.0\pi, \omega_{L_2} = 741.0\pi$	0.7682	1.369	10.52

able mirrors using quadrature variances. Similarly, the quantification of nonclassical correlations in various entropy measures i.e. entanglement using the logarithmic negativity, Gaussian quantum discord (GQD), and Gaussian steering in the mechanical modes become induced due to the effective coupling between the cavity fields and mechanical modes. These nonclassical correlation properties are found to be observed in a wide range of the amplitude χ of a laser that drive the atom. For smaller values of amplitude of this laser, the degree of entanglement and Gaussian steering increase significantly; while the degree of quantum discord shows insignificant difference under the conditions given in Table 4.1.

The exploration of the effect of varying the strength of a bichromatic laser that drive a doubly resonant cavity with regard to their frequencies is shown in Fig. (4.9). To this end, we observe in this figure and Table 4.8 that the degree of these induced quantum correlations of the mechanical modes at steady state as quantified by entropy measures of entanglement using logarithmic negativity (E_N), Gaussian steering ($G^{A|B}$), and Gaussian quantum discord (D_A) varies in similar manner to Fig. (4.1).

As clearly shown in Table (4.8) that the degrees of entanglement, discord and steering of the mechanical modes become enhanced as the strength of field-mirror coupling, which rely directly on the frequency of a bichromatic laser, is found to be increased nonetheless, the degree of quantum discord shows slight difference. Particularly, optimum degree of entanglement $E_N = 1.826$, Gaussian steering $G^{A|B} = 2.43$ at $\chi/\gamma = 4.11$; whereas the value of Gaussian quantum discord is found to be 10.61 in all the ranges

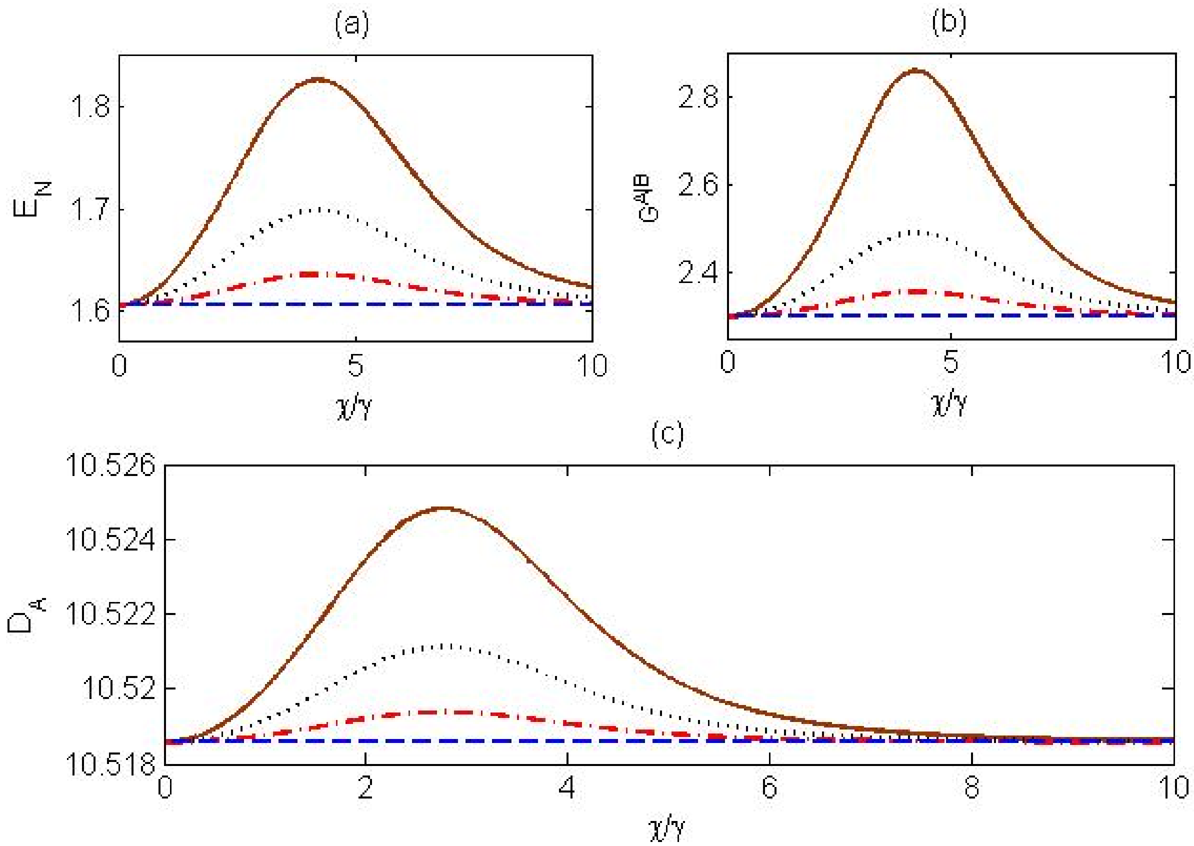

Figure 4.10: Plots of (a) entanglement using logarithmic negativity of the two-mechanical oscillator modes E_N (Eq. (4.15)) (b) steering $G^{A|B}$ of modes of mechanical oscillators (Eq. (4.23)), and (c) quantum discord D_A (Eq. (4.20)) at steady state against $\frac{\chi}{\gamma}$ for different atom-field coupling strengths $g_1 = g_2 = g = 5.0\pi$ MHz (brown solid curve), $g = 4.0\pi$ MHz (black dotted curve), $g = 3.0\pi$ MHz (red dash-dotted curve), and $g = 0$ (blue dashed curve). The other parameters are as shown in Table 4.1.

of $\chi = [0.01, 10]$. This large value of Gaussian quantum discord entails that a lot of information is missed: destroyed by the measurement on the apparatus alone. However, small discord can be considered as almost all information about the system that exists in the system-apparatus correlations can be locally recoverable from the state of the apparatus. On the other hand, it is noted also that the higher degree of steerability amounts to the possibility of altering the state of the remote system without necessarily interacting with it.

Table 4.9: Numerical values of the maximum degrees of entanglement using logarithmic negativity (E_N), Gaussian steering ($G^{A|B}$) and Gaussian quantum discord (D_A) from Fig. 4.10 (a), (b) and (c) for different values of atom-field coupling strength at $\chi/\gamma = 4.11$. But for $g = 0$ these nonclassical features occur in all the ranges of $\chi/\gamma = [0.01, 10]$
.

Atom - field coupling strength (MHz)	E_N	$G^{(A\|B)}$	D_A
$g = 5\pi$	1.826	2.430	10.5250
$g = 4\pi$	1.699	2.351	10.5195
$g = 3\pi$	1.636	2.315	10.5188
$g = 0$	1.606	2.299	10.5185

In Fig. (4.10), we observe that the degree of induced entanglement using logarithmic negativity, Gaussian quantum discord and Gaussian steering of mechanical modes is found to be enhanced with increased strength of atom-field coupling due to the increase in the coherence of atom-field, which can be induced on the modes of movable mirrors so as to enhance its quantum properties. In this context, the variation of quantum discord shows slight difference. It is also revealed from the data given in Table 4.9 that optimum degree of entanglement 1.826, Gaussian steering 2.430, and Gaussian quantum 10.5250 is manifested respectively at $\chi = 4.11\gamma$, $\chi = 4.11\gamma$, and in all the ranges of $\chi/\gamma = [0.01, 10]$. Also, smallest degree of these nonclassical properties are exhibited when there is no coupling between atoms and fields in the cavity. Noticeably, appropriate coupling between the atoms and cavity needs to be used to witness a worthwhile degree of nonclassical correlation in relation to quantum entropy measures.

In order to enhance and control the degree of entanglement of the mechanical-modes, we can also use different parameters of three-level atoms such as atomic injection rates and atomic decay rates.

It is shown in Fig. (4.11) and the data in Table 4.10 that the degrees of entanglement, Gaussian quantum discord and Gaussian steering of the mechanical modes would be enhanced with the rate at which atoms are injected into the doubly resonant cavity due to the increase the correlation in the coupled field-mirror modes. Weakest degrees

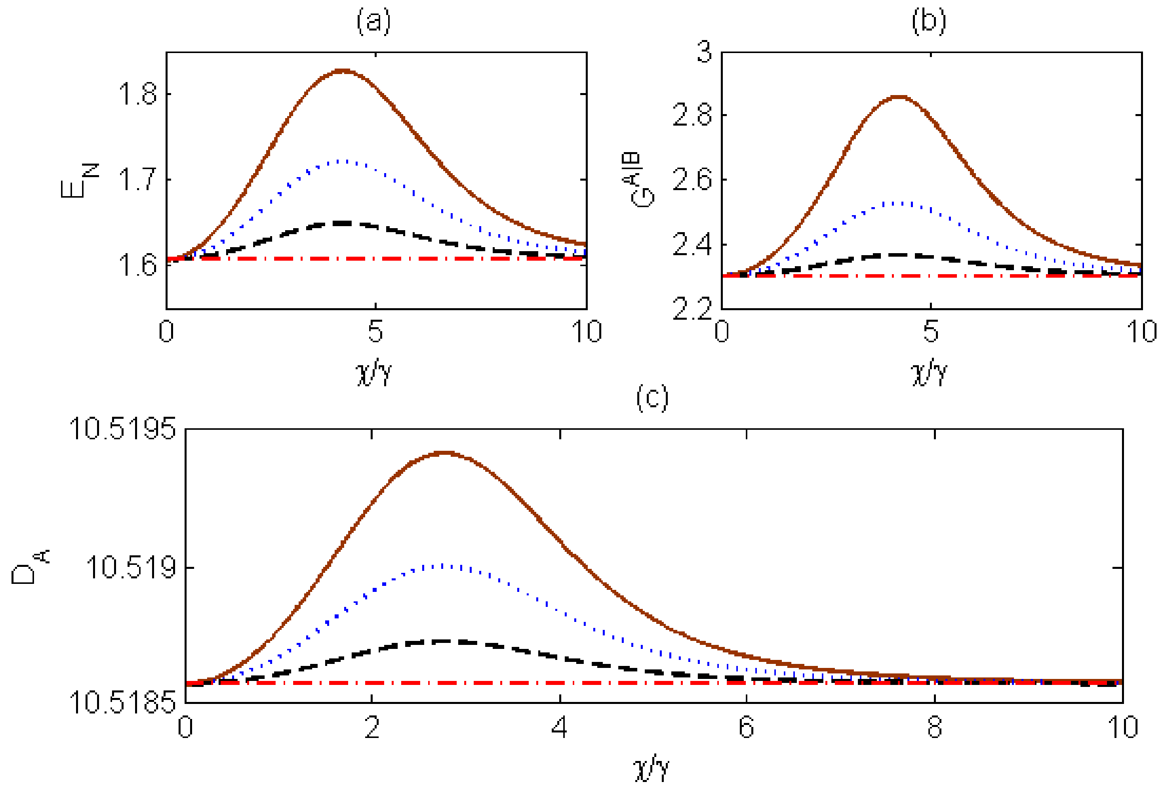

Figure 4.11: Plots of (a) entanglement using logarithmic negativity of the two-mechanical oscillator modes E_N (Eq. (4.15)) (b) steering $G^{A|B}$ of modes of mechanical oscillators (Eq. (4.23)), and (c) quantum discord D_A (Eq. (4.20)) at steady state against $\frac{\chi}{\gamma}$ for different rates of atomic injection $r_a = 0.35$ MHz (brown solid curve), $r_a = 0.25$ MHz (blue dotted curve), $r_a = 0.15$ MHz (red dashed curve), $r_a = 0.0$ MHz (red dash-dotted curve). The other parameters are as shown in Table 4.1.

Table 4.10: Numerical values of maximum degrees of entanglement using logarithmic negativity E_N, Gaussian steering ($G^{A|B}$), and Gaussian quantum discord (D_A) from Fig. 4.10 (a), (b) and (c) for different values of atomic injection rate at $\chi/\gamma = 4.11$. Nonclassical properties for $r_a = 0$ appear in all the ranges of $[0.01, 10]$.

Atomic injection rate strength (MHz)	E_N	$G^{A\|B}$	D_A
$r_a = 0.35$	1.826	2.430	10.5205
$r_a = 0.25$	1.721	2.364	10.5195
$r_a = 0.15$	1.648	2.322	10.5188
$r_a = 0$	1.606	2.299	10.5185

of these nonclassical features are found to be observed when no atoms are injected $(r_a = 0)$ into cavity. These results indicate that the effect of the rate at which the atoms are injected into the cavity in increasing the degrees of induced entanglement, discord and steering of the coupled mirrors may provide a better control over entanglement, and the ability to change the state of one party where the other party doesn't have any information about it. But the degree of quantum discord shows slight difference.

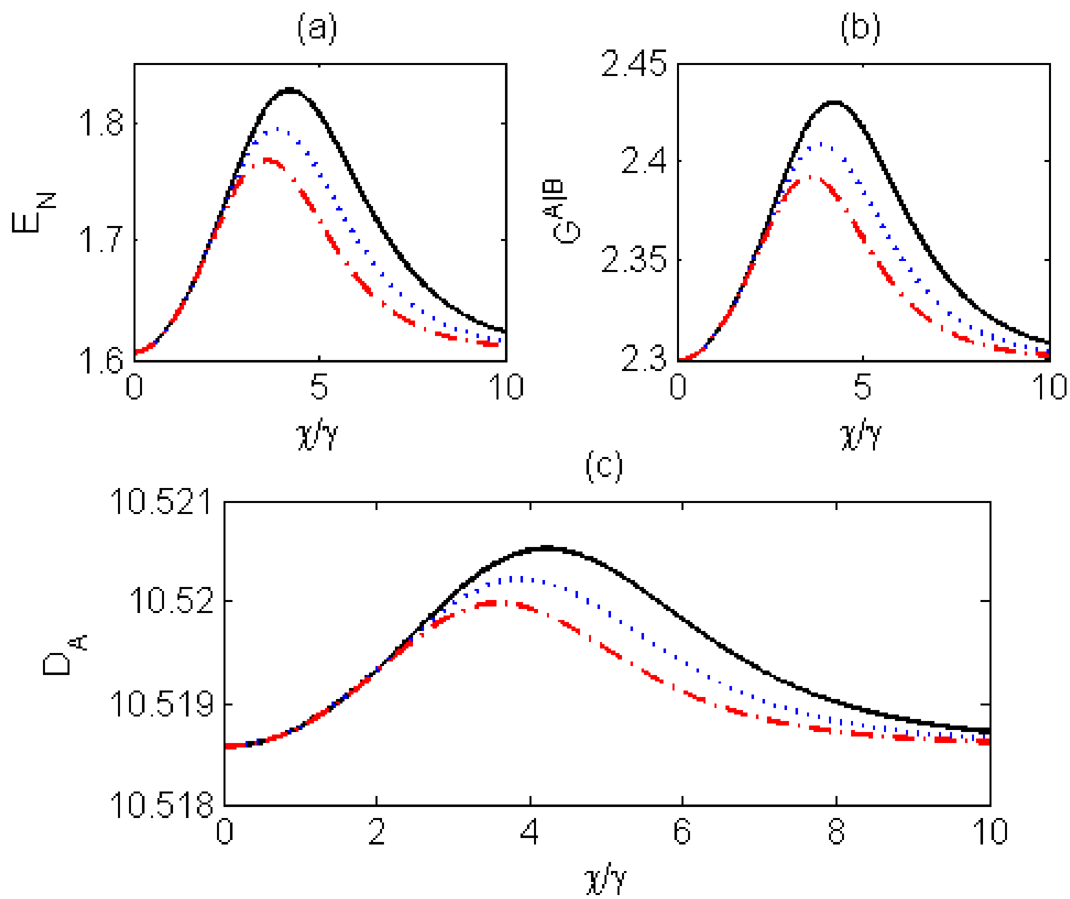

Figure 4.12: Plots of (a) entanglement using logarithmic negativity of the two-mechanical oscillator modes E_N (Eq. (4.15)) (b) steering $G^{A|B}$ of modes of mechanical oscillators (Eq. (4.23)), and (c) quantum discord D_A (Eq. (4.20)) at steady state against $\frac{\chi}{\gamma}$ for different values of atomic injection rates $\gamma = 11.50$ MHz (red dash-dotted curve), $\gamma = 12.50$ MHz (blue dotted curve), and $\gamma = 13.50$ MHz (black solid curve). The other parameters are as shown in Table 4.1.

We also studied the dependence of the degree of induced entanglement, Gaussian steering and Gaussian quantum discord of mechanical modes on the atomic decay rate to see the situation related to atomic parameters more closely.

As we can see from Fig. (4.12) and Table 4.11 that the effect of varying the atomic decay rate depends strongly on the value of χ/γ.

Table 4.11: Numerical values of maximum degrees of entanglement using logarithmic negativity (E_N), Gaussian quantum discord (D_A) and Gaussian steering ($G^{(A|B)}$) from Fig. 4.12 (a), (b) and (c) for different values of atomic decay rate.

Atomic emission rate strength (MHz)	E_N	$G^{(A\|B)}$	D_A	Appearing at χ/γ
$\gamma = 11.5$	1.826	2.430	10.5205	4.11
$\gamma = 12.5$	1.792	2.408	10.5202	3.80
$\gamma = 13.5$	1.768	2.392	10.5199	3.50

Accordingly, the degree of entanglement, steering and discord increase in the same manner irrespective of the values of atomic decay rates, respectively for the values of $\chi/\gamma < 2.75$. But the degrees of these nonclassical features after their optimum values decrease for smaller atomic decay rate. On the the other hand, optimum values of these nonclassical features have been observed to occur at different points due to the effect of various atomic decay rates. These results may reveal the effect of the atomic decay rates in increasing the degree of entanglement, Gaussian steering and Gaussian quantum discord of coupled quantum harmonically oscillating mirrors with regards to how rapidly the atoms are removed from the lower-energy level.

Table 4.12: Numerical value of maximum degree of entanglement using logarithmic negativity (E_N), Gaussian steering $(G^{(A|B)})$, and Gaussian quantum discord (D_A) from Fig. 4.14 (a), (b) and (c) for different values of initial lengths of a doubly resonant cavity at $\chi/\gamma = 4.21$.

Initial lengths of a doubly resonant cavity (mm)	E_N	$G^{(A\|B)}$	D_A
$L_1 = 0.76608$, $L_2 = 0.5832$	4.379	4.708	10.6107
$L_1 = 0.7980$, $L_2 = 0.6075$	3.143	3.523	10.589
$L_1 = 0.8512$, $L_2 = 0.6480$	2.493	2.942	10.580
$L_1 = 0.9576$, $L_2 = 0.7290$	2.017	2.562	10.542

According to the result depicted in Table 4.12 and the plots in Fig. (4.13), a decrease in the initial lengths of a doubly resonant cavity is found to significantly enhance the degree of entanglement, steering and discord of the mechanical modes since it

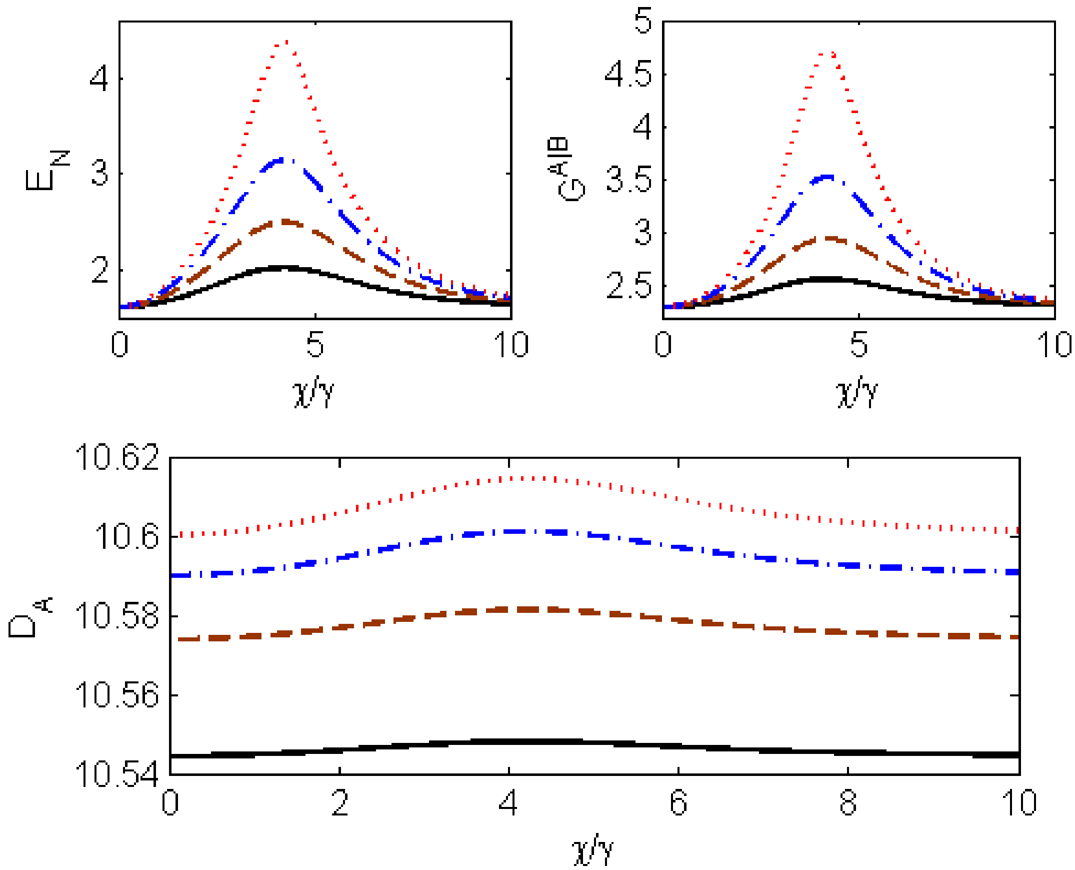

Figure 4.13: Plots of (a) entanglement using logarithmic negativity of the two-mechanical oscillator modes E_N (Eq. (4.15)) (b) steering $G^{A|B}$ of modes of mechanical oscillators (Eq. (4.23)), and (c) quantum discord D_A (Eq. (4.20)) against $\frac{\chi}{\gamma}$ at steady state for different initial lengths of a doubly resonant cavity $L_1 = 0.76608$ mm and $L_2 = 0.58320$ mm (red dotted curve), $L_1 = 0.7980$ mm and $L_2 = 0.6075$ mm (blue dash-dotted curve), $L_1 = 0.8512$ mm and $L_2 = 0.6480$ mm (brown dashed curve), $L_1 = 0.95760$ mm and $L_2 = 0.7290$ mm (black solid curve). The other parameters are as shown in Table 4.1.

.

increases the coherence of radiation in the cavity which can be induced on strength of field-mirror coupling which induce an increase in the effective coupling between mechanical modes that appears in direct relation to the correlations in the CM of a bipartite mechanical modes.

Particularly, the degree of Gaussian quantum discord shows a better variation with regard to the initial lengths of the cavity as compared to the effects of other atomic, cavity and reservoir parameters considered in this study. Markedly, suitable initial lengths of a cavity can be used to control the correlation and therefore various nonclassical properties of mechanical modes.

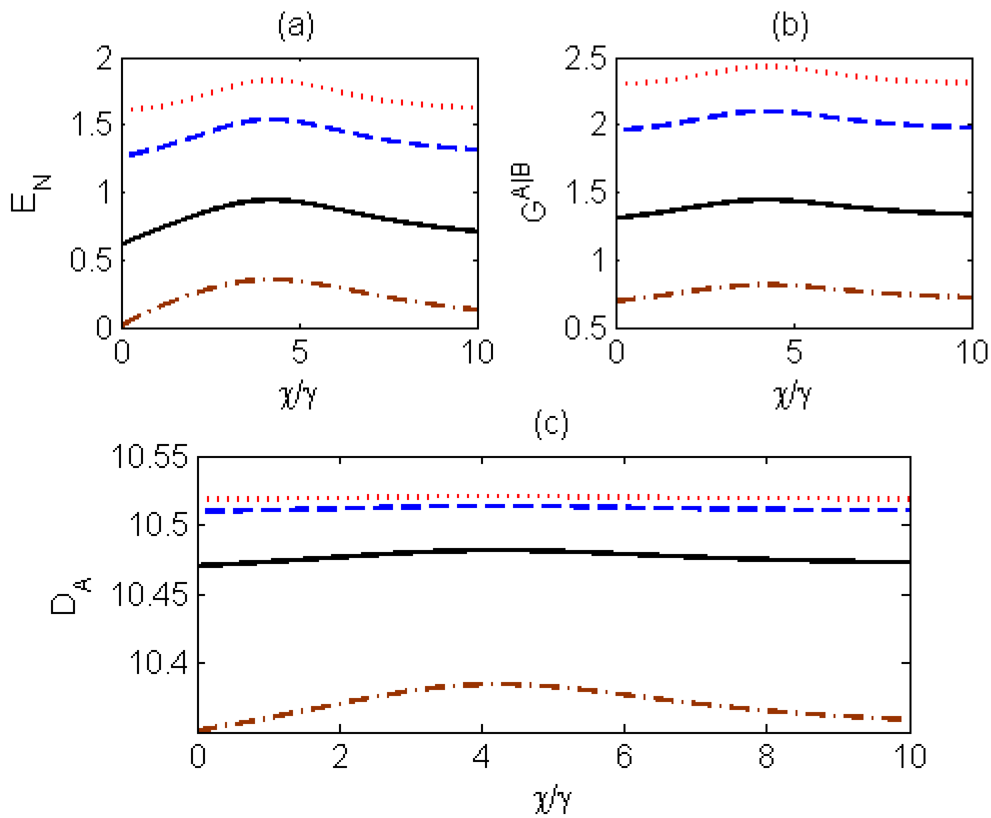

Figure 4.14: Plots of (a) entanglement using logarithmic negativity E_N (Eq. (4.15)) (b) steering $G^{A|B}$ (Eq. (4.23)), and (c) quantum discord D_A (Eq. (4.20)) of the two mechanical modes against $\frac{\chi}{\gamma}$ at steady state for different squeeze parameter of squeezed vacuum reservoir coupled to cavity modes $r = 0.5943$ (brown dash-dotted curve), $r = 0.40$ (black solid curve), $r = 0.20$ (blue dashed curve), and $r = 0.0$ (red dotted curve). The other parameters are as shown in Table 4.1.

We also explore the effect of squeezing parameter of squeezed vacuum reservoir on the degree of induced entanglement, quantum discord and steering of mechanical modes. The degree of quantum properties are found to be enhanced for smaller squeeze parameter as shown in Fig. (4.14) and depicted in Table 4.13 where the direct impact of squeezed vacuum reservoir on the coherence of cavity radiation become induced on the modes of quantum harmonically oscillating mirrors. Maximum degrees of these nonclassical features are found to be observed in the absence of squeezed vacuum

Table 4.13: Numerical value of the degree of entanglement (E_N), Gaussian steering ($G^{(A|B)}$) logarithmic negativity and Gaussian discord (D_A) from Fig. 4.14 (a), (b) and (c) for different values of squeeze parameter at $\chi/\gamma = 4.11$.

Squeeze parameter	E_N	$G^{(A\|B)}$	D_A
$r = 0.000$	1.826	2.430	10.5200 in all the range $[0.01, 10]$
$r = 0.200$	1.538	2.100	10.5075
$r = 0.400$	0.9416	1.442	10.485
$r = 0.5943$	0.3538	0.8131	10.385

reservoir ($r = 0$) as the effect of noise resulting from squeezed vacuum reservoir is neglected. This result entails that the various quantum properties of the two-induced coupled modes of mechanical oscillations can also be controlled via the input external squeezed vacuum reservoir coupled to cavity radiations.

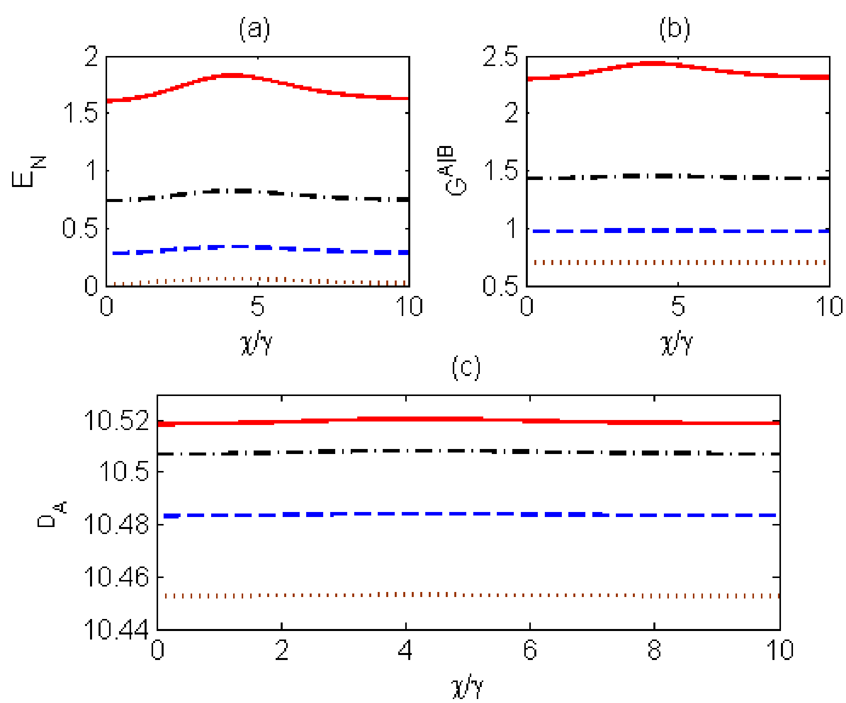

Figure 4.15: Plots of (a) entanglement using logarithmic negativity E_N (Eq. (4.15)) (b) steering $G^{A|B}$ (Eq. (4.23)), and (c) quantum discord D_A (Eq. (4.20)) of the two-mechanical modes against $\frac{\chi}{\gamma}$ at steady state for different temperatures of the reservoirs coupled to mechanical-modes $T = 5.8$ m K (red solid curve), $T = 3.8$ m K (black dash-dotted curve), $T = 1.8$ m K (blue dashed curve), and $T = 0.0$ m K (brown dotted curve). The other parameters are as shown in Table 4.1.

.

The degree of induced entanglement, Gaussian steering and Gaussian quantum discord in the mechanical modes is also found to be enhanced for higher temperature(s) of the reservoir(s) coupled to the mechanical modes as shown in Fig. (4.15). This result express that an increase in the temperature of a thermal bath generally increases the

Table 4.14: Numerical value of the degree of entanglement using logarithmic negativity (E_N), Gaussian steering ($G^{(A|B)}$), and Gaussian quantum discord (D_A) at $\chi/\gamma = 4.11$ from Fig. 4.15 (a), (b) and (c) for different temperatures of a thermal bath coupled to mechanical modes.

Temperature of a reservoir coupled to mechanical modes	E_N	$G^{(A|B)}$	D_A
$T = 0$	0.05556	0.6965	10.450
$T = 1.8$mK	0.3351	0.9777	10.482
$T = 3.8$mK	0.8212	1.454	10.485
$T = 5.8$mK	1.826	2.43	10.525

mean number of mechanical modes of quantum harmonically oscillating mirrors which leads to an increase in their nonclassical correlations such as entanglement, quantum discord and steering. Clearly, it is also shown in Table 4.14 that the degree of these quantum properties become weakest when the temperature of thermal baths coupled to mechanical modes is found to be $T = 0$ K. This can described by the fact that the lower the temperature of a bath coupled to quantum mechanical oscillators the smaller the oscillation of the movable mirror so that the correlation between the mechanical modes reduces.

4.3 Correlations of number of mechanical modes and Statistical properties

In this chapter, the correlation between the number of mechanical modes for instance entanglement witness using the Hillary-Zubairy (HZ) criterion, second order correlations and the statistical properties (the mean, variance, intensity difference and variance of intensity difference) of the mechanical modes is investigated.

4.3.1 Quantification of entanglement via Hillery Zubairy

On account of the relation of the criterion introduced by Hillary and Zubairy Hillery and Zubairy [2006]; Hillery et al. [2010] with the correlation of the number of modes of quantum harmonically oscillating mirrors and the corresponding intermodal correlation, the induced entanglement has been tipped to be quantifiable via simultaneous two-modes count measurement in similar manner to Tesfa [2009].

The first sufficient entanglement HZ criterion 1 (E_{HZ_1}) for the composite state of the modes of mechanical oscillators $\delta\tilde{b}_j$ $(j = 1, 2)$ is given as

$$\left|\langle\delta\tilde{b}_1\delta\tilde{b}_2\rangle\right|^2 - \langle\delta\tilde{b}_1^\dagger\delta\tilde{b}_1\rangle\langle\delta\tilde{b}_2^\dagger\delta\tilde{b}_2\rangle > 0, \tag{4.24}$$

whereas the second sufficient HZ criterion E_{HZ_2} is

$$\left|\langle\delta\tilde{b}_1^\dagger\delta\tilde{b}_2\rangle\right|^2 - \langle\delta\tilde{b}_1^\dagger\delta\tilde{b}_1\delta\tilde{b}_2^\dagger\delta\tilde{b}_2\rangle > 0, \tag{4.25}$$

where $\langle\delta\tilde{b}_1^\dagger\delta\tilde{b}_1\rangle$ and $\langle\delta\tilde{b}_2^\dagger\delta\tilde{b}_2\rangle$ are the mean of fluctuation modes of harmonically oscillating mirrors; whereas $\langle\delta\tilde{b}_1\delta\tilde{b}_2\rangle$ is the intermodal correlation between the mechanical modes.

The measure of entanglement using the HZ criterion as in Eq. (4.24) can also be rewritten as

$$E_{HZ_1} = \left|\langle\delta\tilde{b}_1\delta\tilde{b}_2\rangle\right|^2 - \langle\delta\tilde{b}_1^\dagger\delta\tilde{b}_1\rangle\langle\delta\tilde{b}_2^\dagger\delta\tilde{b}_2\rangle > 0. \tag{4.26}$$

With the aid of Eq.(4.24), and substituting the elements of CM from the solution of Eq.(3.197), we obtain the simplified steady state expression to the HZ criterion as

$$E_{HZ} \;=\; \frac{1}{4}\big|V_{13} - V_{24} + i\big(V_{14} + V_{23}\big)\big|^2 - \frac{1}{16}(V_{11} + V_{22} - 1) * (V_{33} + V_{44} - 1). \tag{4.27}$$

To this end, we investigate the dependence of the quantification of entanglement using the HZ criterion on the atomic parameters such as; the rate at which atoms are

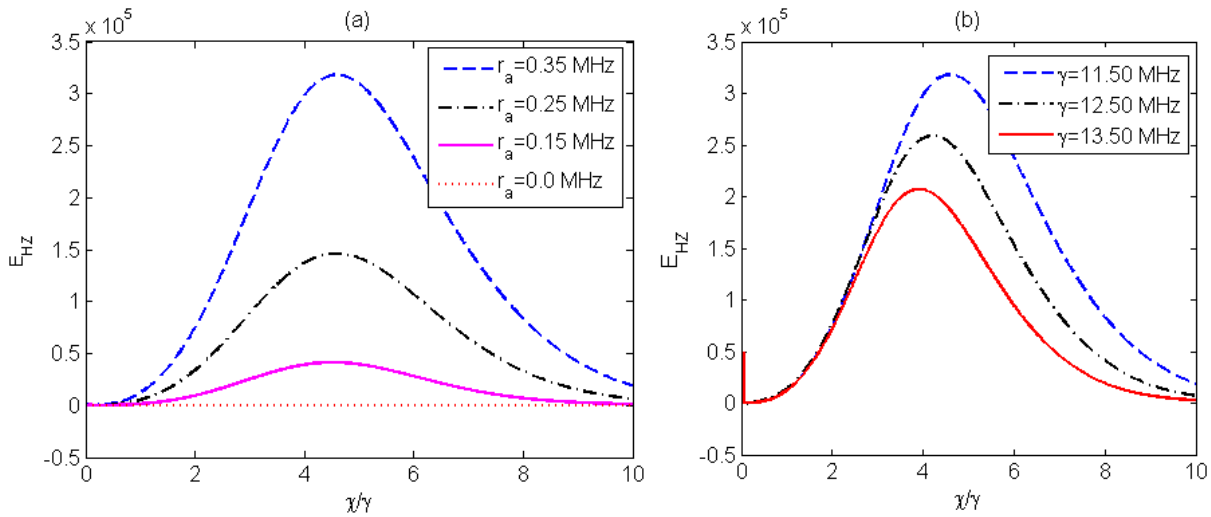

Figure 4.16: Plots of quantification of entanglement of the two-modes of quantum harmonically oscillating mirrors using Hillary-Zubairy criterion (E_{HZ}) against $\frac{\chi}{\gamma}$ at steady state with $g = 824.37$ MHz and various atomic parameters (a) for different atomic injection rate and (b) for different atomic decay rate. The other parameters are as shown in Table 4.1.

.

injected into cavity, the decay rate of atoms, and the strength of coupling between atom and cavity radiation. Besides, we investigate the dependence of this entanglement measure on the cavity parameter (initial lengths of a doubly resonant cavity) and the parameters of reservoirs coupled to cavity radiations and modes of mechanical oscillations.

It is clearly shown in Figs. (4.16)-(4.19) that the quantification of induced entanglement of the two-modes of quantum harmonically oscillating mirrors using the HZ criterion persists in a strong atom-field coupling with all other parameters given as in Table 4.1.

With this consideration, we show in Figs. 4.16 (a) and (4.17) that the degree of entanglement using the HZ criterion increases with the rate at which atoms are injected into cavity and with the strength of atom-field coupling; whereas the degree of entanglement is found to increase for smaller values of atomic decay rates and initial lengths of a doubly resonant cavity as indicated in Fig. 4.16 (b) and Fig. (4.18). This can be

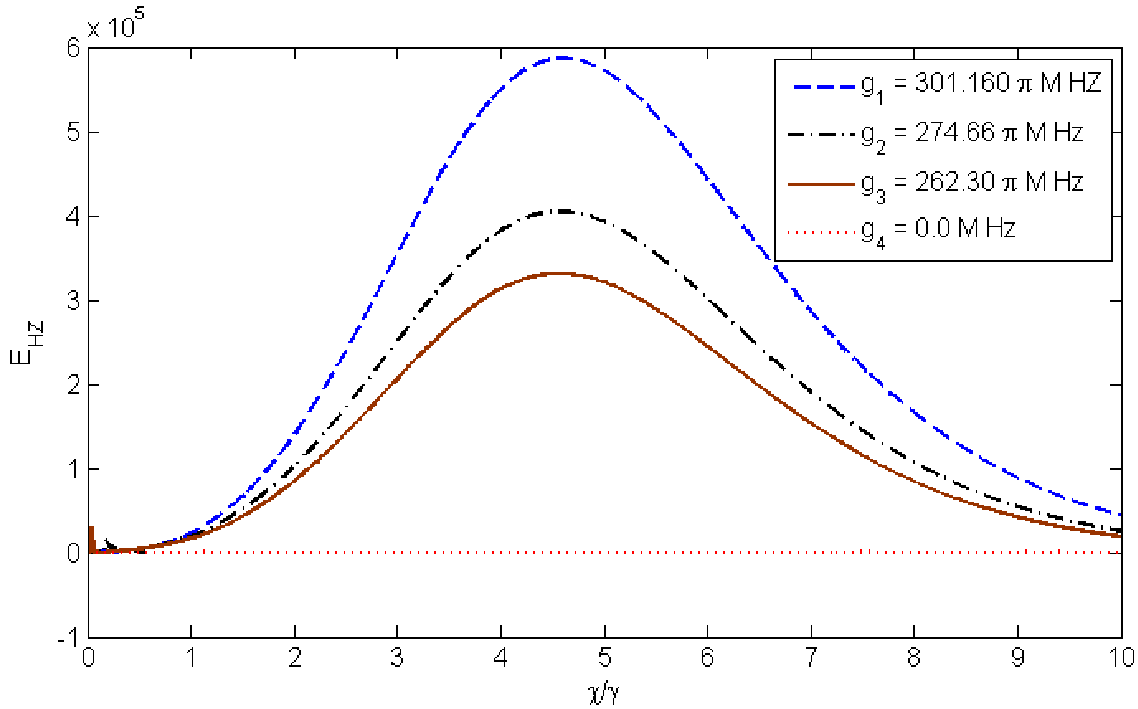

Figure 4.17: Plots of quantification of entanglement of the two-modes quantum harmonically oscillating mirrors using Hillary-Zubairy criterion (E_{HZ}) against $\frac{\chi}{\gamma}$ at steady state with $g = 824.37$ MHz for different initial lengths of the cavity. The other parameters are as shown in Table 4.1.

.

described due to the reason that the intermodal correlation between the mechanical modes is highly affected relative to the mechanical modes number correlation where the enhanced coherence of cavity radiation can lead to increased induced correlation between the mechanical modes.

With regard to the effect of squeeze parameter of a SVR coupled to the cavity radiation, and the impact of temperature(s) of thermal bath(s) coupled to mechanical modes, we observe the degree of entanglement using HZ-criterion as shown in Fig. (4.19). Particularly, the degree of entanglement using HZ-criterion increases significantly with the squeeze parameter even if the variation in the squeeze parameter is too small. Here, least degree of entanglement is observed in the absence of SVR. This result clearly shows that the noise originating from SVR enhances the intermodal correlation between the mechanical modes than that of mechanical modes number correlation.

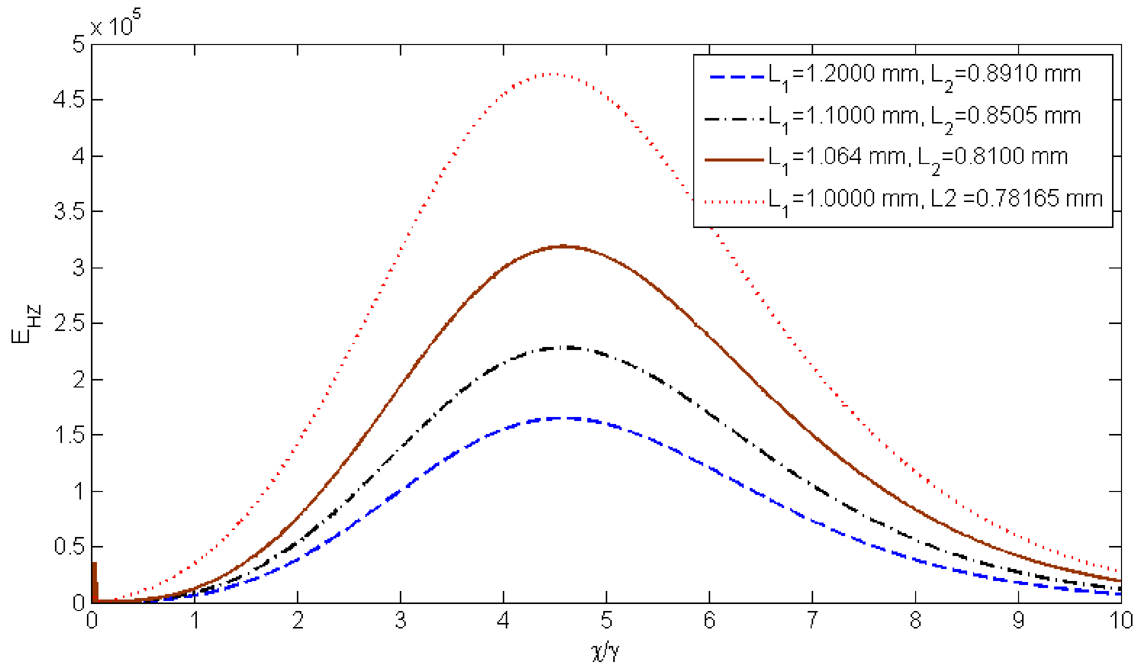

Figure 4.18: Plots of quantification of entanglement of the two-modes of quantum harmonically oscillating mirrors using Hillary-Zubairy criterion (E_{HZ}) against $\frac{\chi}{\gamma}$ at steady state with $g = 824.37$ MHz for different initial lengths of the cavity. The other parameters are as shown in Table 4.1.

.

On the other hand, the degree of entanglement using HZ criterion shows insignificant difference with the variation in temperature of a thermal bath coupled to the modes of quantum harmonically oscillating mirrors as indicated in Fig. (4.19) where these changes doesn't affect the intermodal and the mechanical modes number correlation.

In search of more appropriate and easy means of detecting entanglement, the trend of the detectable entanglement of the mechanical modes can be studied from different perspectives, where the degree of entanglement that can be predicted applying the sum and product of quadrature variances, logarithmic negativity, and HZ criteria are compared with each other. Critical observation indicates that the general tendency corresponding to atomic and cavity parameters follows more or less follow similar pattern except for the squeeze parameter of a two-mode SVR. The criterion obtained from HZ is violated more strongly than the corresponding logarithmic negativity criterion nonetheless these two criteria originate from different sources.

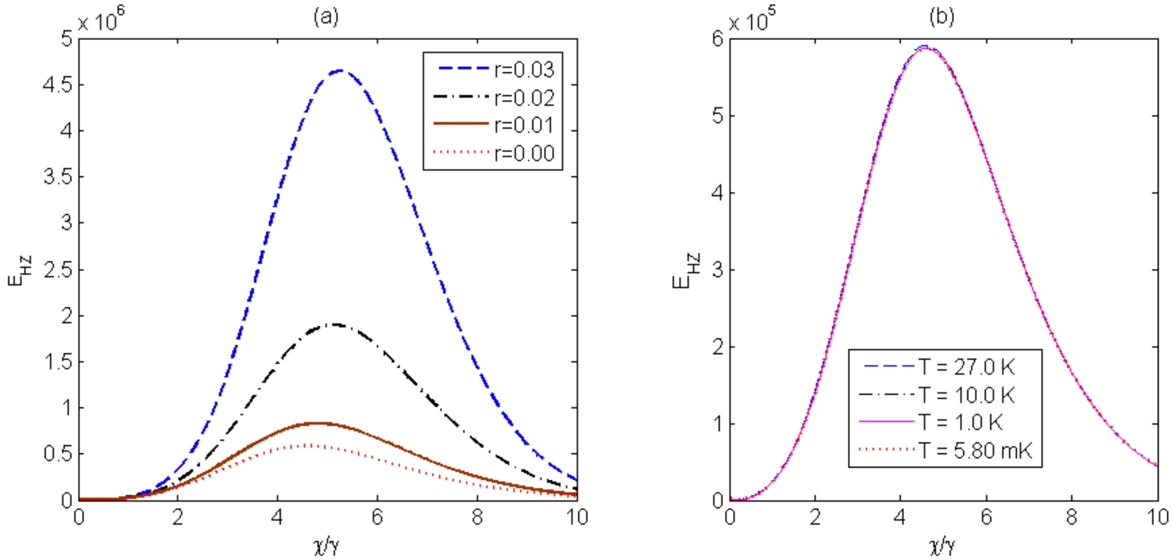

Figure 4.19: Plots of quantification of entanglement of the two-modes of quantum harmonically oscillating mirrors using Hillary-Zubairy criterion (E_{HZ}) against $\frac{\chi}{\gamma}$ at steady state with $g = 946.5$ MHz and various reservoir parameters (a) for different squeeze parameters of a squeezed reservoir coupled to cavity radiations. (b) for different temperature of thermal bath coupled to mechanical modes. The other parameters are as shown in Table 4.1.

.

4.3.2 Second order correlation

The second-order correlation function of the mechanical modes for the superposition of two-modes of the quantum harmonically oscillating mirrors can be expressed in normal order as

$$g^{(2)}_{\delta\tilde{b}_1,\delta\tilde{b}_2}(0) = \frac{\langle \hat{n}_{\delta\tilde{b}_1}\hat{n}_{\delta\tilde{b}_2}\rangle}{\langle \hat{n}_{\tilde{b}_1}\rangle\langle \hat{n}_{\tilde{b}_2}\rangle}, \tag{4.28}$$

where $\hat{n}_{\delta\tilde{b}_1}$ and $\hat{n}_{\delta\tilde{b}_2}$ are represented by $\hat{n}_{\delta\tilde{b}_1} = \delta\tilde{b}_1^\dagger\delta\tilde{b}_1$ and $\hat{n}_{\delta\tilde{b}_2} = \delta\tilde{b}_2^\dagger\delta\tilde{b}_2$.

Since $\delta\tilde{b}_1$ and $\delta\tilde{b}_2$ are Gaussian variables with vanishing means, Eq. (4.28) can be written as

$$g^{(2)}_{\delta\tilde{b}_1,\delta\tilde{b}_2}(0) = 1 + \frac{\langle \delta\tilde{b}_1^\dagger\delta\tilde{b}_2\rangle^2 + \langle \delta\tilde{b}_1\delta\tilde{b}_2\rangle^2}{\langle \delta\tilde{b}_1^\dagger\delta\tilde{b}_1\rangle\langle \delta\tilde{b}_2^\dagger\delta\tilde{b}_2\rangle}. \tag{4.29}$$

On account of the elements of CM from the solution of Eq. (3.197), we find

$$g^{(2)}_{(\delta\tilde{b}_1,\delta\tilde{b}_2)}(0) = 1 + \frac{\big(V_{13} + V_{24} + \mathrm{i}(V_{14} - V_{24})\big)^2 + \big(V_{13} - V_{24} + \mathrm{i}(V_{14} + V_{23})\big)^2}{\big(V_{11} + V_{22} - 1\big)\big(V_{33} + V_{44} - 1\big)}. \tag{4.30}$$

This function would not be a direct measure of various nonclassical features as it deals with correlation between the mechanical modes numbers. However, as we will see below, it would be an indirect inference for the existence of nonclassical features as it exhibits quantum correlation that violates certain classical inequalities.

Therefore, it is also essential to calculate the second-order correlation function for the individual modes to have an insight for the above result. To this end, the second order correlation function for the first mode $\delta\tilde{b}_1$ corresponding to no time delay is given by

$$g^{(2)}_{(\delta\tilde{b}_1,\delta\tilde{b}_1)}(0) = \frac{\langle\delta\tilde{b}_1^{\dagger^2}\delta\tilde{b}_1^2\rangle}{\langle\delta\tilde{b}_1^{\dagger}\delta\tilde{b}_1\rangle\langle\delta\tilde{b}_1^{\dagger}\delta\tilde{b}_1\rangle}. \tag{4.31}$$

$$g^{(2)}_{(\delta\tilde{b}_1,\delta\tilde{b}_1)}(0) = 1 + \frac{\langle\Delta N^2_{\delta\tilde{b}_1}\rangle - \langle N_{\delta\tilde{b}_1}\rangle}{\langle N_{\tilde{b}_1}\rangle^2}. \tag{4.32}$$

The condition of the mode $\delta\tilde{b}_1$ exhibiting sub-Poissonian distribution which may accompany antibunching that appears in Eq. (4.32) can be expressed as

$$G_{\delta\tilde{b}_1} = \langle N_{\delta\tilde{b}_1}\rangle - \langle\Delta N^2_{\delta\tilde{b}_1}\rangle > 0. \tag{4.33}$$

Similarly, the condition for $\delta\tilde{b}_2$ mode is as follows,

$$G_{\delta\tilde{b}_2} = \langle N_{\delta\tilde{b}_2}\rangle - \langle\Delta N^2_{\delta\tilde{b}_2}\rangle > 0. \tag{4.34}$$

Now comparing $[g^{(2)}_{(\delta\tilde{b}_1,\delta\tilde{b}_2)}(0)]^2$ with $g^{(2)}_{(\delta\tilde{b}_1,\delta\tilde{b}_1)}(0)\; g^{(2)}_{(\delta\tilde{b}_2,\delta\tilde{b}_2)}(0)$, we see that

$$\left[g^{(2)}_{(\delta\tilde{b}_1,\delta\tilde{b}_2)}(0)\right]^2 > g^{(2)}_{(\delta\tilde{b}_1,\delta\tilde{b}_1)}(0) g^{(2)}_{(\delta\tilde{b}_1,\delta\tilde{b}_2)}(0).$$

This is a violation of Cauchy-Schwartz in equality Walls and Milburn [2008]. Therefore, we infer from this result that the two-mode quantum harmonically oscillating mirrors exhibits quantum-mechanical correlation which is a source of induced nonclassical features of the mechanical modes.

4.3.3 Mean number of mechanical modes

The statistical properties of modes of harmonically oscillating mirrors is described in terms of the mean and variance of the mechanical-fluctuation modes $\delta\tilde{b}_1$ and $\delta\tilde{b}_2$.

In relation to the robustness of the nonclassical features of mechanical modes to be generated, it is necessary to evaluate the mean photon number, which is directly associated with the intensity of the modes of harmonically oscillating mirrors. In order to attest to the potential of the system under consideration as a reliable source of a two-mode mechanical squeezing, the evolution of the photon number for the mechanical modes cavity radiation is studied.

To determine the mean number of mechanical mode pairs of quantum harmonically oscillating mirrors, it can be described by an operator of the form

$$\delta\tilde{c} = \frac{1}{2}(\delta\tilde{b}_1 + \delta\tilde{b}_2), \tag{4.35}$$

where $\delta\tilde{b}_1$ and $\delta\tilde{b}_2$ represent the separate modes of mechanical oscillation.
To this end, we first write based on Eq. (4.35) that

$$\langle\delta\tilde{c}^\dagger\delta\tilde{c}\rangle = \frac{1}{4}\left(\langle\delta\tilde{b}_1^\dagger\delta\tilde{b}_1\rangle + \langle\delta\tilde{b}_2^\dagger\delta\tilde{b}_2\rangle + \langle\delta\tilde{b}_1^\dagger\delta\tilde{b}_2\rangle + \langle\delta\tilde{b}_2^\dagger\delta\tilde{b}_1\rangle\right). \tag{4.36}$$

Therefore, $\langle\delta\tilde{c}^\dagger\delta\tilde{c}\rangle$ can be interpreted as the mean number of modes of quantum harmonically oscillating pairs, $\bar{n}$.

On account of elements of correlations from the solution of Eqs. (3.197) and (4.36), we find mean number of two modes of quantum harmonically oscillating mirrors at steady state as

$$\bar{n} \;\; = \;\; \frac{1}{4}\left[\frac{V_{11}+V_{22}+V_{33}+V_{44}}{2} + \big(V_{13}+V_{24}\big) - 1\right]_{\mathrm{ss}}. \tag{4.37}$$

With the aid of Eq. (4.37), we plot various graphs of the mean number of the two-mode quantum harmonic oscillator depending on the effect of atomic, cavity and reservoir parameters.

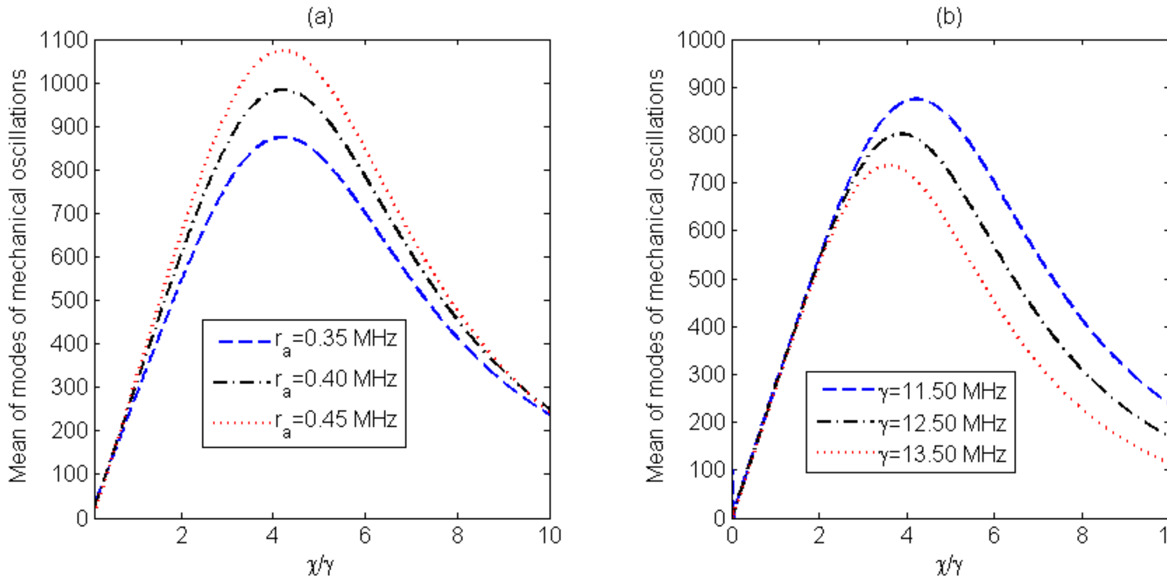

Figure 4.20: Plots of mean number of two-mode quantum harmonically oscillating mirrors $\bar{n}$ against $\frac{\chi}{\gamma}$ at steady state depending on atomic parameters (a) for different atomic injection rate (b) for different atomic decay rate. The other parameters are as shown in Table 4.1.

.

As can readily be inferred from Figs. (4.20), (4.21), and (4.22), the mean number of mechanical mode pairs of the quantum harmonically oscillating mirrors strongly depend on the injection rate and decay rates of the atoms, the initial lengths of the cavity, the amplitude of a laser that driving the atoms, and the temperature as well as squeeze parameter of reservoirs.

Accordingly, the mean number of modes of harmonically oscillating mirror pairs increases for smaller amplitude of the atomic-driving radiation, larger atomic injection rate as in Fig. 4.20 (a), smaller initial lengths of a doubly resonant cavity as indicated in Fig. (4.21). On the other hand, the plots in Fig. 4.20 (b) show that the mean number of mechanical modes decreases for large γ. This must be due to stimulated emission induced by the pump mode. The photons emitted this way do not contribute to the mean photon number of the cavity modes which can be induced to the mechanical

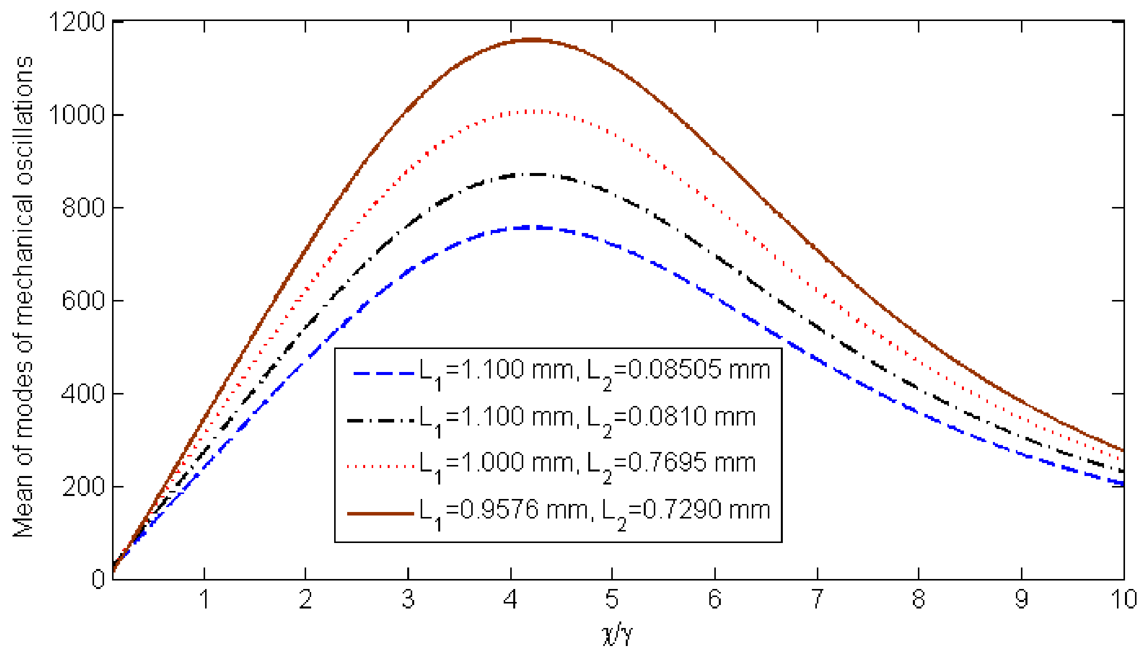

Figure 4.21: Plots of mean number of two-mode quantum harmonically oscillating mirrors $\bar{n}$ against $\frac{\chi}{\gamma}$ at steady state with $g = 9.0\pi$ MHz for different initial lengths of a doubly resonant cavity. The other parameters are as shown in Table 4.1.

.

modes.

It is also observed in Fig. 4.22 (a) that the mean number of mechanical modes is found to be enhanced for larger squeeze parameter of a SVR coupled to cavity radiation as the noise entering the cavity increases the intensity and hence the mean number of the induced modes of quantum harmonically oscillating mirrors. Particularly, the mean number of superposed modes of quantum harmonically oscillating mirrors rapidly increases for slight difference in squeeze parameter.

As we can easily see in Fig. 4.22 (b) that the mean of mechanical modes also increases for higher temperature of thermal baths coupled to mechanical modes as it increases the mean number and intensity of mechanical modes. It is also found that the mean number of mechanical mode pairs attains a maximum value of $\bar{n} = 1073$ for $\chi = 4.11\gamma$.

We realize that the mean number of mechanical mode pairs can be optimized by properly choosing the values of various atomic, cavity and reservoir parameters. This

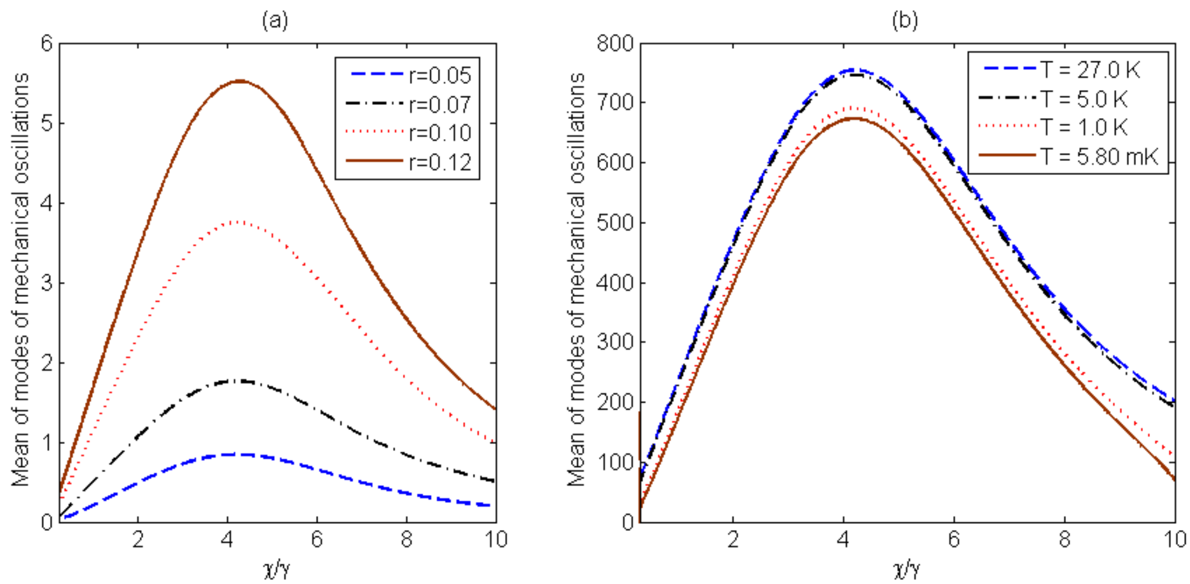

Figure 4.22: Plots of mean number of two-mode quantum harmonically oscillating mirrors $\bar{n}$ against $\frac{\chi}{\gamma}$ at steady state depending on reservoir parameters (a) for different squeeze parameter of a reservoir in which cavity radiations are coupled to squeezed vacuum reservoir (b) for different temperature of thermal baths coupled to modes of quantum harmonically oscillating mirrors. The other parameters are as shown in Table 4.1.

.

entails that the mean number of mechanical modes is significantly higher for the case in which there is a strong nonclassical correlation. Therefore, based on the possibility of increasing the intensity by a proper selection of the involved parameters, this may lead to the conclusion that the system under consideration can be a source of robust nonclassical features of mechanical modes.

4.3.4 Mean of Intensity difference of mechanical modes

Based on the assumption that there is a difference between the mean number of the two mechanical modes of quantum harmonically oscillating mirrors due to the disparity of the absorption-emission mechanism among the involved atomic energy levels that can be transferred to the modes of mechanical oscillations via radiation pressure, and therefore various nonclassical behaviors are induced on these quantum states.

The mean of intensity difference for the two-modes of quantum harmonically oscillating mirrors $\hat{I}_D$ is defined as

$$I_D = \bar{n}_{\delta\tilde{b}_1}(t) - \bar{n}_{\delta\tilde{b}_2}(t), \tag{4.38}$$

where $I_D = \langle \hat{I}_D \rangle$, $\bar{n}_{\delta\tilde{b}_1} = \langle \delta\tilde{b}_1^\dagger(t)\delta\tilde{b}_1(t)\rangle$ and $\bar{n}_{\delta\tilde{b}_2} = \langle \delta\tilde{b}_2^\dagger(t)\delta\tilde{b}_2(t)\rangle$.

On account of the elements of CM from the solution of Eq. (3.197), we obtain the simplified form of the mean of intensity difference at steady state as

$$I_D = \frac{1}{2}\left[V_{11} + V_{22} + V_{33} + V_{44} - 2\right]. \tag{4.39}$$

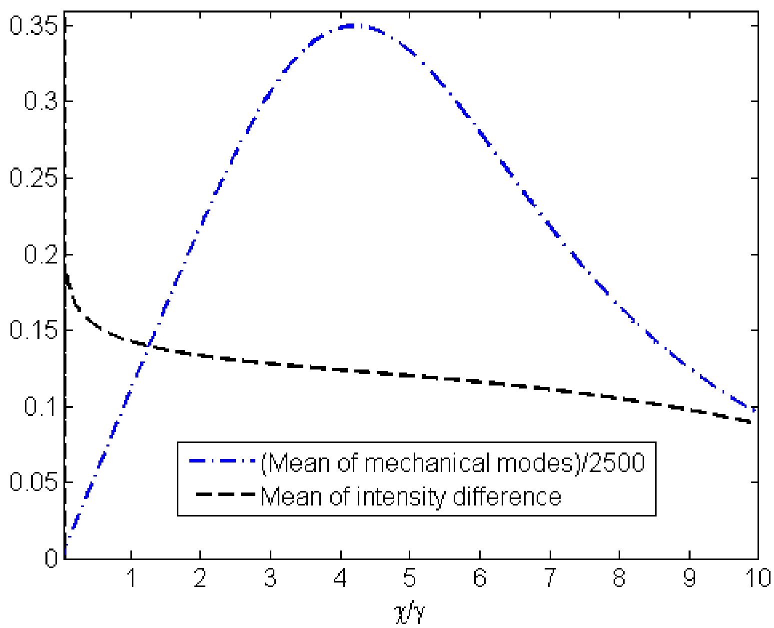

Figure 4.23: Plots of mean number of mechanical mode pairs $\bar{n}$ (blue dash-dotted) and mean of intensity difference I_D (black dashed) against $\frac{\chi}{\gamma}$ at steady state with $g = 900.0$ MHz. The other parameters are as shown in Table 4.1.

.

The extent to which mechanical modes are induced in a successive manner, can be evaluated by comparing the mean number of modes of mechanical oscillation pairs with the mean intensity difference. Based on the mean intensity difference and the mean number of mechanical mode pairs, it is not difficult to see from Fig. (4.23) that the mean number of mechanical modes in mode '$\delta\tilde{b}_1$' is slightly greater than mode '$\delta\tilde{b}_2$'.

This implies that the mean number of pairs of modes of mechanical oscillations due to the transfer of quantum states of the radiation emitted when the atoms spontaneously decay from the upper energy level to the intermediate is larger than that when the atoms go from the intermediate to the lower energy level.

4.3.5 Variance of number of mechanical modes

The variance of the number of two-mechanical modes of quantum harmonically oscillating mirror's number is defined as

$$\Delta n^2 = \langle \hat{n}^2(t)\rangle - \langle \hat{n}(t)\rangle^2, \tag{4.40}$$

where $\hat{n} = \delta\tilde{c}^\dagger(t)\delta\tilde{c}(t)$.

Using the boson commutation relation, it is possible to rewrite Eq. (4.40) in the normal order as

$$\Delta n^2 = \langle \delta\tilde{c}^{\dagger^2}(t)\delta\tilde{c}^2(t)\rangle + \langle \delta\tilde{c}^\dagger(t)\delta\tilde{c}(t)\rangle - \langle \delta\tilde{c}^\dagger(t)\delta\tilde{c}(t)\rangle^2. \tag{4.41}$$

Taking into account that $\delta\tilde{c}(t)$ Gaussian variables with the vanishing mean, we write

$$\langle \delta\tilde{c}^{\dagger^2}(t)\delta\tilde{c}^2(t)\rangle = \left|\langle \delta\tilde{c}^2(t)\rangle\right|^2 + 2\langle \delta\tilde{c}^\dagger(t)\delta\tilde{c}(t)\rangle^2 + \langle \delta\tilde{c}^\dagger(t)\delta\tilde{c}(t)\rangle. \tag{4.42}$$

In view of this, the induced variance of the number of modes of two-harmonically oscillating mirrors can be written as

$$\Delta n^2 = \bar{n}(\bar{n}+1) + \left|\langle \delta\tilde{c}^2(t)\rangle\right|^2. \tag{4.43}$$

We easily see from Eq. (4.43), the modes of mechanical oscillators have super-poissonian photon statistics.

Taking into account Eq. (4.35), we also have

$$\langle \hat{\delta\tilde{c}^2}\rangle = \frac{1}{2}\left(\langle \delta\tilde{b}_1^2(t)\rangle + \langle \delta\tilde{b}_2^2(t)\rangle + 2\langle \delta\tilde{b}_1(t)\delta\tilde{b}_2(t)\rangle\right). \tag{4.44}$$

With the aid of Eqs. (3.191), (3.192), and (4.44), we obtain $\langle\hat{\delta\tilde{c}^2}\rangle$ in terms of the elements of the steady state correlations obtained from the solution of Eq. (3.197) as

$$\langle\hat{\delta\tilde{c}^2}\rangle = \frac{1}{4}\left[\frac{V_{11}+V_{33}-V_{22}-V_{44}}{2}+2\big(V_{13}-V_{24}\big)+i\big(V_{13}+V_{14}+V_{23}+V_{34}\big)\right]_{\rm ss} \quad (4.45)$$

Then, employing Eqs. (4.37) and (4.45) into (4.43), we see that

$$\begin{aligned}\Delta n^2 =& \frac{1}{16}\left|\frac{V_{11}+V_{33}-V_{22}-V_{44}}{2}+2\big(V_{13}-V_{24}\big)+i\big(V_{13}+V_{14}+V_{23}+V_{34}\big)\right|^2_{\rm ss}\\ &+\frac{1}{16}\left[\frac{V_{11}+V_{22}+V_{33}+V_{44}}{2}+\big(V_{13}+V_{24}\big)-1\right]^2_{\rm ss}\\ &+\frac{1}{4}\left[\frac{V_{11}+V_{22}+V_{33}+V_{44}}{2}+\big(V_{13}+V_{24}\big)-1\right]_{\rm ss}. \end{aligned} \quad (4.46)$$

Since $\left|\langle\delta\tilde{c}^2(t)\rangle\right|^2$ is positive, we see from Eq. (4.43) that $\Delta n^2 > \bar{n}$. We therefore observe that the two-mode harmonical oscillation exhibits a super-Poissonian mechanical modes statistics for all cases.

4.3.6 Variance of Intensity difference of mechanical modes

The variance of intensity difference of mechanical modes can be expressed as

$$\Delta I_D^2 = \langle\hat{I}_D^2(t)\rangle - \langle\hat{I}_D(t)\rangle^2, \quad (4.47)$$

where the quantum state of harmonically oscillating mirrors number difference $\hat{I}_D$ is defined as

$$\hat{I}_D = \delta\tilde{b}_1^\dagger(t)\delta\tilde{b}_1(t) - \delta\tilde{b}_2^\dagger(t)\delta\tilde{b}_2(t). \quad (4.48)$$

One can easily see using Eq. (4.48) that

$$\langle\hat{I}_D^2(t)\rangle = \langle\delta\tilde{b}_1^\dagger(t)\delta\tilde{b}_1(t)\delta\tilde{b}_1^\dagger(t)\delta\tilde{b}_1(t)\rangle + \langle\delta\tilde{b}_2^\dagger(t)\delta\tilde{b}_2(t)\delta\tilde{b}_2^\dagger(t)\delta\tilde{b}_2(t)\rangle - 2\langle\delta\tilde{b}_1^\dagger(t)\delta\tilde{b}_1(t)\delta\tilde{b}_2^\dagger(t)\delta\tilde{b}_2(t)\rangle. \quad (4.49)$$

which can also be put applying the usual boson commutation relation in the form

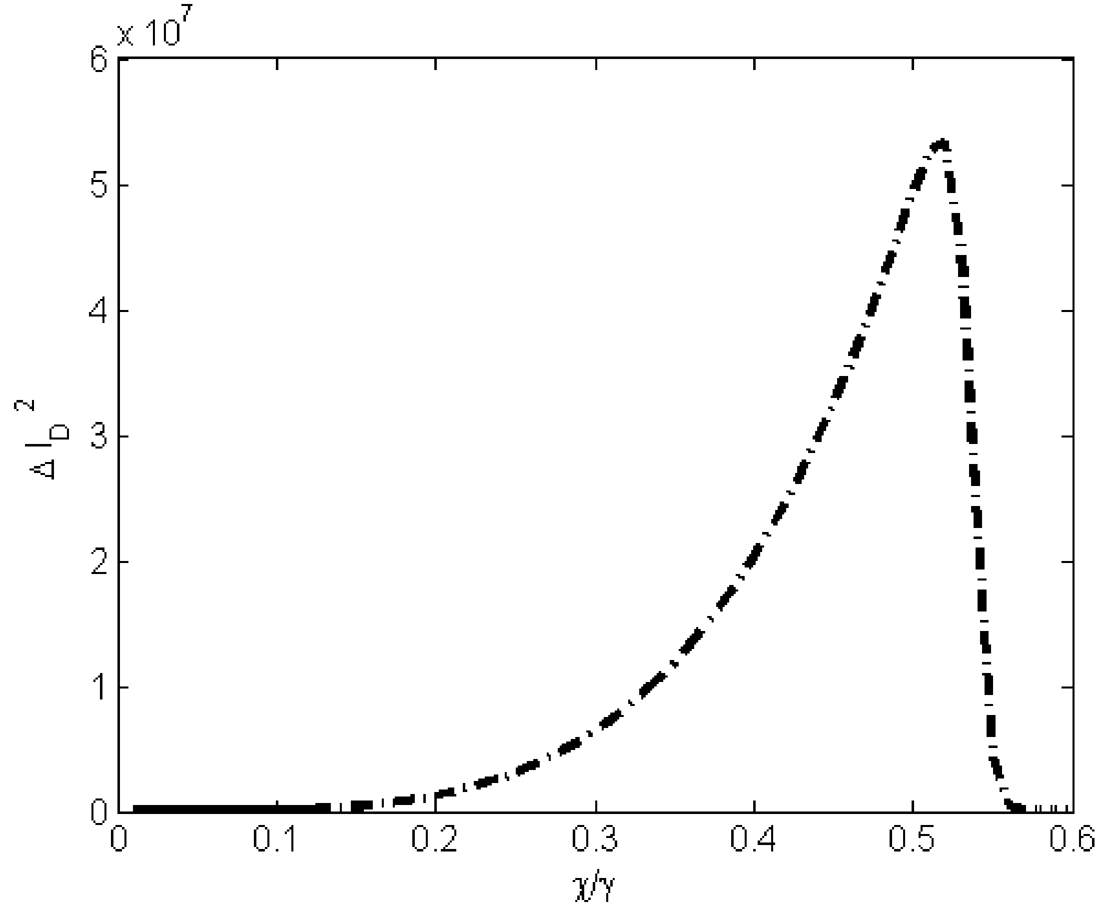

Figure 4.24: Plots of Variance of intensity difference of two-mode quantum harmonically oscillating mirrors ΔI_D^2 against $\frac{\chi}{\gamma}$ at steady state. The other parameters are as shown in Table 4.1.

.

$$\begin{aligned}\langle \hat{I}_D^2(t)\rangle =&\langle \delta\tilde{b}_1^{\dagger^2}(t)\delta\tilde{b}_1^2(t)\rangle + \langle \delta\tilde{b}_2^{\dagger^2}(t)\delta\tilde{b}_2^2(t)\rangle - 2\langle \delta\tilde{b}_1^\dagger(t)\delta\tilde{b}_1(t)\delta\tilde{b}_2^\dagger(t)\delta\tilde{b}_2(t)\rangle\\ &+ \langle \delta\tilde{b}_1^\dagger(t)\delta\tilde{b}_1(t)\rangle + \langle \delta\tilde{b}_2^\dagger(t)\delta\tilde{b}_2(t)\rangle.\end{aligned} \tag{4.50}$$

In view of this, the variance of the intensity difference can rewritten as

$$\begin{aligned}\Delta I_D^2 =&\langle \delta\tilde{b}_1^{\dagger^2}(t)\delta\tilde{b}_1^2(t)\rangle + \langle \delta\tilde{b}_2^{\dagger^2}(t)\delta\tilde{b}_2^2(t)\rangle - 2\langle \delta\tilde{b}_1^\dagger(t)\delta\tilde{b}_1(t)\delta\tilde{b}_2^\dagger(t)\delta\tilde{b}_2(t)\rangle\\ &+ \langle \delta\tilde{b}_1^\dagger(t)\delta\tilde{b}_1(t)\rangle + \langle \delta\tilde{b}_2^\dagger(t)\delta\tilde{b}_2(t)\rangle - \Big(\langle \delta\tilde{b}_1^\dagger(t)\delta\tilde{b}_1(t)\rangle - \langle \delta\tilde{b}_2^\dagger(t)\delta\tilde{b}_2(t)\rangle\Big)^2.\end{aligned} \tag{4.51}$$

Noting that $\delta\tilde{b}_1$ and $\delta\tilde{b}_2$ are Gaussian variables with vanishing mean, we see that

$$\langle\delta\tilde{b}_1^{\dagger^2}(t)\delta\tilde{b}_1^2(t)\rangle = \big|\langle\delta\tilde{b}_1^2(t)\rangle\big|^2 + 2\langle\delta\tilde{b}_1^\dagger(t)\delta\tilde{b}_1(t)\rangle^2, \tag{4.52}$$

$$\langle\delta\tilde{b}_2^{\dagger^2}(t)\delta\tilde{b}_2^2(t)\rangle = \big|\langle\delta\tilde{b}_2^2(t)\rangle\big|^2 + 2\langle\delta\tilde{b}_2^\dagger(t)\delta\tilde{b}_2(t)\rangle^2, \tag{4.53}$$

$$\langle\delta\tilde{b}_1^\dagger(t)\delta\tilde{b}_1(t)\delta\tilde{b}_2^\dagger(t)\delta\tilde{b}_2(t)\rangle = \big|\langle\delta\tilde{b}_1(t)\delta\tilde{b}_2(t)\rangle\big|^2 + \big|\langle\delta\tilde{b}_1^\dagger(t)\delta\tilde{b}_2(t)\rangle\big|^2 + \langle\delta\tilde{b}_1^\dagger(t)\delta\tilde{b}_1(t)\rangle\langle\delta\tilde{b}_2^\dagger(t)\delta\tilde{b}_2(t)\rangle. \tag{4.54}$$

With the aid of Eqs. (4.52) - (4.54), the variance of intensity difference can be expressed as

$$\begin{aligned}\Delta I_D^2 =& \big|\langle\delta\tilde{b}_1^2(t)\rangle\big|^2 + \big|\langle\delta\tilde{b}_2^2(t)\rangle\big|^2 + \langle\delta\tilde{b}_1^\dagger(t)\delta\tilde{b}_1(t)\rangle^2 + \langle\delta\tilde{b}_2^\dagger(t)\delta\tilde{b}_2(t)\rangle^2 + \langle\delta\tilde{b}_2^\dagger(t)\delta\tilde{b}_2(t)\rangle \\ &+ \langle\delta\tilde{b}_1^\dagger(t)\delta\tilde{b}_1(t)\rangle - 2\big|\langle\delta\tilde{b}_1(t)\delta\tilde{b}_2(t)\rangle\big|^2 - 2\big|\langle\delta\tilde{b}_1^\dagger(t)\delta\tilde{b}_2(t)\rangle\big|^2. \end{aligned} \tag{4.55}$$

With the aid of the elements of CM from the solution of Eq. (3.197), we can write the steady state form of Eq. (4.55) as

$$\begin{aligned}\Delta I_D^2 =& \frac{1}{4}\big(V_{11} + V_{22} - 1\big)^2_{\text{ss}} + \frac{1}{4}\big(V_{33} + V_{44} - 1\big)^2_{\text{ss}} + \frac{1}{2}\big[V_{11} + V_{22} + V_{33} + V_{44} - 2\big]_{\text{ss}} \\ &- \frac{1}{4}\big|V_{13} + V_{24} + \mathrm{i}(V_{14} - V_{24})\big|^2_{\text{ss}} - \frac{1}{4}\big|V_{13} - V_{24} + \mathrm{i}(V_{14} + V_{23})\big|^2_{\text{ss}} \\ &+ \frac{1}{4}\big|V_{11} - V_{22} + 2\mathrm{i}V_{13}\big|^2_{\text{ss}} + \frac{1}{4}\big|V_{33} - V_{44} + 2\mathrm{i}V_{34}\big|^2_{\text{ss}}. \end{aligned} \tag{4.56}$$

We observe from Fig. (4.24) that, the variance of intensity difference of the modes of quantum harmonically oscillating mirrors show significant increase for some smaller amplitude of a laser pumping an atom.

The variance of the photon number difference turns out to be zero for certain values of χ. On top of this, there is an indication that $\Delta(\delta\tilde{c}_+)^2$ can be related to ΔI_D^2. In this context, the quantification of the available degree of squeezing can be carried out by ordinary bosonic state counting techniques which is far more easy when compared to the otherwise employed hetrodyne measurement.

5

Conclusion

In this dissertation, we investigated the nonclassical correlations such as squeezing, entanglement, Gaussian quantum discord, Gaussian steering of the two quantum harmonically oscillating mirrors (mechanical modes) that can be caused by the transfer of coherence from two mode cavity radiation to two separate mechanical modes via radiation pressure in an optomechanical cavity comprising of three-level atoms injected into cavity when all atoms are initially at the lower-energy level and the top and bottom levels of the atoms are coupled by a strong radiation, a bichromatic cavity drive laser, two separate harmonically oscillating mirrors coupled to two separate thermal baths, and cavity radiations coupled to a two-mode Markovian squeezed vacuum reservoir with the aid of quantum Langevin equation. Afterwards, we determined the correlation between the noise forces associated to the evolution of cavity modes and mechanical modes in a good cavity limit. The nonclassical correlations of the two-mechanical modes have been obtained with the aid of the linearized quantum Langevin equation in adiabatic approximation when the atom-field coupling turns out to be much stronger than the optomechanical coupling. In connection to these, the covariance matrix at steady state is obtained using the Lyapunov equation that can be used to investigate the various nonclassical correlations.

The results show that the mechanical modes exhibit induced nonclassical correlations. We have also seen that these nonclassical correlations persist in a wide range of amplitude χ of a strong laser driving the atoms and the degree of nonclassical features increase for smaller values of χ. It is also found that the degree of the nonclassical properties are sensitive to the specific choices of the frequencies of a bichromatic drive laser. Particularly, strongest degree of nonclassical correlations is manifested when the higher frequency of a bichromatic laser drives the cavity and enforces the cavity radiation of higher frequency, which is in a direct relation to the strength of field-mirror coupling that can be transferred to the mechanical modes. It also turns out that the degree of these nonclassical correlations would be enhanced with increasing rates of injection of the atoms, for stronger atom-field coupling, for higher temperature of thermal baths but with decreasing initial lengths of a cavity, atomic decay rate (just after obtaining maximum values of nonclassical properties) and with squeeze parameter.

We also observed that the degree of various nonclassical correlations increase (almost up to optimum values) irrespective of the values of atomic decay rates. Critical observation indicate that there are threshold coupling between the atoms and the fields, atomic injection rate, initial lengths of a cavity, temperature and squeeze parameter of reservoirs above which these nonclassical features would not be manifested under the parameters given in Table 4.1. On the other hand, these threshold values can be larger when the power of a bichromatic laser driving the cavity gets smaller.

There also appear strong degree of nonclassical features for increased temperature of thermal baths coupled to mechanical modes. Nonetheless, the degree of entanglement measures using HZ criterion shows insignificant difference with the variation of temperature. This can be expressed using the fact that the increase in temperature results in larger amplitude of atomic vibration, and in quantum terms this is considered as an increase in the number of mechanical modes in the system where the resulting nonclassical correlation of the mechanical modes is found to be altered leading to a stronger degree of squeezing, entanglement, Gaussian steering and GQD. Even at absolute zero (0K) temperature, a non-zero quantum features are still found to be manifested due to the non-zero energy of the vibrational mode of oscillating mirrors.

We have also found robust degree of entanglement using different different detection mechanisms, Gaussian quantum discord and Gaussian steering when a SVR is coupled to two-mode cavity radiations; whereas the degree of squeezing (when the power of lasers driving the cavity is high, 554 mW, and the strength of atom-field coupling is weaker, 1.95π MHz) and that of the entanglement using HZ criterion is found to be least when the cavity radiations are coupled to a vacuum reservoir.

Besides, weakest nonclassical correlation is manifested when cavity field fails to couple with atoms, no atoms are injected into cavity, and when the temperature of a reservoir coupled to mechanical modes acquires absolute zero value. It is also clearly shown that the degree of entanglement detected in the different criteria developed using quadrature variance and von Neumann entropy behave qualitatively in the same way, while the slight disparity between the magnitudes is basically attributed to the variations related to the difference in the correlations leading to these phenomena.

We noticed that the mean number of pair of mechanical modes increases for larger atomic injection rate, larger squeeze parameter of a SVR coupled to cavity radiation, higher temperature of thermal baths coupled to mechanical modes but for smaller amplitude of the atomic-driving radiation, initial lengths of a cavity, and atomic decay rate. Hence, we realize that the mean number of mechanical mode pairs can be optimized by properly choosing the values of various atomic, cavity and reservoir parameters. This entails that the mean number of mechanical modes is significantly higher for the case in which there is a strong nonclassical correlation. We also remarked that the mechanical modes exhibit super-Poissonian photon statistics.

By comparing the mean intensity difference and the mean number of pairs of mechanical modes, it has been observed that the mean number of mechanical modes in mode '$\delta\tilde{b}_1$' is slightly greater than mode '$\delta\tilde{b}_2$'. This implies that the mean number of pairs of modes of mechanical oscillations due to the transfer of quantum states of the radiation emitted when the atoms spontaneously decay from the upper energy level to the intermediate is larger than that when the atoms go from the intermediate to the lower energy level.

Therefore, based on the possibility of increasing the nonclassical correlations and the intensity of the mechanical modes by a proper choice of the involved parameters, may lead us to the conclusion that our system can be an attractive viable scheme to produce a robust nonclassical features, which can be implemented in the current quantum technology.

FUTURE RESEARCHES AND RECOMMENDATIONS

From an overall outlook, lack of time, the effects of the parameters of quantum harmonically oscillating mirrors (such as the masses of mirrors, frequency of the mirrors, mechanical mode decay rate, cavity finnese) on the nonclassical behaviours of mechanical modes haven't been covered. By altering the input quantum resource in application of quantum information science will be the other focusing area. Since the change in atomic, cavity, and reservoir parameters affect the properties of various nonclassical correlations, we suggest the quantum information processing scientists to consider the issue in quantum communication, and metrology. In the future, we will also further investigate other nonclassical correlations such as mechanical modes bistability, fidelity, quantum monogamy and others theoretically and experimentally applying other mechanisms.

LIST OF PUBLICATIONS

1. Bekele, M., Yirgashewa, T., & Tesfa, S. (2022). Effects of a three-level laser on mechanical squeezing in a doubly resonant optomechanical cavity coupled to biased noise fluctuations. *Physical Review A*, 105(5), 053502. http://doi.org/10.1103/PhysRevA.105.053502

2. Bekele, M., Yirgashewa, T., & Tesfa, S. (2023). Entanglement of mechanical modes in a doubly resonant optomechanical cavity of a correlated emission laser. *Phys. Rev. A* 107, 012417. http://doi.org/10.1103/PhysRevA.107.012417

3. Three different manuscript are prepared for publication in the near future.

LIST OF CONFERENCE PARTICIPATION

I have been participating in different national and international conferences such as

1. 7th Ethiopian Physical Society Symposium at Adama Science and Technology University on November, 2018. (Participant)

2. 1st International Conference at Bule Hora University on May, 2018. (Participant)

3. 8th EPS at Arba-Minch University February on March, 2019. (Participant)

4. 2nd International Conference at Bule Hora University on June, 2021. (Presenter)

5. 3rd International Conference at Bule Hora University on May, 2022. (Participant)

In addition, the finding of this research was presented in abroad international conferences

1. 3rd International Quantum Africa Conference (Presenter) on September 16-21, (2022).

2. Invited to present on ICTP Conference in 2023.

Bibliography

Adesso, G., Bromley, T. R., and Cianciaruso, M. (2016). Measures and applications of quantum correlations. *Journal of Physics A: Mathematical and Theoretical*, 49(47):473001.

Adesso, G. and Datta, A. (2010). Quantum versus classical correlations in gaussian states. *Physical review letters*, 105(3):030501.

Adesso, G., Girolami, D., and Serafini, A. (2012). Measuring gaussian quantum information and correlations using the rényi entropy of order 2. *Physical review letters*, 109(19):190502.

Adesso, G., Ragy, S., and Lee, A. R. (2014). Continuous variable quantum information: Gaussian states and beyond. *Open Systems & Information Dynamics*, 21(01n02):1440001.

Adesso, G., Serafini, A., and Illuminati, F. (2004a). Determination of continuous variable entanglement by purity measurements. *Physical review letters*, 92(8):087901.

Adesso, G., Serafini, A., and Illuminati, F. (2004b). Extremal entanglement and mixedness in continuous variable systems. *Physical Review A*, 70(2):022318.

Agarwal, G. S. (2012). *Quantum optics*. Cambridge University Press.

Aguirregabiria, J. and Bel, L. (1987). Delay-induced instability in a pendular fabry-perot cavity. *Physical Review A*, 36(8):3768.

Alber, G., Beth, T., Horodecki, M., Horodecki, P., Horodecki, R., Rötteler, M., Weinfurter, H., Werner, R., and Zeilinger, A. (2003). *Quantum information: An introduction to basic theoretical concepts and experiments*, volume 173. Springer.

Amazioug, M., Jebli, L., Nassik, M., and Habiballah, N. (2020a). Dynamics of classical-quantum correlations between two movable mirrors in optomechanics. *International Journal of Modern Physics B*, 34(08):2050066.

Amazioug, M., Jebli, L., Nassik, M., and Habiballah, N. (2020b). Quantifying non-classical correlations under thermal effects in a double cavity optomechanical system. *Chinese Physics B*, 29(2):020304.

Amazioug, M., Maroufi, B., and Daoud, M. (2020c). Creating mirror–mirror quantum correlations in optomechanics. *The European Physical Journal D*, 74:1–9.

Amazioug, M., Nassik, M., and Habiballah, N. (2018a). Entanglement, epr steering and gaussian geometric discord in a double cavity optomechanical systems. *The European Physical Journal D*, 72:1–9.

Amazioug, M., Nassik, M., and Habiballah, N. (2018b). Measure of general quantum correlations in optomechanics. *International Journal of Quantum Information*, 16(05):1850043.

Ansari, N. A. (1993). Effect of atomic coherence on the second-and higher-order squeezing in a two-photon three-level cascade atomic system. *Physical Review A*, 48(6):4686.

Arcizet, O., Cohadon, P.-F., Briant, T., Pinard, M., and Heidmann, A. (2006). Radiation-pressure cooling and optomechanical instability of a micromirror. *Nature*, 444(7115):71–74.

Armstrong, S., Wang, M., Teh, R. Y., Gong, Q., He, Q., Janousek, J., Bachor, H.-A., Reid, M. D., and Lam, P. K. (2015). Multipartite einstein–podolsky–rosen steering and genuine tripartite entanglement with optical networks. *Nature Physics*, 11(2):167–172.

Aspect, A., Grangier, P., and Roger, G. (1982). Experimental realization of einstein-podolsky-rosen-bohm gedankenexperiment: A new violation of bell's inequalities. *Physical review letters*, 49(2):91.

Aspelmeyer, M., Kippenberg, T. J., and Marquardt, F. (2014). Cavity optomechanics nano-and micromechanical resonators interacting with light preface. In *CAVITY OPTOMECHANICS: NANO-AND MICROMECHANICAL RESONATORS INTERACTING WITH LIGHT*, pages V–V. SPRINGER-VERLAG BERLIN.

Bagci, T., Simonsen, A., Schmid, S., Villanueva, L. G., Zeuthen, E., Appel, J., Taylor, J. M., Sørensen, A., Usami, K., Schliesser, A., et al. (2014). Optical detection of radio waves through a nanomechanical transducer. *Nature*, 507(7490):81–85.

Barchielli, A. and Vacchini, B. (2015). Quantum langevin equations for optomechanical systems. *New Journal of Physics*, 17(8):083004.

Bell, J. (1964a). Physics (long island city, ny) 1 195 go to reference in article google scholar (reprinted in bell js 1987 speakable and unspeakable in quantum mechanics (cambridge.

Bell, J. S. (1964b). On the einstein podolsky rosen paradox. *Physics Physique Fizika*, 1(3):195.

Bell, J. S. (1975). The theory of local beables. Technical report.

Benguria, R. and Kac, M. (1981). Quantum langevin equation. *Physical review letters*, 46(1):1.

Bennet, A. J., Evans, D. A., Saunders, D. J., Branciard, C., Cavalcanti, E. G., Wiseman, H. M., and Pryde, G. J. (2012). Arbitrarily loss-tolerant einstein-podolsky-rosen steering allowing a demonstration over 1 km of optical fiber with no detection loophole. *Physical Review X*, 2(3):031003.

Bennett, C. H., Grudka, A., Horodecki, M., Horodecki, P., and Horodecki, R. (2011). Postulates for measures of genuine multipartite correlations. *Physical Review A*, 83(1):012312.

Bochmann, J., Vainsencher, A., Awschalom, D. D., and Cleland, A. N. (2013). Nanomechanical coupling between microwave and optical photons. *Nature Physics*, 9(11):712–716.

Bowles, J., Vértesi, T., Quintino, M. T., and Brunner, N. (2014). One-way einstein-podolsky-rosen steering. *Physical Review Letters*, 112(20):200402.

Braginsky, V. and Khalili, F. Y. (1992). Quantum measurement, cambridge university press.

Branciard, C., Cavalcanti, E. G., Walborn, S. P., Scarani, V., and Wiseman, H. M. (2012). One-sided device-independent quantum key distribution: Security, feasibility, and the connection with steering. *Physical Review A*, 85(1):010301.

Braunstein, S. L. and Van Loock, P. (2005). Quantum information with continuous variables. *Reviews of modern physics*, 77(2):513.

Brunner, N., Cavalcanti, D., Pironio, S., Scarani, V., and Wehner, S. (2014). Bell nonlocality. *Reviews of modern physics*, 86(2):419.

Caldeira, A. O. and Leggett, A. J. (1983). Path integral approach to quantum brownian motion. *Physica A: Statistical mechanics and its Applications*, 121(3):587–616.

Calucci, G. (1992). Casimir effect for moving bodies. *Journal of Physics A: Mathematical and General*, 25(13):3873.

Cavalcanti, E. G., Hall, M. J., and Wiseman, H. M. (2013). Entanglement verification and steering when alice and bob cannot be trusted. *Physical Review A*, 87(3):032306.

Cavalcanti, E. G., He, Q. Y., Reid, M. D., and Wiseman, H. M. (2011). Unified criteria for multipartite quantum nonlocality. *Physical Review A*, 84(3):032115.

Cavalcanti, E. G., Jones, S. J., Wiseman, H. M., and Reid, M. D. (2009). Experimental criteria for steering and the einstein-podolsky-rosen paradox. *Physical Review A*, 80(3):032112.

Caves, C. M., Thorne, K. S., Drever, R. W., Sandberg, V. D., and Zimmermann, M. (1980). On the measurement of a weak classical force coupled to a quantum-mechanical oscillator. i. issues of principle. *Reviews of Modern Physics*, 52(2):341.

Cerf, N. J. and Adami, C. (1997). Negative entropy and information in quantum mechanics. *Physical Review Letters*, 79(26):5194.

Černotík, O. and Hammerer, K. (2016). Measurement-induced long-distance entanglement of superconducting qubits using optomechanical transducers. *Physical Review A*, 94(1):012340.

Chakraborty, S. and Sarma, A. K. (2017). Enhancing quantum correlations in an optomechanical system via cross-kerr nonlinearity. *JOSA B*, 34(7):1503–1510.

Corbitt, T., Chen, Y., Innerhofer, E., Müller-Ebhardt, H., Ottaway, D., Rehbein, H., Sigg, D., Whitcomb, S., Wipf, C., and Mavalvala, N. (2007). An all-optical trap for a gram-scale mirror. *Physical review letters*, 98(15):150802.

Costa, A., Beims, M., and Angelo, R. (2016). Generalized discord, entanglement, einstein–podolsky–rosen steering, and bell nonlocality in two-qubit systems under (non-) markovian channels: Hierarchy of quantum resources and chronology of deaths and births. *Physica A: Statistical Mechanics and its Applications*, 461:469–479.

Cover, T. M. (1999). *Elements of information theory*. John Wiley & Sons.

Dakić, B., Vedral, V., and Brukner, Č. (2010). Necessary and sufficient condition for nonzero quantum discord. *Physical review letters*, 105(19):190502.

DeJesus, E. X. and Kaufman, C. (1987). Routh-hurwitz criterion in the examination of eigenvalues of a system of nonlinear ordinary differential equations. *Physical Review A*, 35(12):5288.

Dirac, P. A. M. (1927). The quantum theory of the emission and absorption of radiation. *Proceedings of the Royal Society of London. Series A, Containing Papers of a Mathematical and Physical Character*, 114(767):243–265.

Duan, L.-M., Giedke, G., Cirac, J. I., and Zoller, P. (2000). Inseparability criterion for continuous variable systems. *Physical review letters*, 84(12):2722.

Eberle, T., Händchen, V., Duhme, J., Franz, T., Werner, R. F., and Schnabel, R. (2011). Strong einstein-podolsky-rosen entanglement from a single squeezed light source. *Physical Review A*, 83(5):052329.

Einstein, A., Podolsky, B., and Rosen, N. (1935). Can quantum-mechanical description of physical reality be considered complete? *Physical review*, 47(10):777.

Eisert, J., Plenio, M., Bose, S., and Hartley, J. (2004). Towards quantum entanglement in nanoelectromechanical devices. *Physical review letters*, 93(19):190402.

Eisert, J., Scheel, S., and Plenio, M. B. (2002). Distilling gaussian states with gaussian operations is impossible. *Physical review letters*, 89(13):137903.

El Qars, J., Daoud, M., and Laamara, R. A. (2017). Dynamical gaussian quantum steering in optomechanics. *The European Physical Journal D*, 71:1–10.

Feng, L.-J., Lin, G.-W., Deng, L., Niu, Y.-P., and Gong, S.-Q. (2018). Strong mechanical squeezing in an electromechanical system. *Scientific Reports*, 8(1):3513.

Ferraro, A., Aolita, L., Cavalcanti, D., Cucchietti, F. M., and Acín, A. (2010). Almost all quantum states have nonclassical correlations. *Physical Review A*, 81(5):052318.

Fesseha, K. (2001). Three-level laser dynamics with squeezed light. *Physical Review A*, 63(3):033811.

Fiurášek, J. (2002). Gaussian transformations and distillation of entangled gaussian states. *Physical review letters*, 89(13):137904.

Ford, G., Lewis, J., and O'Connell, R. (1988). Independent oscillator model of a heat bath: exact diagonalization of the hamiltonian. *Journal of statistical physics*, 53:439–455.

Ge, W., Al-Amri, M., Nha, H., and Zubairy, M. S. (2013). Entanglement of movable mirrors in a correlated-emission laser. *Physical Review A*, 88(2):022338.

Gebremariam, T., Mazaheri, M., Zeng, Y., and Li, C. (2019). Dynamical quantum steering in a pulsed hybrid opto-electro-mechanical system. *JOSA B*, 36(2):168–177.

Genes, C., Vitali, D., and Tombesi, P. (2008). Emergence of atom-light-mirror entanglement inside an optical cavity. *Physical Review A*, 77(5):050307.

Gerry, C. and Knight, P. L. (2005). *Introductory quantum optics.* Cambridge university press.

Giorda, P. and Paris, M. G. (2010). Gaussian quantum discord. *Physical review letters*, 105(2):020503.

Giovannetti, V., Mancini, S., and Tombesi, P. (2001). Radiation pressure induced einstein-podolsky-rosen paradox. *Europhysics Letters*, 54(5):559.

Giovannetti, V. and Vitali, D. (2001). Phase-noise measurement in a cavity with a movable mirror undergoing quantum brownian motion. *Physical Review A*, 63(2):023812.

Gröblacher, S., Hammerer, K., Vanner, M. R., and Aspelmeyer, M. (2009). Observation of strong coupling between a micromechanical resonator and an optical cavity field. *Nature*, 460(7256):724–727.

Groisman, B., Popescu, S., and Winter, A. (2005). Quantum, classical, and total amount of correlations in a quantum state. *Physical Review A*, 72(3):032317.

Gu, W.-j. and Li, G.-x. (2013). Squeezing of the mirror motion via periodic modulations in a dissipative optomechanical system. *Optics Express*, 21(17):20423–20440.

Gu, W.-j., Li, G.-x., and Yang, Y.-p. (2013). Generation of squeezed states in a movable mirror via dissipative optomechanical coupling. *Physical Review A*, 88(1):013835.

Händchen, V., Eberle, T., Steinlechner, S., Samblowski, A., Franz, T., Werner, R. F., and Schnabel, R. (2012). Observation of one-way einstein–podolsky–rosen steering. *Nature Photonics*, 6(9):596–599.

He, Q. and Ficek, Z. (2014). Einstein-podolsky-rosen paradox and quantum steering in a three-mode optomechanical system. *Physical Review A*, 89(2):022332.

He, Q., Gong, Q., and Reid, M. (2015). Classifying directional gaussian entanglement, einstein-podolsky-rosen steering, and discord. *Physical review letters*, 114(6):060402.

He, Q., Rosales-Zarate, L., Adesso, G., and Reid, M. (2014). Secure continuous variable quantum teleportation and einstein-podolsky-rosen steering. *arXiv preprint arXiv:1410.1041*.

He, Q. Y. and Reid, M. D. (2013). Genuine multipartite einstein-podolsky-rosen steering. *Physical Review Letters*, 111(25):250403.

Henderson, L. and Vedral, V. (2001). Classical, quantum and total correlations. *Journal of physics A: mathematical and general*, 34(35):6899.

Hillery, M., Dung, H. T., and Zheng, H. (2010). Conditions for entanglement in multipartite systems. *Physical Review A*, 81(6):062322.

Hillery, M. and Zubairy, M. S. (2006). Entanglement conditions for two-mode states. *Physical review letters*, 96(5):050503.

Holevo, A. S. and Werner, R. F. (2001). Evaluating capacities of bosonic gaussian channels. *Physical Review A*, 63(3):032312.

Horodecki, M., Horodecki, P., and Horodecki, R. (1996). On the necessary and sufficient conditions for separability of mixed quantum states. *arXiv preprint quant-ph/9605038*.

Horodecki, R., Horodecki, P., Horodecki, M., and Horodecki, K. (2009). Quantum entanglement. *Reviews of modern physics*, 81(2):865.

Hu, X. and Nori, F. (1996). Squeezed phonon states: modulating quantum fluctuations of atomic displacements. *Physical review letters*, 76(13):2294.

Huang, S. and Agarwal, G. (2009). Entangling nanomechanical oscillators in a ring cavity by feeding squeezed light. *New Journal of Physics*, 11(10):103044.

Hurwitz, A. et al. (1964). On the conditions under which an equation has only roots with negative real parts. *Selected papers on mathematical trends in control theory*, 65:273–284.

Jacobs, K., Tittonen, I., Wiseman, H., and Schiller, S. (1999). Quantum noise in the position measurement of a cavity mirror undergoing brownian motion. *Physical Review A*, 60(1):538.

Jones, S. J., Wiseman, H. M., and Doherty, A. C. (2007). Entanglement, einstein-podolsky-rosen correlations, bell nonlocality, and steering. *Physical Review A*, 76(5):052116.

Karrai, K., Favero, I., and Metzger, C. (2008). Doppler optomechanics of a photonic crystal. *Physical review letters*, 100(24):240801.

Kassahun, F. (2016). Refined quantum analysis of light, revised edition.

Kiffner, M., Zubairy, M. S., Evers, J., and Keitel, C. (2007). Two-mode single-atom laser as a source of entangled light. *Physical Review A*, 75(3):033816.

Kippenberg, T. J. and Vahala, K. J. (2007). Cavity opto-mechanics. *Optics express*, 15(25):17172–17205.

Kocsis, S., Hall, M. J., Bennet, A. J., Saunders, D. J., and Pryde, G. J. (2015). Experimental measurement-device-independent verification of quantum steering. *Nature Communications*, 6(1):5886.

Kogias, I., Lee, A. R., Ragy, S., and Adesso, G. (2015). Quantification of gaussian quantum steering. *Physical review letters*, 114(6):060403.

Kok, P. and Lovett, B. W. (2010). *Introduction to optical quantum information processing*. Cambridge university press.

Kronwald, A., Marquardt, F., and Clerk, A. A. (2013). Arbitrarily large steady-state bosonic squeezing via dissipation. *Physical Review A*, 88(6):063833.

Law, C. (1995). Interaction between a moving mirror and radiation pressure: A hamiltonian formulation. *Physical Review A*, 51(3):2537.

Leggett, A. (1984). Quantum tunneling in the presence of an arbitrary linear dissipation mechanism. *Physical Review B*, 30(3):1208.

Li, J., Haghighi, I. M., Malossi, N., Zippilli, S., and Vitali, D. (2015). Generation and detection of large and robust entanglement between two different mechanical resonators in cavity optomechanics. *New Journal of Physics*, 17(10):103037.

Liao, J.-Q., Law, C., et al. (2011). Parametric generation of quadrature squeezing of mirrors in cavity optomechanics. *Physical Review A*, 83(3):033820.

Lindblad, G. (1976). Brownian motion of a quantum harmonic oscillator. *Reports on Mathematical Physics*, 10(3):393–406.

Loudon, R. and Knight, P. L. (1987). Squeezed light. *Journal of modern optics*, 34(6-7):709–759.

Lü, X.-Y., Liao, J.-Q., Tian, L., and Nori, F. (2015a). Steady-state mechanical squeezing in an optomechanical system via duffing nonlinearity. *Physical Review A*, 91(1):013834.

Lü, X.-Y., Wu, Y., Johansson, J., Jing, H., Zhang, J., and Nori, F. (2015b). Squeezed optomechanics with phase-matched amplification and dissipation. *Physical review letters*, 114(9):093602.

Luo, S. (2008a). Quantum discord for two-qubit systems. *Physical Review A*, 77(4):042303.

Luo, S. (2008b). Using measurement-induced disturbance to characterize correlations as classical or quantum. *Physical Review A*, 77(2):022301.

Mancini, S., Giovannetti, V., Vitali, D., and Tombesi, P. (2002). Entangling macroscopic oscillators exploiting radiation pressure. *Physical review letters*, 88(12):120401.

Mancini, S. and Tombesi, P. (1994). Quantum noise reduction by radiation pressure. *Physical Review A*, 49(5):4055.

Mari, A. and Eisert, J. (2009). Gently modulating optomechanical systems. *Physical Review Letters*, 103(21):213603.

Marshall, W., Simon, C., Penrose, R., and Bouwmeester, D. (2003). Towards quantum superpositions of a mirror. *Physical Review Letters*, 91(13):130401.

Meng, C., Brawley, G. A., Bennett, J. S., Vanner, M. R., and Bowen, W. P. (2020). Mechanical squeezing via fast continuous measurement. *Physical Review Letters*, 125(4):043604.

Meystre, P. (2013). A short walk through quantum optomechanics. *Annalen der Physik*, 525(3):215–233.

Midgley, S., Ferris, A., and Olsen, M. (2010). Asymmetric gaussian steering: when alice and bob disagree. *Physical Review A*, 81(2):022101.

Modi, K., Brodutch, A., Cable, H., Paterek, T., and Vedral, V. (2012). The classical-quantum boundary for correlations: Discord and related measures. *Reviews of Modern Physics*, 84(4):1655.

Neveu, P., Clarke, J., Vanner, M. R., and Verhagen, E. (2021). Preparation and verification of two-mode mechanical entanglement through pulsed optomechanical measurements. *New Journal of Physics*, 23(2):023026.

Nielsen, Michael A, I. C. (2000). Quantum information cambridge university press.

Olivares, S. (2012). Quantum optics in the phase space: a tutorial on gaussian states. *The European Physical Journal Special Topics*, 203(1):3–24.

Ollivier, H. and Zurek, W. H. (2001). Quantum discord: a measure of the quantumness of correlations. *Physical review letters*, 88(1):017901.

Olsen, M. (2015). Asymmetric steering in coherent transport of atomic population with a three-well bose–hubbard model. *JOSA B*, 32(4):A15–A19.

Olsen, M. (2017). Controlled asymmetry of einstein-podolsky-rosen steering with an injected nondegenerate optical parametric oscillator. *Physical Review Letters*, 119(16):160501.

Paternostro, M., Vitali, D., Gigan, S., Kim, M., Brukner, C., Eisert, J., and Aspelmeyer, M. (2007). Creating and probing multipartite macroscopic entanglement with light. *Physical Review Letters*, 99(25):250401.

Peres, A. (1996). Separability criterion for density matrices. *Physical Review Letters*, 77(8):1413.

Peres, A. (1997). *Quantum theory: concepts and methods*, volume 72. Springer.

Piani, M. and Watrous, J. (2015). Necessary and sufficient quantum information characterization of einstein-podolsky-rosen steering. *Physical review letters*, 114(6):060404.

Pinard, M., Dantan, A., Vitali, D., Arcizet, O., Briant, T., and Heidmann, A. (2005). Entangling movable mirrors in a double-cavity system. *Europhysics Letters*, 72(5):747.

Plenio, M. B. (2005). Logarithmic negativity: a full entanglement monotone that is not convex. *Physical review letters*, 95(9):090503.

Plenio, M. B. and Virmani, S. (2007). An introduction to entanglement measures. *Quantum Inf. Comput.*, 7(1):1–51.

Poderini, D., Polino, E., Rodari, G., Suprano, A., Chaves, R., and Sciarrino, F. (2022). Ab initio experimental violation of bell inequalities. *Physical Review Research*, 4(1):013159.

Pramanik, T., Kaplan, M., and Majumdar, A. S. (2014). Fine-grained einstein-podolsky-rosen–steering inequalities. *Physical Review A*, 90(5):050305.

Purdy, T. P., Yu, P.-L., Peterson, R. W., Kampel, N. S., and Regal, C. A. (2013). Strong optomechanical squeezing of light. *Physical Review X*, 3(3):031012.

Reid, M. (2013a). Signifying quantum benchmarks for qubit teleportation and secure quantum communication using einstein-podolsky-rosen steering inequalities. *Physical Review A*, 88(6):062338.

Reid, M., Drummond, P., Bowen, W., Cavalcanti, E. G., Lam, P. K., Bachor, H., Andersen, U. L., and Leuchs, G. (2009). Colloquium: the einstein-podolsky-rosen paradox: from concepts to applications. *Reviews of Modern Physics*, 81(4):1727.

Reid, M. D. (1989). Demonstration of the einstein-podolsky-rosen paradox using nondegenerate parametric amplification. *Physical Review A*, 40(2):913.

Reid, M. D. (2013b). Monogamy inequalities for the einstein-podolsky-rosen paradox and quantum steering. *Physical Review A*, 88(6):062108.

Rogers, B., Paternostro, M., Palma, G. M., and De Chiara, G. (2012). Entanglement control in hybrid optomechanical systems. *Physical Review A*, 86(4):042323.

Safavi-Naeini, A. H., Gröblacher, S., Hill, J. T., Chan, J., Aspelmeyer, M., and Painter, O. (2013). Squeezed light from a silicon micromechanical resonator. *Nature*, 500(7461):185–189.

Saunders, D. J., Jones, S. J., Wiseman, H. M., and Pryde, G. J. (2010). Experimental epr-steering using bell-local states. *Nature Physics*, 6(11):845–849.

Schneeloch, J., Broadbent, C. J., Walborn, S. P., Cavalcanti, E. G., and Howell, J. C. (2013). Einstein-podolsky-rosen steering inequalities from entropic uncertainty relations. *Physical Review A*, 87(6):062103.

Schrödinger, E. (1935a). Discussion of probability relations between separated systems. In *Mathematical Proceedings of the Cambridge Philosophical Society*, volume 31, pages 555–563. Cambridge University Press.

Schrödinger, E. (1935b). Mathematical proceedings of the cambridge philosophical society. In *Mathematical Proceedings of the Cambridge Philosophical Society*, volume 31, pages 555–563.

Scully, M. and zubairy ms 1997 quantum optics.

Serafini, A. (2006). Multimode uncertainty relations and separability of continuous variable states. *Physical review letters*, 96(11):110402.

Sete, E. A. and Eleuch, H. (2015). Anomalous optical bistability and robust entanglement of mechanical oscillators using two-photon coherence. *JOSA B*, 32(5):971–982.

Skrzypczyk, P., Navascués, M., and Cavalcanti, D. (2014). Quantifying einstein-podolsky-rosen steering. *Physical review letters*, 112(18):180404.

Smith, D. H., Gillett, G., De Almeida, M. P., Branciard, C., Fedrizzi, A., Weinhold, T. J., Lita, A., Calkins, B., Gerrits, T., Wiseman, H. M., et al. (2012). Conclusive quantum steering with superconducting transition-edge sensors. *Nature communications*, 3(1):625.

Steinlechner, S., Bauchrowitz, J., Eberle, T., and Schnabel, R. (2013). Strong einstein-podolsky-rosen steering with unconditional entangled states. *Physical Review A*, 87(2):022104.

Sun, K., Xu, J.-S., Ye, X.-J., Wu, Y.-C., Chen, J.-L., Li, C.-F., and Guo, G.-C. (2014). Experimental demonstration of the einstein-podolsky-rosen steering game based on the all-versus-nothing proof. *Physical review letters*, 113(14):140402.

Svelto, O. and Svelto, O. (1998). Solid-state, dye, and semiconductor lasers. *Principles of Lasers*, pages 365–418.

Săndulescu, A. and Scutaru, H. (1987). Open quantum systems and the damping of collective modes in deep inelastic collisions. *Annals of Physics*, 173(2):277–317.

Tan, H., Zhang, X., and Li, G. (2015). Steady-state one-way einstein-podolsky-rosen steering in optomechanical interfaces. *Physical Review A*, 91(3):032121.

Taylor, M. A., Janousek, J., Daria, V., Knittel, J., Hage, B., Bachor, H.-A., and Bowen, W. P. (2013). Biological measurement beyond the quantum limit. *Nature Photonics*, 7(3):229–233.

Tesfa, S. (2006). Entanglement amplification in a nondegenerate three-level cascade laser. *Physical Review A*, 74(4):043816.

Tesfa, S. (2008). Externally induced continuous variable entanglement in a correlated emission laser. *Journal of Physics B: Atomic, Molecular and Optical Physics*, 41(14):145501.

Tesfa, S. (2009). Effect of dephasing on quantum features of the cavity radiation of an externally pumped correlated emission laser. *Physical Review A*, 79(6):063815.

Tesfa, S. (2011). Dependence of the evolution of the cavity radiation of a coherently pumped correlated emission laser on dephasing and phase fluctuation. *Physical Review A*, 83(2):023809.

Tesfa, S. (2021). *Quantum Optical Processes: From Basics to Applications*, volume 976. Springer Nature.

Vacchini, B. (2002). Quantum optical versus quantum brownian motion master equation in terms of covariance and equilibrium properties. *Journal of Mathematical Physics*, 43(11):5446–5458.

Vallone, G. (2013). Einstein-podolsky-rosen steering: Closing the detection loophole with non-maximally-entangled states and arbitrary low efficiency. *Physical Review A*, 87(2):020101.

Verhagen, E., Deléglise, S., Weis, S., Schliesser, A., and Kippenberg, T. J. (2012). Quantum-coherent coupling of a mechanical oscillator to an optical cavity mode. *Nature*, 482(7383):63–67.

Vidal, G. and Werner, R. F. (2002). Computable measure of entanglement. *Physical Review A*, 65(3):032314.

Vitali, D., Gigan, S., Ferreira, A., Böhm, H., Tombesi, P., Guerreiro, A., Vedral, V., Zeilinger, A., and Aspelmeyer, M. (2007). Optomechanical entanglement between a movable mirror and a cavity field. *Physical review letters*, 98(3):030405.

Walborn, S., Salles, A., Gomes, R., Toscano, F., and Ribeiro, P. S. (2011). Revealing hidden einstein-podolsky-rosen nonlocality. *Physical review letters*, 106(13):130402.

Walk, N., Hosseini, S., Geng, J., Thearle, O., Haw, J. Y., Armstrong, S., Assad, S. M., Janousek, J., Ralph, T. C., Symul, T., et al. (2016). Experimental demonstration of gaussian protocols for one-sided device-independent quantum key distribution. *Optica*, 3(6):634–642.

Walls, D. and Milburn, G. J. (2008). Cqed. In *Quantum Optics*, pages 213–229. Springer.

Wang, D.-Y., Bai, C.-H., Wang, H.-F., Zhu, A.-D., and Zhang, S. (2016a). Steady-state mechanical squeezing in a double-cavity optomechanical system. *Scientific reports*, 6(1):38559.

Wang, G., Huang, L., Lai, Y.-C., and Grebogi, C. (2014). Nonlinear dynamics and quantum entanglement in optomechanical systems. *Physical review letters*, 112(11):110406.

Wang, J., Cao, H., Jing, J., and Fan, H. (2016b). Gaussian quantum steering and its asymmetry in curved spacetime. *Physical Review D*, 93(12):125011.

Weedbrook, C., Pirandola, S., García-Patrón, R., Cerf, N. J., Ralph, T. C., Shapiro, J. H., and Lloyd, S. (2012). Gaussian quantum information. *Reviews of Modern Physics*, 84(2):621.

Werner, R. F. and Wolf, M. M. (2001). Bound entangled gaussian states. *Physical review letters*, 86(16):3658.

Wheeler, J. A. and Zurek, W. H. (2014). *Quantum theory and measurement*, volume 40. Princeton University Press.

Wilde, M. M. (2013). *Quantum information theory*. Cambridge university press.

Williamson, J. (1936). On the algebraic problem concerning the normal forms of linear dynamical systems. *American journal of mathematics*, 58(1):141–163.

Wipf, C., Corbitt, T., Chen, Y., and Mavalvala, N. (2008). Route to ponderomotive entanglement of light via optically trapped mirrors. *New Journal of Physics*, 10(9):095017.

Wiseman, H. M., Jones, S. J., and Doherty, A. C. (2007). Steering, entanglement, nonlocality, and the einstein-podolsky-rosen paradox. *Physical review letters*, 98(14):140402.

Wittmann, B., Ramelow, S., Steinlechner, F., Langford, N. K., Brunner, N., Wiseman, H. M., Ursin, R., and Zeilinger, A. (2012). Loophole-free einstein–podolsky–rosen experiment via quantum steering. *New Journal of Physics*, 14(5):053030.

Wollman, E. E., Lei, C., Weinstein, A., Suh, J., Kronwald, A., Marquardt, F., Clerk, A. A., and Schwab, K. (2015). Quantum squeezing of motion in a mechanical resonator. *Science*, 349(6251):952–955.

Wu, L.-A., Kimble, H., Hall, J., and Wu, H. (1986). Generation of squeezed states by parametric down conversion. *Physical review letters*, 57(20):2520.

Xiong, H., Scully, M. O., and Zubairy, M. S. (2005). Correlated spontaneous emission laser as an entanglement amplifier. *Physical Review Letters*, 94(2):023601.

Xiong, H.-N., Zhang, W.-M., Wang, X., and Wu, M.-H. (2010). Exact non-markovian cavity dynamics strongly coupled to a reservoir. *Physical Review A*, 82(1):012105.

Yang, L.-P., Cai, C., Xu, D., Zhang, W.-M., Sun, C., et al. (2013). Master equation and dispersive probing of a non-markovian process. *Physical Review A*, 87(1):012110.

Yang, R.-G., Li, N., Zhang, J., Li, J., and Zhang, T.-C. (2017). Enhanced entanglement of two optical modes in optomechanical systems via an optical parametric amplifier. *Journal of Physics B: Atomic, Molecular and Optical Physics*, 50(8):085502.

Zhang, J., Peng, K., and Braunstein, S. L. (2003). Quantum-state transfer from light to macroscopic oscillators. *Physical Review A*, 68(1):013808.

Zhang, J.-S. and Chen, A.-X. (2020). Large mechanical squeezing beyond 3db of hybrid atom-optomechanical systems in a highly unresolved sideband regime. *Optics Express*, 28(9):12827–12836.

Zhang, W.-M., Lo, P.-Y., Xiong, H.-N., Tu, M. W.-Y., and Nori, F. (2012). General non-markovian dynamics of open quantum systems. *Physical review letters*, 109(17):170402.

Zhang, Z.-C., Wang, Y.-P., Yu, Y.-F., and Zhang, Z.-M. (2018). Quantum squeezing in a modulated optomechanical system. *Optics Express*, 26(9):11915–11927.

Zhou, L., Han, Y., Jing, J., and Zhang, W. (2011). Entanglement of nanomechanical oscillators and two-mode fields induced by atomic coherence. *Physical Review A*, 83(5):052117.

Zurek, W. H. (2000). Einselection and decoherence from an information theory perspective. *Annalen der Physik*, 512(11-12):855–864.